GEOMAR
Helmholtz-Zentrum für Ozeanforschung Kiel

C A U
Christian-Albrechts-Universität zu Kiel

Master Thesis

Local adaptation of the common sea star *Asterias rubens* to different salinities

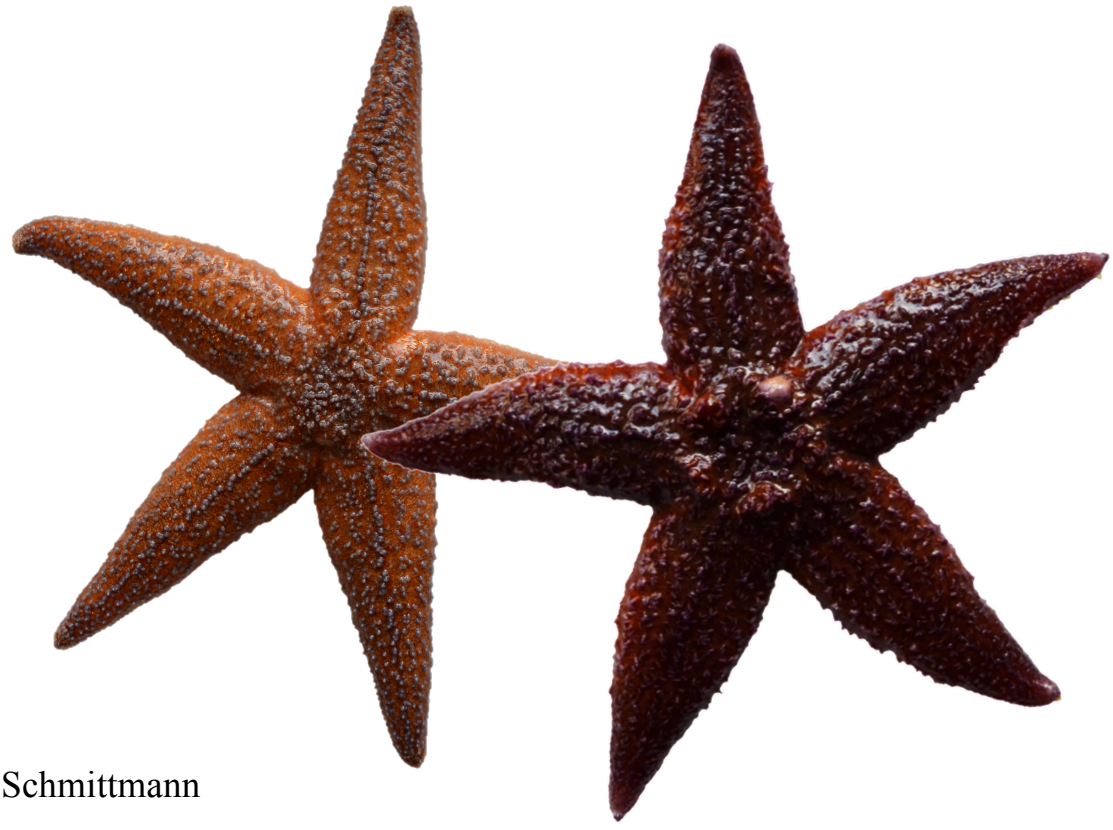

Lara Schmittmann

28th August 2017

1st Supervisor: PD Dr Frank Melzner

2nd Supervisor: Prof Thorsten Reusch

Declaration of Authorship

I, Lara Schmittmann, declare that this thesis and the work presented in it are my own and has been generated by me as the result of my own original research.

Title of thesis: Local adaptation of the common sea star *Asterias rubens* to low salinities

I confirm that:

1. This work was done wholly while in candidature for a research degree at this University;

2. Where any part of this thesis has previously been submitted for a degree or any other qualification at this University or any other institution, this has been clearly stated;

3. Where I have consulted the published work of others, this is always clearly attributed;

4. Where I have quoted from the work of others, the source is always given. With the exception of such quotations, this thesis is entirely my own work;

5. I have acknowledged all main sources of help;

6. Where the thesis is based on work done by myself jointly with others, I have made clear exactly what was done by others and what I have contributed myself;

7. None of this work has been published before submission.

Signed:

Date:

Summary

Hyposaline environments impose stressful conditions to marine organisms and limit their distribution. The common sea star *Asterias rubens* is one of the few echinoderm species that is able to survive and reproduce in hyposaline areas, like the brackish Baltic Sea. We expect populations inhabiting low salinity regions to be selected towards hyposalinity tolerance, visible in their physiology and population structure. As an osmoconformer, *A. rubens* relies on compatible organic osmolytes (OO) to adapt its cellular osmolality to that of the surrounding medium while intracellular ion concentrations are kept stable. The salinity at which OO are depleted was previously shown to correlate with fitness loss and is thus considered the critical salinity an organism can tolerate. For sea stars from the Baltic Sea, we experimentally determined the critical salinity to be 9.2 PSU which correlates with their distribution border in the field and our observations in the laboratory. Further, we conducted a reciprocal transplant experiment with animals from the North Sea (32 PSU) and the Baltic Sea (16 PSU) to investigate the effect of changing salinities on OO concentration and composition. Growth, feeding rate and righting time were determined and proton nuclear magnetic resonance spectroscopy was conducted on digestive tissue to quantify OO. Growth, feeding rate and righting time were negatively affected by low salinities whereas animals from the Baltic Sea showed higher growth and activity in 16 PSU than animals from the North Sea. Glycine was found to be the main osmolyte in *A. rubens* and contributed with up to 90 % to the total pool. We found no evidence for adaptation to hyposalinity on the level of OO and suggest the investigation of inorganic ions. To analyse the population structure of *A. rubens* in the North Atlantic, we sampled 14 populations from the Baltic Sea, the North Sea, Iceland and the Canadian East coast. Based on 7 newly developed microsatellites, we analysed the population structure with the aid of F-statistics, Bayesian clustering algorithms and NJ-trees. We applied Pearson's correlation and Mantel tests to investigate IBD and IBE (salinity). The population structure of *A. rubens* in the North Atlantic is neither shaped by salinity nor by geographical distance. Nevertheless, a population structure is visible and probably shaped by water depth and stratification of water masses due to salinity. We show that sea stars from the same coordinates but from different water depth (5 m and 25 m) are genetically isolated. Additionally, Canadian *A. rubens* populations possess unique genotypes that hint towards a dispersal barrier to European populations. Despite the adaptation potential of *A. rubens* the critical salinity of 9.2 PSU and the projected desalination for the Baltic Sea due to climate change suggest a depression of the suitable habitat for *A. rubens*. This would lead to the loss of an important keystone species in some areas.

List of figures

List of tables

Table of contents

1 Introduction

1.1 Hyposaline environments: the Baltic Sea as an example

Hyposaline environments impose stressful conditions for marine organisms and are mostly found in coastal regions in form of estuaries, lagoons, mangroves or intertidal zones (Rivera-Ingraham and Lignot 2017). Salinity stress in these regions differs in form of magnitude and rate of change: sudden and intense decreases characterize intertidal zones, while slower changes of longer duration occur after strong rainfalls and thus increased river outflow. Permanently hyposaline conditions are found in enclosed brackish lagoons and big estuaries. The exposure time to low salinities and the extent of salinity fluctuations determine the ability of an organism to cope with hyposaline conditions (Harley *et al.,* 2006). In a fluctuating environment with the possibility to migrate towards more saline waters, the pressure to genetically adapt is probably lower than in geographically isolated regions. An example for a both geographically and ecologically marginal ecosystem is the Baltic Sea, a semi enclosed basin of the North Atlantic (Johannesson *et al.,* 2011).

The North Sea – Baltic Sea complex in the North Atlantic comprises of the fully marine North Sea and the brackish to fresh Baltic Sea connected by the narrow Danish Straight region. The Baltic Sea is a semi-enclosed basin and characterized by its strong horizontal surface salinity gradient from almost marine conditions in the Kattegat region (~ 25 PSU = practical salinity units) to fresh water in the North East (Hansson and Gustafsson, 2011). Additionally, a vertical salinity gradient is created by a halocline that divides a hyposaline surface layer with fluctuating salinity from a more stable bottom layer of higher salinity. Irregular saltwater influx from the North Sea combined with fresh water river run-off from inland create the prominent halocline and regional salinity fluctuations (Hansson and Gustafsson, 2011). Nutrient input from agriculture provides the basis for high primary productivity and thus biomass as it is often found in coastal regions (Woodland *et al.,* 2015). Due to the brackish conditions in the Baltic Sea and its recent formation after the last glacial maximum (~ 10,000 BP) the biodiversity is very low and consists of both fresh water and marine organisms and a few glacial relict species (Andrén *et al.,* 2011; Pawlak *et al.,* 2009; Ojaveer *et al.,* 2010; Wennerström *et al.,* 2013). Different species exhibit various strategies to cope with hyposaline conditions resulting in species-specific physiological thresholds and flexibility (Sanford and Kelly 2011). This makes it a perfect Darwinian Laboratory, a study

site for adaptation and population connectivity along an environmental gradient together with geographical constraints.

Within population genetic diversity is suggested to be much lower in the Baltic Sea when compared to the same species in the North Atlantic, especially in the entrance region of the basin (Johannesson and André 2006). From 20 analysed species, only the barnacle *Balanus improvises* was found panmictic over the salinity gradient. Such genetic shift over the entrance of the Baltic Sea can be the result of different processes, including genetic drift, divergent selection of certain genotypes or increased phenotypic plasticity (Johannesson and André 2006; Johannesson *et al.,* 2011). One example for rapid evolution in response to extreme conditions is the just recently described brown algae species, *Fucus radicans* (Bergstrom *et al.,* 2005). This dwarf relative of the Atlantic *Fucus vesiculosus* is endemic to the Baltic Sea and characterized by one extremely successful clone that dominates the population (Tatarenkov *et al.,* 2005; Pereyra *et al.,* 2009). A different strategy to cope with low salinities was found for the isopod *Idotea baltica* which successfully invades the Baltic Sea basin down to salinities of 3 PSU (Wood *et al.,* 2014). It has an extremely high phenotypic plasticity that facilitates the tolerance to a wide range of abiotic conditions while it additionally benefits from low competition on its main food source *Fucus sp.* Further, hybridization can favour genetic diversity and thus evolutionary potential as was shown for the clam, *Macoma baltica* (Johannesson and André 2006; Nikula *et al.,* 2008). Due to hybridization of two distinct genetic lineages the gene pool and effective population size is increased and genetic variability is higher compared to North Sea populations. Additionally, hybridization and finally out-competition of certain lineages in low salinity areas was shown to be beneficial in the blue mussel species complex (Stuckas *et al.,* 2009). Selection for certain genes in Baltic Sea populations and therefore potential local adaptation was proposed for different species including cod (Berg *et al.,* 2015), blue mussels (Riginos and Cunningham 2005) and herring (Lamichhaney *et al.,* 2012).

1.2 Adaptation to hyposaline environments

Two main strategies have evolved in the marine environment to maintain cell homeostasis in saline water. Osmoregulators, such as fish, are permanently hyposaline to the marine environment. Both their cellular and blood osmolality are kept constant at around ~ 400 mOsm (Figure 1) regardless of the environmental salinity (Hochachka and Somero 2002; Willmer *et al.,* 2005). This strategy can only be achieved through osmoregulatory

organs such as gills or kidneys and active ion transport. In contrast, many marine invertebrates osmoconform with their environment, i.e. adjust the intracellular osmotic pressure to that of the external medium while the osmotic composition of the extracellular body fluid or hemolymph resembles seawater (Figure 1) and passively adapts by diffusion (Hochachka and Somero, 2002). However, osmolality is to some extent regulated at the body fluid-cell interface by regulation of organic osmolyte (OO) concentrations. In a fully marine osmoconformer, intracellular ions and proteins add up to ~ 300-400 mOsm, whereas OO contribute to the remaining portion to achieve the final cellular osmotic pressure resembling seawater (~ 1000 mOsm) (Hochachka and Somero, 2002**,** Figure 1). The intracellular ionic composition with a high concentration of potassium is crucial for cellular transport, protein function and integrity and is carefully maintained at constant levels (Hochachka and Somero, 2002). OO on the other hand, are so called compatible micromolecules as they do not interfere with enzyme or cell function (Yancey 2005). Different compounds can serve as OO, such as amino acids, methylamines and sugars (Yancey 2005), while utilization of certain OO differs between species.

Organisms inhabiting brackish areas are either phenotypically flexible enough to cope with a high range of salinities (euryhaline) or genetically adapted to salinity stress (Cognetti and Maltagliati, 2000). When seawater salinity decreases rapidly, the short term response of an osmoconformer is an efflux of ions through passive ion channels to prevent cell swelling due to water uptake (Silva and Wright 1994). In the following, ion concentrations are actively restored to initial levels (Diehl and Lawrence 1985; Silva and Wright 1994; Hochachka and Somero 2002), and OO concentrations are down regulated as a long-term response e.g. by excretion from the cells into the body cavity or by turnover of many small amino acids into a few large ones (Silva and Wright 1994; Yancey 2001, 2005). The Na^+/K^+-ATPase (NKA) is responsible for active cellular export of sodium and import of potassium ions and involved in intracellular osmoregulation (Lucu *et al.,* 2000). Also, the importance of other active ion pumps, like the apical V-type H^+ ATPase, was shown for the freshwater invading copepod *Eurytemora affinis* (Lee *et al.,* 2011). This ion pump creates a proton gradient over the cell membrane allowing different cations to enter the cell in exchange (Beyenbach 2006). Maintenance of intracellular ion concentrations is expected to be extremely energy demanding with a resting metabolic rate of 17-20 % of the total ATP production under marine conditions (Maar *et al.,* 2015). Under hyposaline conditions in half of the optimal salinity, this energy expenditure is estimated to increase around 3.8-4.7 times in the blue mussel, *Mytilus edulis* to around 74-87 % of the total costs (Maar *et al.,* 2015). Nevertheless, estimations are

rather based and accumulative results and theoretical models than on specific experiments and are probably variable between species and under different conditions. Increased respiration under salinity stress is interpreted as higher energy demand due to costs of osmoregulation and shown for some species (Sarà *et al.,* 2008; Shin *et al.,* 2011; Yu *et al.,* 2012). Another proxy for metabolic cost is an altered activity or expression of the NKA (Henry *et al.,* 2002; Lv *et al.,* 2016). Costs of ion regulation also heavily depend on the analysed tissue as demonstrated for the Mediterranean shore crab, *Carcinus aestuarii* (Rivera-Ingraham *et al.,* 2016). In this study, a part of the gills entered metabolic arrest under hypoosmotic conditions while another part was heavily involved in osmoregulation as shown by high mitochondria activity and thus ATP production.

For the invasive sea anemone, *Diadumene lineata* it has been proposed that the depletion of OO at a critical salinity (S_{crit}) of 7 PSU correlates with the inability of asexual reproduction (Podbielski *et al.,* 2016). As an adaptation to hyposaline conditions, S_{crit} is possibly shifted towards lower salinities by alteration of the OO pool. Such adaptations could be the result of utilizing more efficient osmolyte species or rather aggregation than efflux of OO (Willmer *et al.,* 2005). Other strategies of adaptation to hyposaline conditions include accumulation of certain ions such as sodium in the mussel *Mytilus sp.* and potassium in echinoderms (Willmer 1978a,b; Russell 2013), changes in membrane permeability by altered expression of ion pumps (Havird *et al.,* 2013), higher activity of the ion pumps (Lee *et al.,* 2011) or increased water efflux (Willmer *et al.,* 2005).

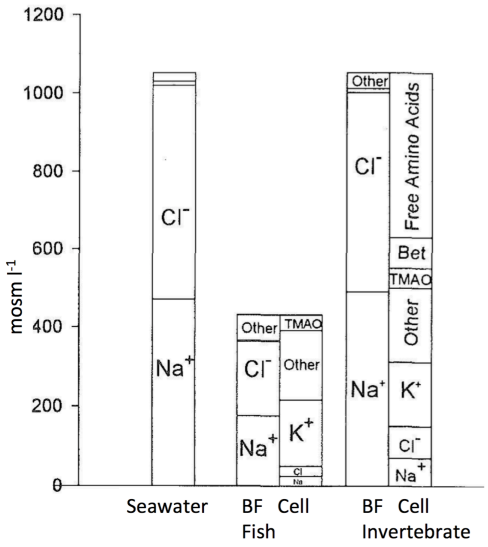

Figure 1: Composition of osmotically active substances in seawater, osmoregulating fish and osmoconforming invertebrates. BF = bodyfluid (adapted from Hochachka and Somero, 2002)

1.3 Climate change in the Baltic Sea

The atmospheric chemist Paul Crutzen coined the term 'Anthropocene' for the current geological epoch as its main characteristic is human activity (Crutzen 2002). The oceans as the largest habitat on earth are immensely altered by climate change (Harley *et al.,* 2006; Hickling *et al.,* 2006; Halpern 2010). Suitable habitats for many marine organisms are being compressed and/or geographically shifted. Next to the main effects of global change, namely ocean warming, deoxygenation and acidification (IPCC 2014), an important stressor in coastal regions will be changes in salinity patterns. Predictions for the Baltic Sea include increased precipitation and river run-off (10 %) leading to a decrease in sea surface salinity and bottom water salinity by 1.5-2 PSU (Meier *et al.,* 2012; Gräwe *et al.,* 2013; IPCC 2014). Different models agree on shifts of salinity isolines, most pronounced in the shift of the 7 PSU isoline by approximately 100 km south-west wards (Gräwe *et al.,* 2013) (Figure 2). Desalinization might result in a complete restructuring of the ecosystem: while marine species already living at their salinity limit will be forced to migrate into deeper waters or the South West of the Baltic Sea, freshwater species will be able to advance further into the Baltic Sea Proper. Migration to deeper waters is however limited by oxygen minimum zones and constraints species distribution further (Conley *et al.,* 2002). Although, predictions of physical and geochemical conditions are uncertain, most models mostly agree on resulting changes even under different greenhouse gas emission scenarios (A1B and A2 from Nakićenović *et al.,* 2000 equivalent to RCP8.5 from IPCC 2014 report; Meier *et al.,* 2012). Nevertheless, models do not include organismic responses. The response of ecosystems or single species, particularly the higher trophic levels, cannot be modelled precisely without a greater understanding of organismic biology and adaptation potential. Experiments and field studies are urgently needed to investigate responses in vivo and incorporate this knowledge into ecological climate change models. Factors including phenotypic plasticity, genetic adaptation, species-interaction and migration are species-specific and thus need to be based on experimental data for at least a number of species in each taxonomic or functional clade. It is crucial to understand possible limitations and interaction of organisms in order to address future climate changes by implementation of conservation efforts according to regional demands.

Genetic variability favours adaptation to novel conditions such as confronted during anthropogenic climate change (Bell and Gonzalez 2009). Therefore, the combination of little genetic variance, reduced gene flow due to geographical constraints and changing conditions in the Baltic Sea will impose a great threat for species already living at their physiological

distribution boarder (Johannesson *et al.,* 2011). As single species play an important role in ecosystem functioning of the species poor Baltic Sea, the loss of key species can result in a potential negative impact on the whole ecosystem (Kappel 2005).

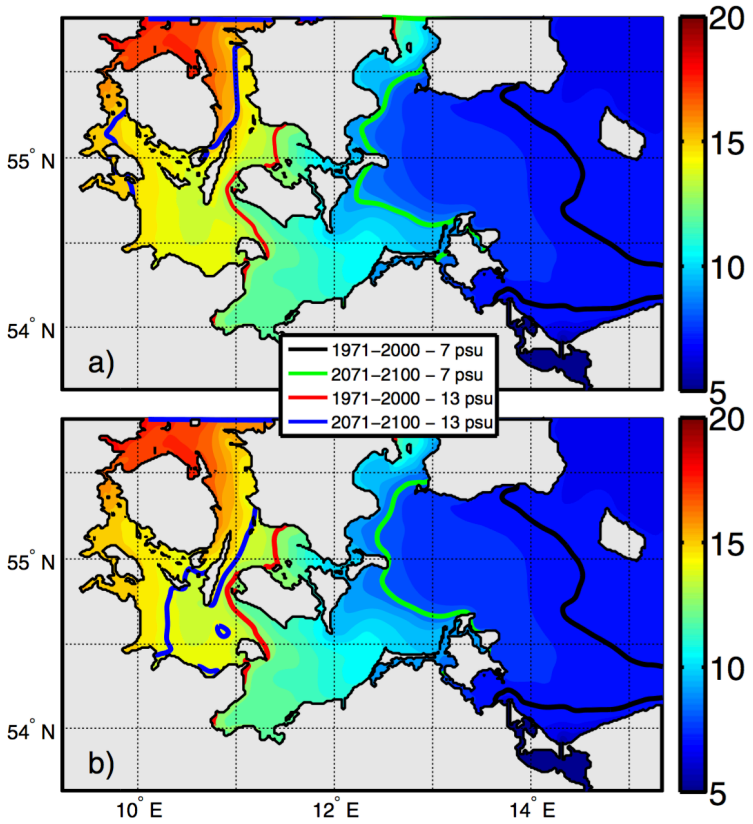

Figure 2: Mean sea surface salinity distribution in PSU for the year 2071-2100. The thick lines indicate the shift of the 7 and 13 PSU isoline for the greenhouse gas emission scenarios (a) RCP8.5 and (b) RCP4.5 (from Gräwe et al 2013).

1.4 The common sea star *Asterias rubens*

The common sea star *Asterias rubens* (Linnaeus 1758) is a secondary consumer in the Baltic Sea, already experiencing salinity stress at the boarder of their current distribution. Echinoderms are an exclusively marine phylum with more than 7000 living species, lacking osmoregulatory organs like kidneys or gills. *A. rubens* represents the only echinoderm species that penetrates into the Baltic Sea basin down to salinities as low as 8 PSU (Brattström 1941; Schlieper 1957). Further, it is an important keystone predator on *Mytilus* beds, controlling mussel populations by reducing their abundance by up to 70 % annually (Reusch and Chapman, 1997). For the osmoconforming *A. rubens* it has been reported that potassium is

constantly upregulated in the extracellular ambulacral fluid and intestinal and muscle cells (Binyon 1962; Diehl 1986). So far, it is not known which OOs are utilized by *A. rubens* and if the composition varies with salinity. For the related asteroid species *Luidia clathrata* the amino acid glycine was mainly utilized during low salinity stress (Diehl and Lawrence, 1985). Although, adult *A. rubens* are able to establish populations in salinities down to 8 PSU, fertilization and development of larvae are only possible in salinities of 14 PSU or higher (Casties *et al.,* 2015). In areas with strong salinity fluctuations like the Kiel Fjord (~10 and 27 PSU), recruitment of *A. rubens* is only successful in years of stable salinities during reproductive season (continuous logging of salinity by German Federal Maritime and Hydrographic Agency (BSH) between 2004 and 2006). It was estimated that during the period of 2005-2010 only the year 2009 fulfilled the necessary requirements (Casties *et al.,* 2015). Populations in salinities lower than 14 PSU must have been formed by recruitment from animals living in areas of higher salinities. Larval stages and juveniles are able to disperse with currents, whereas adult organisms are sessile.

1.5 Population structure and isolation by environment

Despite the ability of *A. rubens* to tolerate salinities down to 8 PSU in the Baltic Sea, no animals are found in regions of similarly reduced salinities off the British coasts (Binyon 1961). In the Barents Sea and the enclosed, less saline White Sea, however, *A. rubens* shows similar behaviour as in the North Sea – Baltic Sea system and tolerates salinities from 16-34 PSU (Sarantchova 2001). This suggests adaptation of single populations, rather than each genotype representing the physiological requirements to survive diluted seawater (Binyon 1961). In larvae of the *Mytilus edulis trossolus* complex in the Baltic Sea, extreme local adaptation to salinity was shown: although this species is able to successfully recruit at 7 PSU and lower (Sanders *et al.,* unpublished), offspring of parents from regions with a mean salinity of 11 PSU showed significantly reduced settlement at 9 PSU (Nascimento Schulze *et al.,* unpublished). To investigate both adaptation and phenotypic plasticity of less adapted populations of *A. rubens* will help estimate the probable impact of desalination on their distribution. From personal observation and previous descriptions (Kowalski 1955) (Figure 3), *A. rubens* from the North Sea and the Baltic Sea display phenotypic differences. Animals from the North Sea have an orange-brownish colour, a stronger exoskeleton and are more active. In contrast, animals from the Baltic Sea are generally red-violet, slack and respond slower. It was found, that salinity is associated with colour in *A. rubens* (Weber and Holmes, 2010) and that it correlates with activity (Kowalski 1955) although the latter finding

has to be interpreted with caution due to partially low replication. Local adaptation and isolation of populations by environment (salinity) can be investigated with different population genetic methods based on molecular markers. Single nucleotide polymorphisms (SNPs) from DNA or mRNA are commonly used and can be acquired in different ways (De Wit *et al.,* 2015). SNPs hold detailed information of long-term divergence, overall genomic diversity and gene function. A more feasible and faster method but with less resolution is microsatellite genotyping (Guichoux *et al.,* 2011). Microsatellites are repeated motifs of one to six nucleotides. They are highly polymorphic between individuals with a higher mutation rate than SNPs, which qualifies them for detecting early population differences like in a recently populated area such as the Baltic Sea (Guichoux *et al.,* 2011; Selkoe and Toonen, 2006). So far, only one microsatellite has been available for *A. rubens* (Harper and Hart, 2005), but for application to population structure analysis more loci have to be established.

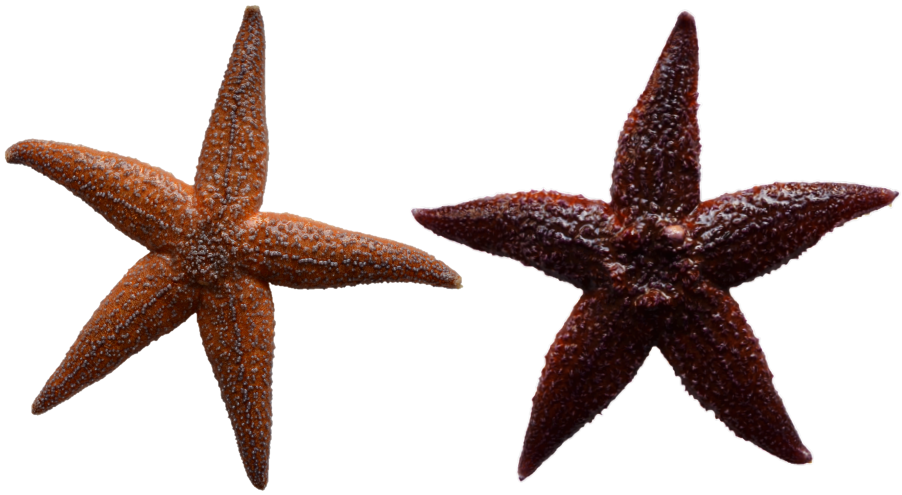

Figure 3: *Asterias rubens* specimen collected from the island of Sylt in the North Sea (left) and one specimen collected from the Baltic Sea at Kiel fjord (right).

1.6 Biogeography of Asterias species in the Atlantic Ocean

Asterias rubens is native to North Atlantic Ocean. On the east coast, it occurs from Norway, Iceland and the Barents Sea and south to Senegal, excluding the Mediterranean Sea (Mortensen 1927). Recently, it was found in as a non-indigenous species in the Black Sea (Karhan *et al.,* 2008). On the west coast of the Atlantic, it can be found from the Labrador Sea to New Jersey, USA. The *Asterias* genus participated in the trans-Arctic interchange (3.5 Ma) during which many species invaded the Atlantic from the Pacific (Worley and Franz, 1983).

With the formation of the Labrador current (3 Ma BP) and the physical separation of the east and west coast of the Atlantic by cold water, two species diverged: *Asterias forbesi* on the American coast and *Asterias rubens* on the European coast (Wares 2001). The current hypothesis is, that as recent as ~ 20,000 BP the water warmed up enough for *Asterias rubens* to reinvade North America, where the two species now co-occur and hybridize (Harper and Hart, 2007; Wares 2001). As markers used so far did not reveal unique haplotypes in American *A. rubens* populations to estimate the time of arrival the hypothesis is not fully validated (Wares 2001; Harper *et al.,* 2007). An alternative hypothesis would be that *A. rubens* arrived via human vectors much later, which is supported by little population differences across the Atlantic. Unfortunately, no fossil evidence are available that could support either hypothesis.

1.7 Aim of the study

The aim of this study was to assess local adaptation to salinity by comparison of *Asterias rubens* from different salinity environments using experimental and population genetic approaches. This project will help to understand the adaptation/acclimation potential of *A. rubens* regarding salinity fluctuations and future decreases in sea surface salinity. Furthermore, the biogeography of the *Asterias* genus in the Atlantic Ocean was investigated.

1. Experimental physiology:

Asterias rubens populations from the Baltic Sea were expected to have locally adapted to low salinities due to geographical separation from North Sea populations over several generations. Adaptation towards an increased capability of intracellular osmoregulation to diluted seawater can theoretically happen through different strategies from which some are displayed in Figure 4. During intracellular osmoregulation it is expected that the intracellular ion concentration is maintained stable while the organic osmolyte concentration has a linear relationship with salinity (Diehl and Lawrence 1985; Diehl 1986). We aimed to test the following hypotheses with this study:

1. The salinity at which OO are depleted coincides with death of sea stars and thus can be described as the critical salinity S_{crit}.

2. a) Growth, feeding rate and righting time of sea stars is lower in 16 PSU. b) Growth, feeding rate and righting time of sea stars is lower in animals from Sylt in 16 PSU than in animals from Kiel.

3. *Asterias rubens* from Kiel are locally adapted to low salinities through potentially one of the following strategies (see Figure 4 for more details):

   a) higher OO concentrations.
   b) higher ion concentrations.
   c) higher tolerance of ion loss.
   d) a combination of ion and OO manipulation.

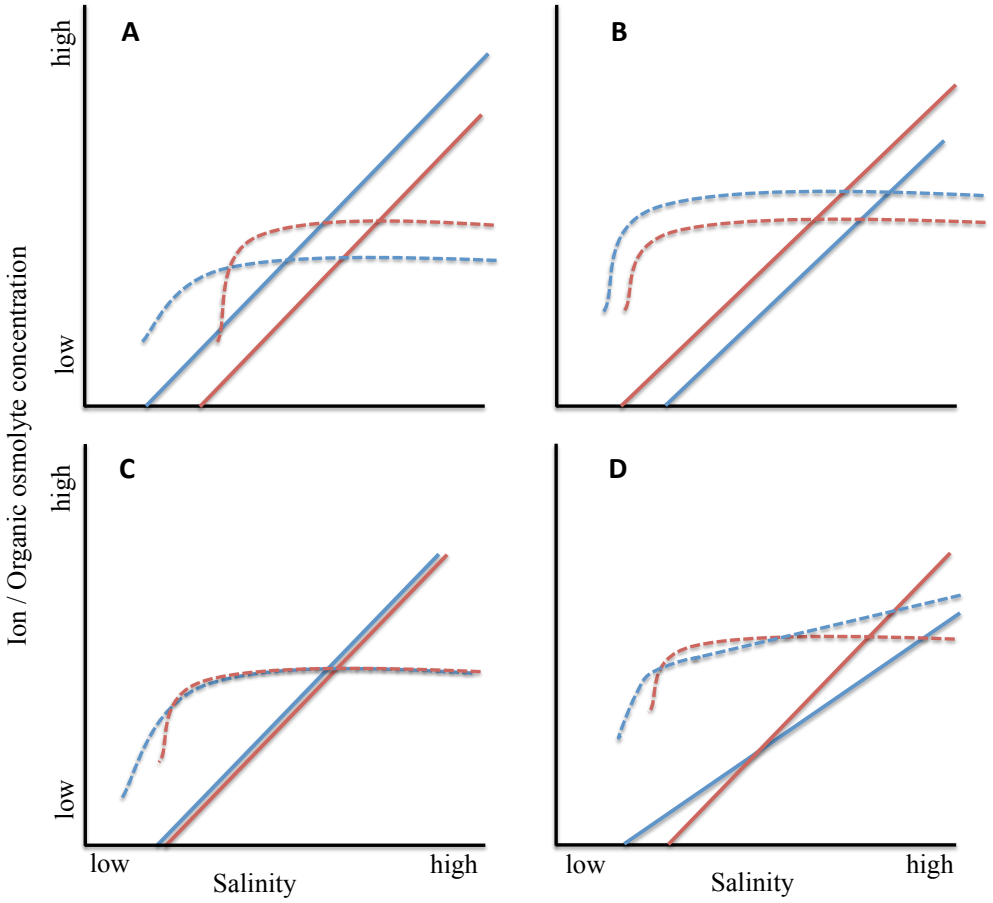

Figure 4: Theoretical adaptation mechanisms to hyposaline environments. Intracellular ion (dashed lines) and OO (solid lines) concentrations are plotted against a salinity gradient. Blue lines depict a population that is adapted to low salinities in comparison to a less adapted population visualized by red lines in four different scenarios. A: adaptation through higher OO concentrations; B: adaptation through higher ion concentrations; C: adaptation through tolerance of ion loss; D: adaptation through a combination of ion and OO manipulation.

2. Population structure:

Due to local adaptation, the population structure of *A. rubens* over the North Atlantic was investigated with a focus on salinity. Additionally, as shown for many other species (Johannesson *et al.,* 2011) Baltic Sea populations were expected to exhibit one form of adaptation to low salinities which should reflect in the population structure. Based on the following hypotheses we conducted a population genetic analysis:

4. Isolation by environment (salinity) is shaping the population structure of *Asterias rubens* in the North Atlantic.

5. Populations in the Baltic Sea show lower genetic diversity than from the North Sea and North Atlantic.

6. If the current hypothesis of colonization of North America by *A. rubens* 20.000 years ago is not discarded, the microsatellite study is expected to reveal unique haplotypes in American populations.

2 Methods

2.1 Experiment 1: Acclimation of *Asterias rubens* from Kiel to different salinity levels

2.1.1 Animal collection and maintenance

Thirty sea stars between 6 and 16.4 g were collected from Kiel Fjord (54°19'45.2"N 10°08'54.9"E) on 20th of April 2016 from a depth of 2 m by snorkelling. The salinity was 16.4 PSU and the water temperature was 4.7 °C (measured with Cond 3110, WTW). Animals were transported in a cooling box equipped with a portable aerator (Pulsator, Zebco) to the laboratory facilities of the GEOMAR Helmholtz Centre for Ocean Research, Kiel. Sea stars were placed individually into 2 L aquaria filled with filtered seawater with a salinity of 16.4 PSU from Kiel Fjord (filter series of 50 µm, 20 µm and 5 µm). The water was aerated with compressed air dispersed by air stone diffusers (HOBBY Angular airstone, large) and changed 2-3 times per week with filtered seawater. Salinity was adjusted to the desired level using either artificial sea salt (Tropic Marine Sea Salt) or de-ionised water (dH2O). Addition of dH2O leads to a decline in seawater alkalinity and was counteracted by addition of NaHCO3 from a 1 M stock solution according to the salinity-alkalinity relationship from Beldowski et al. 2010. Aquaria were kept in a climate chamber with a constant temperature of 10 °C and a 12:12 h light:dark cycle. Water was always prepared one day in advance and stored at 10 °C to adjust the temperature. Water temperature and salinity were checked every second day with a conductivity portable meter (Cond 3110, WTW). Food was offered in form of fish (COSTA Lachsfilet) five times within the first two weeks after the experiment started. 5 % of the sea stars body weight was offered as fish and the rest removed two days after each feeding to prevent bacterial growth.

2.1.2 Experimental design

Sea stars were separated into 6 treatments with 5 replicated tanks, containing one individual each. The initial weight of sea stars ranged from 5.9 to 16.4 g (mean per treatment 10.5 g). Starting salinity of all treatments was 16.4 PSU according to the salinity in Kiel Fjord the day of sampling. Kiel Fjord is characterized by a mean salinity of 16 PSU (Hansson and Gustafsson 2011) with fluctuations between 10 and 27 PSU (continuous logging of salinity by German Federal Maritime and Hydrographic Agency (BSH) between 2004 and 2006). The treatment levels were 8 PSU, 12 PSU, 16 PSU, 20 PSU, 24 PSU and 28 PSU with 16 PSU

being the control treatment. With every water exchange, the salinity was increased or decreased by 1 PSU until the desired level was reached (1-4 weeks depending on the treatment). From that point, the salinity was kept stable until the end of the experiment on 24th of June 2016. Animals in the 8 PSU treatment were not able to attach to the aquaria walls anymore as soon as salinity was below 10 PSU and showed no signs of activity. We decided to increase the salinity to 10 PSU and keep it stable. Nevertheless, all animals from this treatment died within 2 weeks.

2.1.3 Metabolic profiling

Animals were dissected at the end of the experiment and depending on the available tissue mass 1-3 replicates of ~ 300 µg pyloric caecae tissue was placed in 1.8 ml tubes (SARSTEDT CryoPure). Samples were flash frozen in liquid nitrogen and stored at – 80 °C until further preparation.

Frozen tissue was ground in liquid nitrogen and a known amount of tissue powder per animal was filled in a 2 ml Eppendorf tube, flash frozen and stored in – 80 °C. Extracts were prepared from frozen samples. Samples were homogenized for 1 min in 1 ml ice-cold methanol with an ULTRA-TURRAX until no clumps were visible anymore (VWR VDI 12). Extracts were centrifuged for 5 min at 14000 rpm and 4 °C and the supernatant was discarded (Eppendorf centrifuge 5415 R). The pellets were dried in the Eppendorf tubes with a speed vac (Eppendorf concentrator 5301) and stored in a desiccator to prevent hydration.

Non-targeted metabolic profiling was performed with high- resolution magic angle spinning (HR-MAS) nuclear magnetic resonance (^{1}H-NMR) spectroscopy at the Alfred-Wegener-Institute for Polar and Marine Research in Bremerhaven, Germany. Pellets were re-dissolved in 1 µl D_2O per mg sample containing 0.05 % trimethylsilylpropanoic acid (TSP) as a reference standard. 70 µl from that solution were used for analysis and transferred to a rotor that was injected into an NMR spectrometer operating at 400 MHz (Bruker WB AVANCE III 400 9.4 T, Bruker Biospin GmbH, Germany). ^{1}H-NMR spectra were acquired at 4 °C and a spinning rate pf 3 kHz with the Bruker TopSpin 3.5 software. The following parameters were used: Bruker protocol cpmgpr1d, ns = 64, TD = 70,656, SW = 8802 Hz; acquisition time of 4 s and a relaxation delay of 4 s. Manual shimming with a line width of 2-4 Hz was performed. Samples were measured in a random order to prevent an effect of the machine. After spectra acquisition, phase- and baseline corrections were performed with the TopSpin 3.5 Software and spectra were transferred to the Chenomx Software for metabolic identification and

quantification (Chenomx NMR Suite 7.6, Chenomx Inc., Canada). Spectra were calibrated to the internal standard TSP (at 0.0 ppm). Metabolites were identified using the Chenomx Software database and 26 target compounds were chosen based on literature. To quantify metabolites, ^{1}H-NMR signals were automatically integrated by the Chenomx Software and manually validated.

2.1.4 Statistical analysis

All statistical analyses and graphical display of results were conducted with the R software (Version 3.4.0) implemented in Rstudio (Version 0.98.1083). Single tanks were regarded as units of replication. Normality of data and homogeneity of variances were assessed graphically prior to applying the Shapiro-Wilks-W Test and the Levene's Test, respectively. One-way ANOVA was applied for single osmolyte concentrations followed by Tukey's HSD post hoc tests. Changes in the total osmolyte concentration across salinities were analysed with linear regression to calculate the critical salinity S_{crit}. If the data did not meet assumptions of normality and homogeneity, either transformations (logarithmic, square root, Box-Cox) were applied or the non-parametric Kruskal-Wallis-Test, followed by Nemenyi post hoc tests. All p-values < 0.05 were considered significant.

2.2 Experiment 2: Reciprocal transplant experiment

2.2.1 Animal collection and maintenance

Sea stars from List on the island of Sylt (55°01'36.6"N 8°25'53.9"E) were collected by hand from oyster beds at low tide in August 2016 and directly transported in an aerated cooling box (Pulsator, Zebco) to the laboratory facilities of the GEOMAR Helmholtz Centre for Ocean Research, Kiel. They arrived at a salinity of 28.2 PSU and a temperature of 18.4 °C and were transferred to aerated 80 l tanks for an acclimation period to laboratory conditions of one week. The salinity was adjusted to 32 PSU during that week and kept at 16 °C and a 12:12 h light:dark cycle. Animals from Kiel Fjord (54°19'45.2"N 10°08'54.9"E) were collected around a pier at a depth of 2-3 m by snorkelling. The salinity was 15.7 PSU during sampling with a temperature of 17.1 °C. Animals were directly transferred to aerated 80 L tanks for one week with a salinity of 16 PSU and a temperature of 16 °C. The seawater for both populations was pumped from Kiel Fjord, treated with UV light (Strahler UV-C Water sterilizer 500) and filtered with a serious of three filters (50 µm, 20 µm and 5 µm). Water was

prepared always one day before water exchange to let the temperature adjust to the experimental conditions, while salinity was adjusted either by salt (Tropic Marine Sea Salt) or dH_2O addition. Alkalinity was correct by addition of $NaHCO_3$ according to the control salinities. Ammonium concentrations were monitored daily using colour scale measurements (JBL GmbH & Co. KG) for 1-2 randomly selected tanks and concentrations never exceeded 0.05 mg/L. Salinity and temperature in each tank were monitored every day (WTW Cond3110) for the first week and every second day in the following weeks.

2.2.2 Experimental set-up and treatments

After the acclimation period, four treatments with eight 10 l aquaria each were set up: the control treatments Kiel 16 with a stable salinity of 16 PSU and Sylt 32 with a stable salinity of 32 PSU; and the cross-acclimation treatments Kiel 32 with a gradually increasing salinity from 16 to 32 PSU and Sylt 16 with a gradually decreasing salinity from 32 to 16 PSU. Each replicate tank held a small (between 2.5 and 4.9 g, mean 3. g) and a slightly bigger sea star (5.2 and 8.7 g, mean 6. g), resulting in 16 animals per treatment. Animals were dispersed between treatments in a way that the mean biomass in each tank and the standard deviation was similar within and between treatments. Water quality was maintained through water exchanges every second day, simultaneously adjusting the salinity of the acclimation treatments by 1 PSU. After 4 weeks the final treatment level was reached (acclimation phase), followed by 4 weeks of stable salinities (stable phase). The timeline of the experiments including sampling points is displayed in Figure 5. Two days after the treatment had been initiated, *ad libitum* feeding with the mussel *Mytilus edulis* had been started. Mussels in different size classes according to the size of the sea stars that shared an aquarium were individually chosen. It was shown that larger sea stars eat larger mussels, therefore no food competition was expected between small and big animals (Sommer *et al.,* 1999).

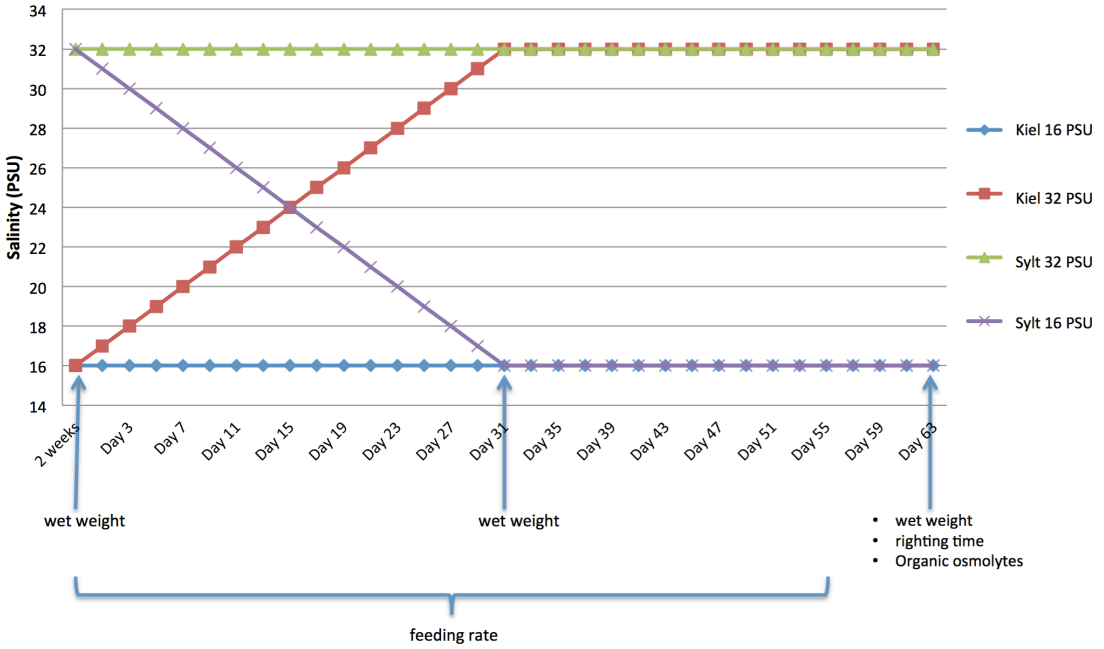

Figure 5: Timeline of the reciprocal transplant experiment to determine local adaptation to salinity in *Asterias rubens*. Salinity changes in the different treatments (blue Kiel 16 PSU, red Kiel 32 PSU, green Sylt 32 PSU, purple Sylt 16 PSU) is plotted against time. Arrows and brackets indicate sampling points and planned measurements.

2.2.3 Weight and feeding rate

All animals were weighed separately at three time points throughout the experiment: at the beginning of the experiment (initial weight), after the acclimation phase (after acclimation) and after the stable salinity phase (end weight). For that, animals were gently tapped on paper tissue to remove access water and placed on a scale (Sartorius Lab Instruments GmbH LC2215).

Empty shells of *Mytilus edulis* were collected weekly from each tank and shell lengths were measured using an automatic caliper. In a currently conducted long-term study, ten mussels from Kiel Fjord in the range of approximately 1 cm to 9 cm are collected weekly to create calibration curves of the ratio of shell length to dry weight over different seasons and years (Ulrike Findeisen). With the formula of those specific calibration curves that were calculated for the time mussels were collected for feeding, the consumed biomass was calculated from empty shells. R^2 values for calibration curves ranged between 0.765 and 0.951. We could not differentiate reliably between mussel consumption of small and big sea stars that shared a tank, thus feeding rates were calculated per tank. For statistical analysis, feeding rates of the stable salinity phase were added up per tank and divided by the total sea star biomass per tank at the end of the experiment.

2.2.4 Righting time

After the stable salinity phase, righting time was measured as the time it takes an individual sea star to return to its oral side when placed on its aboral side. Therefore, animals were carefully detached from the aquarium wall and placed on their aboral side in the middle of the aquarium so that they were not able to use any corner or wall as support. The process was considered finished only when all five arms touched the ground. If animals showed no sign of successful turning, measurements were stopped after 15 min. Righting time was assessed four times for each individual and in a random order across treatments. No increase or decrease in righting time was observed with repetition of the procedure. For statistical analysis, righting time per individual was divided by the end weight of the animal and expressed in seconds per g wet weight.

2.2.5 Metabolic profiling

The same protocol as described in 2.1.3 was followed.

2.2.6 Statistical analysis

All statistical analyses and graphical display of results were conducted with the R software (Version 3.4.0) implemented in Rstudio (Version 0.98.1083). Single sea stars were regarded as units of replication. Normality of data and homogeneity of variances were assessed graphically prior to applying the Shapiro-Wilks-W Test and the Levene's Test, respectively. Two-way ANOVA was applied for analysis of weight, feeding rate, righting time and single osmolyte concentrations followed by Tukey's HSD post hoc tests. If the data did not meet assumptions of normality and homogeneity, either transformations (logarithmic, square root, Box-Cox) were applied or the non-parametric Kruskal-Wallis-Test, followed by Nemenyi post hoc tests. All $p < 0.05$ were considered significant.

2.3 Population genetics

2.3.1 Primer design

For *Asterias rubens*, one microsatellite was already available from Harper and Hart 2005. Additionally, 29 were designed from transcriptomic data and tested for genotyping (appendix Table 11).

One publicly available transcriptome from gonad tissue was downloaded from NCBI (PRJNA236087) (81470 contigs) and a second transcriptome obtained from tube foot tissue was provided directly by Patrick Flammang (Hennebert *et al.,* 2014, 2015, PRJNA268905) (97945 contigs). As both data sets were used separately for primer design and yielded different results, it will be referred to the gonad transcriptome and the tube foot transcriptome from here on.

With the command line version of tandem repeats finder (TRF Version 4.09), contigs were automatically scanned for repetitive motifs (Settings: 2 7 7 80 10 50 500 –f-d-m) (Benson *et al.,* 1999). 8518 hits were found for the gonad transcriptome and 8279 hits for the tube foot transcriptome. Repeats were then filtered manually to obtain motifs that were di-, tri- or tetra-nucleotides, repeated at least 10 times. Microsatellite repeats that were found in more than one contig were excluded, as well as motifs that had no flanking sequences for primer design. In total, 15 sequences from the gonad transcriptome were chosen for primer design using the online interface of Primer3web (Version 4.0.0) (default settings except Max tm difference 1, GC content 30-70 %, Product size: 100-130, 150-170, 180-200) (Untergasser *et al.,* 2012, Koressaar and Remm 2007). Primers were designed to amplify products of three different length classes to later combine primer pairs in the same PCR reaction. The 5' end of each forward primer was labelled with a fluorescent dye (FAM and HEX used).

For the tube foot transcriptome, 14 sequences were chosen for primer design. The settings were the same as for the tube foot transcriptome, except that here only products of a maximal length of 130 bp were chosen to minimize the risk that products span intron-exon boarders.

As more than half of the primers designed from the gonad transcriptome did not amplify any product, sequences for the second trial were analyzed in more detail beforehand. Transcriptomic contigs containing microsatellites were blasted against the genome of the bat star *Patiria miniata* and the crown of thorns starfish *Acanthaster planci* acquired from Echinobase (http://www.echinobase.org last accessed June 2017, Cameron *et al.,* 2009). Although both sea stars belong to different orders than *Asterias rubens*, all contigs could be aligned. Gene models did not cover the whole genome and most contigs aligned outside annotated regions while some where located within exons. Using Exonerate (Slater and Birney 2005) the intron and exon structure was predicted for the transcriptomic data. If the designed amplification product including primers spanned an intron exon boarder, it was excluded. Additionally, we used the transcriptomic contigs to predict open reading frames

(ORF) with ORFfinder from NCBI where only for 3 from 17 sequences were found to be within ORFs (Wheeler *et al.,* 2003).

6 primers from the gonad transcriptome and 8 from the tube foot transcriptome amplified reliably, and 7 in total were polymorphic and can be used for analysis (Table 1).

Noticeable, di-nucleotide repeats were only found in the tube foot transcriptome and only in extremely low number (2, while one was present in 9 different contigs). Usually, di-nucleotide motifs are the most prevalent microsatellites (Fan and Chu 2007) but apparently very rare in *Asterias rubens* which was already suggested by Harper and Hart 2005 after conducting Southern Blots on *A. rubens* DNA. For the Pacific sister species *Asterias amurensis* on the other hand, 8 from 27 published microsatellites are di-nucleotide repeats (Richardson *et al.,* 2012). It could be argued that di-nucleotide repeats cannot be expected in a transcriptome as a deletion or duplication would lead to a reading frame shift in coding regions. Nevertheless, many tetra-nucleotide repeats that impose the same problems were found and used for microsatellite design. Furthermore, only in the tube foot transcriptome but not in the gonad transcriptome mono-nucleotide repeats were found.

2.3.2 Sample collection and DNA extraction

Asterias rubens from 14 populations were sampled between 2000 and 2016 by 13 different collaborators (Table 2, Figure 6). Approximately 20 tube feet of each animal was cut with dissection scissors and preserved in RNA-later, or directly frozen at - 20 °C. Usually, this method is only minimally invasive to the sea stars and they survive. Dissecting instruments were disinfected with ethanol after each sample. Size of collected animals ranged from 3 – 25 cm diameter.

DNA was extracted with the QIAGEN Blood and Tissue Kit using the protocol for animal tissue with slight modifications. A microspoon of tube feet was pestled in lysis buffer with 20 µl proteinase K and incubated 2-3 h in a programmed FlexCycler block (Biozym, Block assembly T48) until all tissue was completely dissolved. Elution was performed using 70 µl elution buffer and an incubation time of 5 min at room temperature. DNA concentration and contamination were tested for a few samples of each population with the spectrophotometer nanodrop Nd-1000 and the NanoDrop software version 3.7.1 (preQLab Biotechnologie GmBH).

PCR reactions were performed according to the protocol in Table 3 (Applied Biosystems Inc Veriti™ Thermal Cycler). After, 1 µl PCR product was mixed with Hi-Di formamide and the size standard GeneScan™ 350 ROX™ (1:40) (both ThermoFischer Scientific, Schwerte, Germany) in a final volume of 10 µl. Initial denaturation was performed in a PCR cycler (Analytik Jena Flexcycler) at 95 °C for 2 min and samples were then separated with capillary electrophoresis on an ABI3130 Genetic Analyser (Applied Biosystems Inc). Resulting allelic lengths were analysed using the genotyping software GeneMarker AFLP (Version 1.91, Biogene Ltd, Kimbolton, UK).

Table 1: List of microsatellite primers used for this study with amplified repeat motif and number of detected alleles in 14 populations of *A. rubens*.

Primer	motif	# alleles
Ar1	[CAG]16	2
Ar5	[TGTC]13	4
Ar14	[TGTT]12	12
Ar17	[TGTC]13	4
Ar19	[CAG]29	6
Ar26	[TCT]13	4
Ar29	[AG]16	13

Table 2: Information on sampled populations for assessing the genetic population structure of *Asterias rubens* in the North Atlantic. The location, date and sample size as well as the mean habitat salinity can be found. For salinity data reference see appendix **Table 6**. The responsible person and the method of collection are listed.

Population	Population Ident.	Coordinates	Sampling date	Salinity	Salinity	Salinity	Water depth	Sampling method	Sample size	Collector
Kiel, Germany	K	54.329103, 10.148522	April 2016	15.89 PSU	15.89 PSU	15.89 PSU	2 m	snorkelling	31	Lara Schmittmann
Schilksee, Germany	Sch	54.424487 10.174697	May 2016	15.89 PSU	15.89 PSU	15.89 PSU	2 m	snorkelling	17	Fabian Wolf, Isabel Grieveson
Sylt, Germany	S	55.020963 8.440199	April 2016	30 PSU?	30 PSU?	30 PSU		dredging	24	AWI Sylt
Kattegat	Kat	56°24,67' N 11°21,46' E	June 2014	32 PSU	32 PSU	32 PSU	24 m	dredging	16	Rieke Findeisen
Helgoland, Germany	H	54.182747 7.891490	May 2016	32 PSU	32 PSU	32 PSU	20 m	dredging	19	AWI Helgoland
Bear cove (Nova Scotia) Canada	B	44.536465 -63.540516	August 2002	31 PSU	31 PSU	31 PSU	?	?	5	Fiona Harper
Quebec, Canada	Q	50.233333 -63.600000	August 2000	32 PSU	32 PSU	32 PSU	?	?	24	Fiona Harper
Reykjavik, Iceland	Ice	64.151155 -21.942407	July 2016	35 PSU	35 PSU	35 PSU	1 m at low tide	hand	14	Trystan Sanders, Josephine Watson
Kristineberg, Schweden	Krist	58.248889, 11.441111	July 2016	24 PSU	24 PSU	24 PSU	1-3m	snorkelling	20	Isabel Casties
Oslo, Norway	O	59.903375, 10.744465	August 2016	25.2 PSU	25.2 PSU	25 PSU	2 m	net	13	Felix Mittermayer
Tjärnö, Norway	T	58.875613 11.145748	October 2016	26.23 PSU	26.23 PSU	26.23 PSU	2 m	net	31	Felix Mittermayer
Bergen, Norway	Be	60.400683 5.300411	October 2016	22 PSU	22 PSU	22 PSU	?	Diving	30	David Thor
Vattenholmen Deep, Sweden	VD	58.811300, 11.159765	?	26-32?	26-32?	30 PSU	25 m	Diving	15	Swantje Enge
Vattenholmen Shallow, Sweden	VSH	58.811300, 11.159765	?	26.23 PSU	26.23 PSU	26.23 PSU	5 m	Diving	22	Swantje Enge

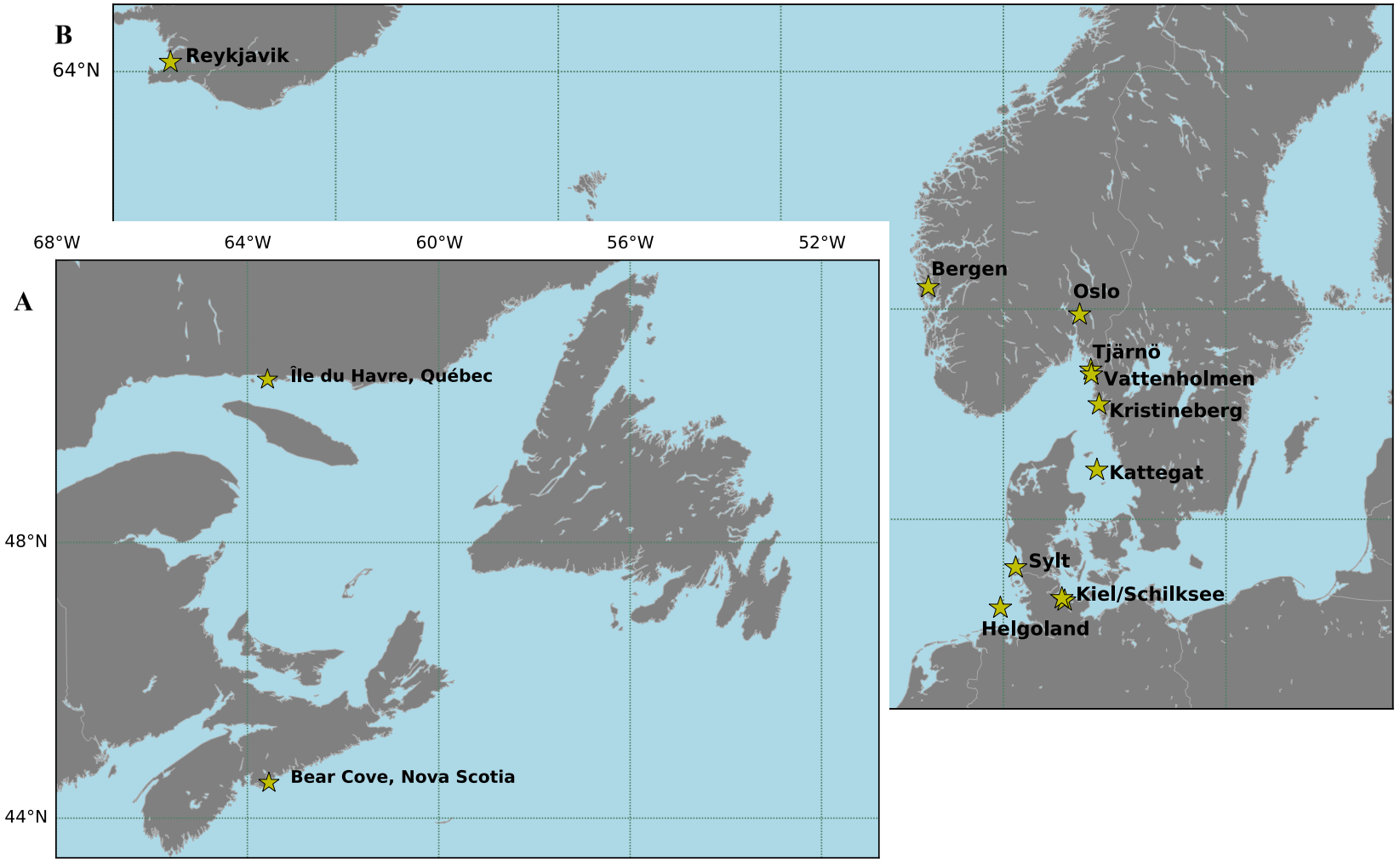

Figure 6: Sample sites of *A. rubens* populations in the North Atlantic. A: Sampling sides on Canadian east coast. **B:** Sampling sites in Europe. See **Table 2** for exact coordinates.

Table 3: PCR mix and protocol for microsatellite amplification.

PCR mix		PCR protocol		
Multiplex PCR Mastermix 3 mM $MgCl_2$ (QIAGEN)	5 µl	Initial denaturation 95 °C		15 min
RNase free water	3 µl	Denaturation 94 °C		30 sec
Primer forward (1 µM)	1 µl	Elongation 57 °C	24 cycles	90 sec
Primer reverse (1 µM)	1 µl	Annealing 72 °C		60 sec
DNA template	1 µl	Final extension 60 °C		60 min
Total volume	10 µl			

2.3.3 Data analysis

GENETIX was used to calculate pairwise F_{st} values after Weir and Cockerham (1984), allele frequencies and heterozygosities (Version 4.0.2) (Belkhir *et al.,* 1998). Deviations from Hardy-Weinberg equilibrium, linkage disequilibrium (LD) as well as p-values associated to F_{st} statistics were tested with the online version of GENEPOP for both microsatellite loci and populations (Version 4.2) (Rousset 2008). All loci were tested for null alleles with the R software (Version 3.4.0) package PopGenReport (Adamack and Gruber 2014). Allelic richness as the mean number of alleles per locus per population was assessed after resampling the populations to 15 individuals per populations, excluding populations with less than 15 individuals (Bear cove, Iceland and Oslo). Based on allele frequencies, a principal component analysis (PCA) was conducted using the R software package 'adegenet' (Jombart and Bateman 2008).

To assess the genetic population structure, genotypes were analysed with a Bayesian clustering algorithm within the STRUCTURE software (Version 2.3.2) (Pritchard *et al.,* 2000). Settings were chosen according to the guidelines of Porras-Hurtado and colleagues (2013). There is no previous information about admixture or allele correlation levels in *Asterias rubens*. Therefore, both the genetic admixture and the no-admixture model were run assuming correlated allele frequencies. Populations were set as prior to increase the chance of detecting population structure with a small number of markers. Clusters from $K = 1$ to $K = 10$ were tested while each calculation was repeated 10 times with a burnin length of 1000 followed by 10 000 iterations of MCMC (Markov Chain Monte Carlo). With the online software Structure Harvester (Earl and VonHoldt 2012) and the implemented Evanno (2005) method, the most likely number of clusters K was inferred by analysing the increase in log-likelihood.

A phylogeographic analysis was conducted by calculating a neighbour joining (NJ) tree with Cavalli-Sforza's and Edwards chord distance (as suggested by Takezaki and Nei 1996 for microsatellite data). All programs were implemented into the package PHYLIP (Version 3.695). Prior to calculation of the distance matrix with GENDIST, 1000 bootstrap runs were performed on allele frequencies with SEQBOOT. NEIGHBOUR created NJ trees based on the bootstrap distance matrices and the most likely consensus tree was calculated based on multiple trees with CONSENSE and visualized with DRAWTREE.

The online program IBDWS (Isolation by distance, Version 3.23) calculated the correlation of genetic and geographic distance based on a distance matrix of F_{st} values and approximate geographic distance between populations in km (https://www.freemaptools.com/ accessed 01.04.2017). Four different linear models (Mantel tests) that differ in the way input data is transformed were applied. Additionally, Pearson's correlation and linear regression models were applied to F_{st} and geographic distance data with the R software (Version 3.4.0) (Dutilleul *et al.,* 2000). As suggested by Rousset (1997), a correlation was performed between $F_{st}/(1-F_{st})$ and the logarithm of the geographical distance. To detect isolation by environment (IBE), Pearson's correlation and linear regression models were applied to F_{st} and environmental distance data, in this case differences in salinity. Mean habitat salinity was estimated for each population from different sources (appendix Table 6).

3 Results

3.1 Experiment 1: Acclimation of *Asterias rubens* from Kiel to different salinities

A. rubens from a Baltic Sea population that experience strong salinity fluctuations and a mean annual salinity of 16 PSU were acclimated to salinities of 8-28 PSU. Sea stars in the 8 PSU treatment had a distinctively swollen body (Figure 7) and stopped activity as soon as a salinity of 10 PSU was reached. Although we decided to not further decrease the salinity, all replicate animals from this treatment died after 7-19 days at 10 PSU. One animal from the 12 PSU treatment died after one month at 12 PSU. It had consumed notably little food compared to the other replicate animals.

Twenty-six metabolites were quantified with ^{1}H-NMR spectroscopy. 5 compounds significantly changed in concentration with salinity and where thus considered organic osmolytes: the amino acids alanine, glycine and phenylalanine, and the organic compounds betaine and taurine (Figure 9). From a second experiment (see methods 2.2 and results 3.2), 7 other compounds were found to change with salinity and therefore also taken into account to calculate S_{crit}, namely the amino acids leucine, lysine, methionine, threonine, tyrosine and valine; and the organic compound methylamine. By calculating a linear model of decrease of osmolyte concentration with decreasing salinity the critical salinity for *A. rubens* could be estimated at $y = 0$ (Figure 8) (p-value < 0.001, $R^2 = 72.99$). S_{crit} was found to be slightly below 10 PSU.

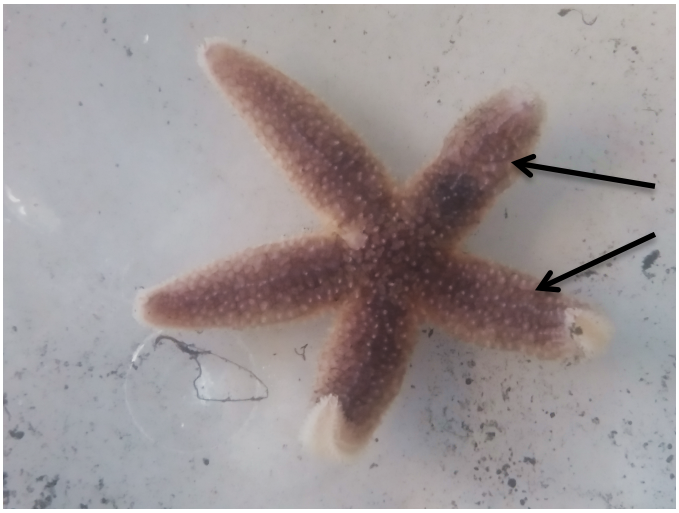

Figure 7: Sea stars right after water exchange and shortly before death in 9 PSU. Black arrows mark swollen parts of the arms.

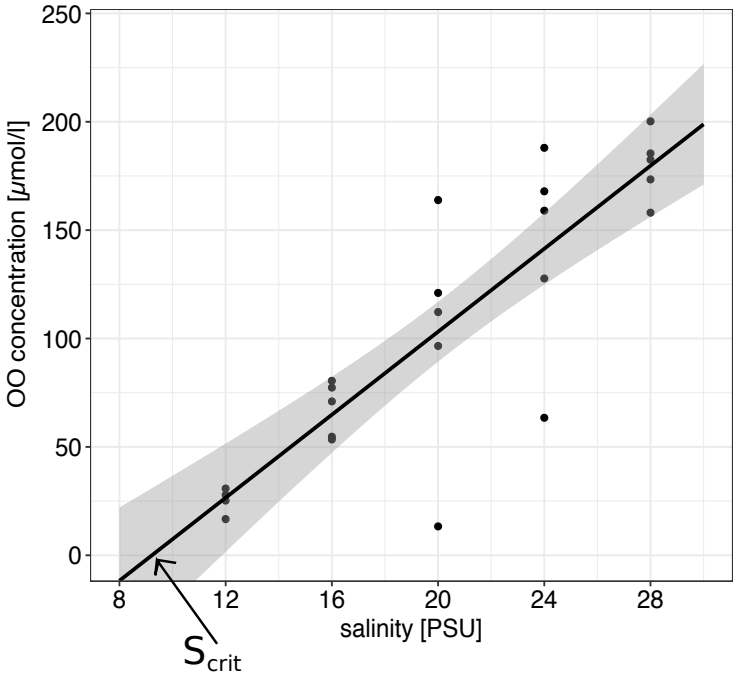

Figure 8: Mean total organic osmolyte concentration of *A. rubens* from the Baltic Sea in salinities of 12-28 PSU. Dots indicate mean concentrations of replicates. Total osmolyte concentration consisted of alanine, betaine, glycine, leucine, lysine, methionine, methylamine, phenylalanine, taurine, threonine, tyrosine and valine. Regression line with estimation of S_{crit} . = -88.300 + 9.572 x, R^2 = 72.99, p-value < 0.001.

The total osmolyte concentration in 28 PSU was around 175 µmol/l and decreased linearly with salinity as expected for osmoconformers (p-value < 0.001) (Figure 9, appendix Table 7). The main osmolyte utilized by *A. rubens* was found to be glycine, which contributed with up to 90 % to the total OO pool and thereby drove the total concentration. Its proportion of the total pool decreased from around 90 % in 28 PSU to 50 – 60 % in 12 PSU. Therefore, the relative content of the other osmolytes increased, especially from alanine, betaine, lysine and taurine.

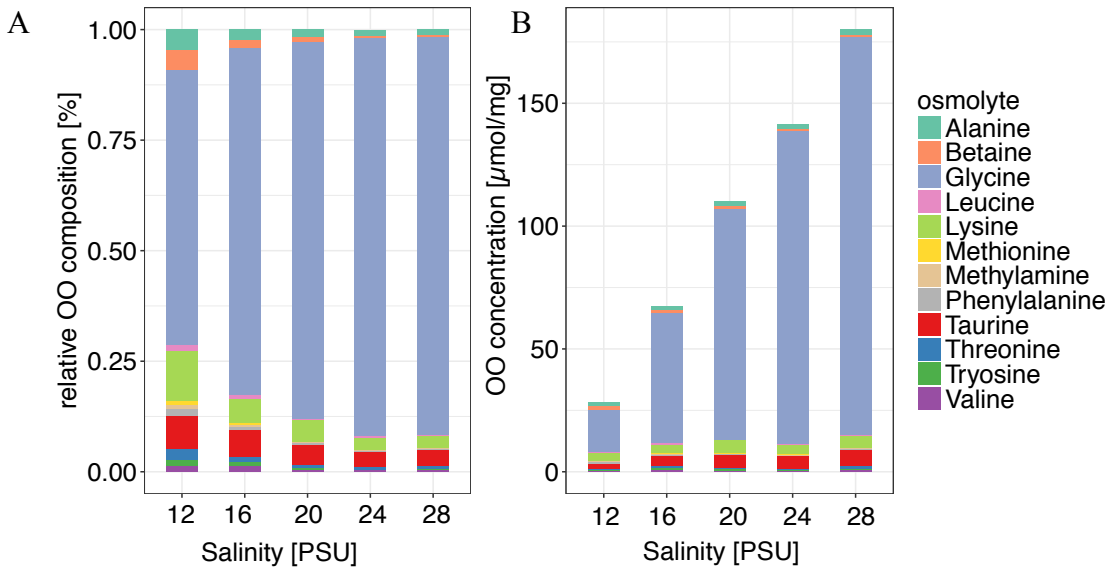

Figure 9: Composition of organic osmolytes utilized by *Asterias rubens* in salinities of 12-28 PSU. Compounds quantified by ^{1}H-NMR spectroscopy: alanine, betaine, glycine, leucine, lysine, methionine, methylamine, phenylalanine, taurine, threonine, tyrosine and valine. A: Relative composition of intracellular osmolytes (%). B: Absolute concentration of intracellular osmolytes per mg tissue (µmol mg^{-1}).

To visualize the difference between treatments, a PCA was conducted on osmolyte concentrations. The 12 compounds that vary with salinity were chosen for the analysis. More than 40 % of the variance can be explained by the first and second dimension of the PCA (Figure 10). None of the treatments was clearly separated from the others, while sea stars from 12 PSU built the narrowest cluster and overlapped only slightly with the 28 PSU cluster.

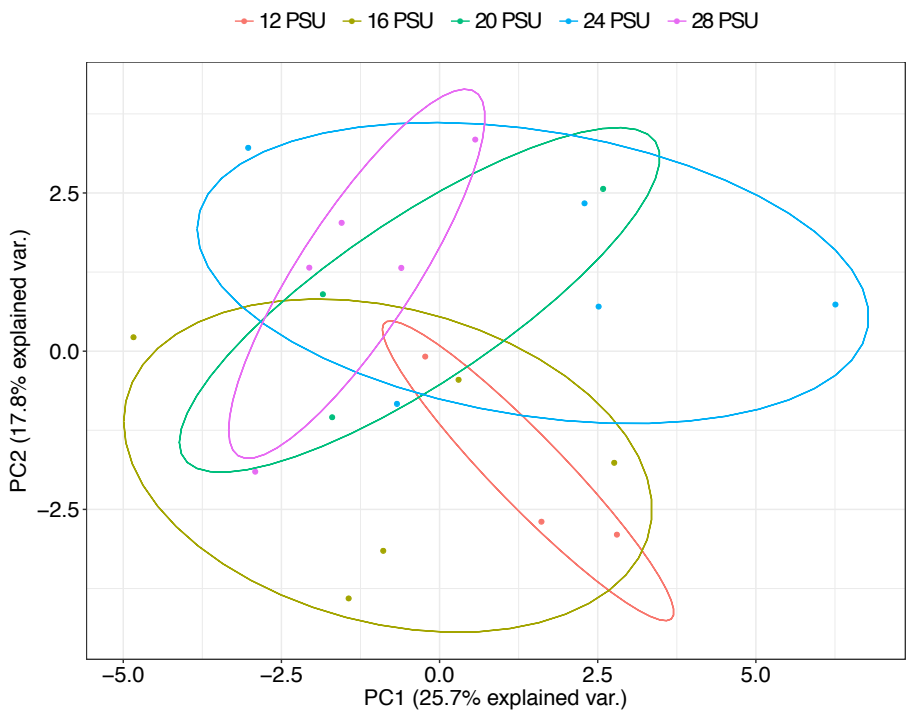

Figure 10: PCA of main organic osmolyte concentrations. Analysis based on alanine, betaine, glycine, leucine, lysine, methionine, methylamine, phenylalanine, taurine, threonine, tyrosine and valine. Colours indicate different treatments: 12 PSU (red), 16 PSU (light green), 20 PSU (dark green), 24 PSU (blue), 28 PSU (purple).

3.2 Experiment 2: Reciprocal transplant experiment

The experiment was conducted on two size classes of sea stars (small ~ 3 g and big ~ 6 g). Between treatments, there was no significant difference within the size class groups in the beginning of the experiment. Due to changing salinity conditions during the first 4 weeks of the experiment, we could not conduct statistical analyses on this time period. During the second part with stable salinity, the mean absolute weight change was largest for small and big sea stars from Kiel in 32 PSU (mean + 1.75 and + 2.61 g) (Figure 11). Animals from Sylt in 16 PSU even lost weight (mean - 0.42 and - 1.28). Prior to statistical analysis, the absolute weight change was divided by the sea star wet weight at the end of the experiment to correct for size differences between animals. Salinity and population origin both significantly affect weight change during this stable salinity phase (both p-value < 0.01) (Figure 12, appendix Table 8).

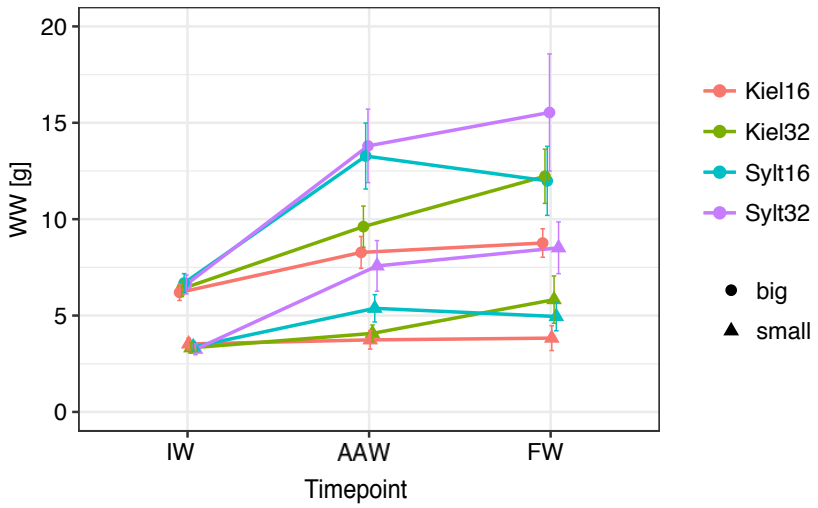

Figure 11: Wet weight (WW) of sea stars throughout the experiment. Animals were measured individually at three time points: at the beginning of the acclimation period = initial weight (IW), at the end of the acclimation period = after acclimation (AAW), and at the end of the experiment = final weight (FW). Colours indicate the different treatments: Kiel 16 PSU (red), Kiel 32 PSU (green), Sylt 16 PSU (turquoise), Sylt 32 PSU (purple). The two size classes are marked by different symbols: big (circle), small (triangle).

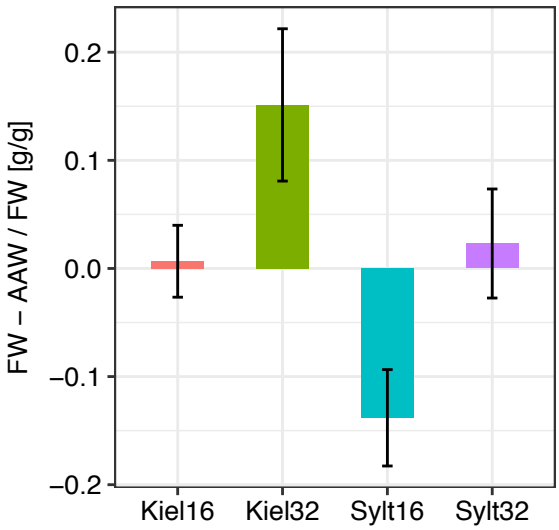

Figure 12: The mean weight change between end of the acclimation period (AAW) and the end of the experiment (FW) normalized for FW is displayed for the four treatments.

Sea stars kept in 32 PSU fed 2-3 times more than in 16 PSU, while animals from Kiel had higher feeding rates per g wet weight than animals from Sylt in 16 PSU (Figure 13). Salinity had a significant effect on feeding rate (p-value < 0.01) while population origin had not (appendix Table 8).

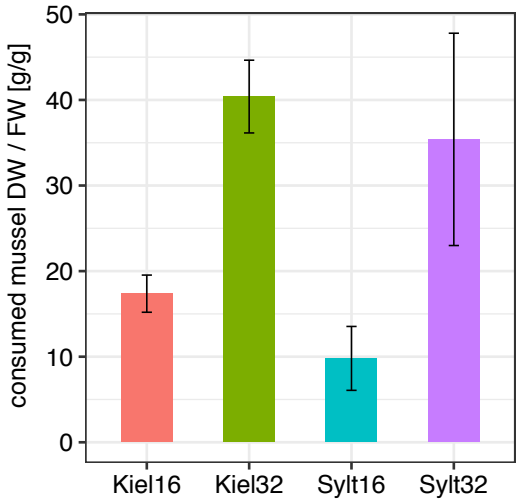

Figure 13: Mean total consumption of mussel tissue dry weight (DW) normalized for sea star weight (FW) during the stable salinity phase. Empty shells were measured and consumed mussel tissue dry weight was calculated from calibration curves. Total consumption per tank after the acclimation period was divided by the total sea star biomass per tank.

The mean righting time of *A. rubens* was affected by population origin, as animals from Kiel needed half the time to turn from their aboral to their oral side than animals from Sylt (p-value < 0.0001) (Figure 14, appendix Table 8). Higher salinities of 32 PSU decreased righting time significantly (p-value < 0.01). When normalized for weight, small animals showed a slower righting response per g tissue mass, which was significant (p-value < 0.01).

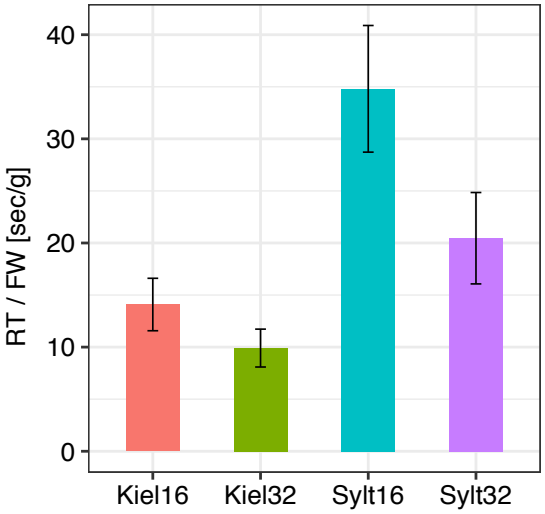

Figure 14: Mean righting time (RT) normalized by weight of animals (FW).

Twenty-six metabolites were quantified with ^{1}H-NMR spectroscopy. From that, 11 were identified as osmolytes as their concentration changes significantly with salinity: the amino acids alanine, glycine, leucine, lysine, methionine, phenylalanine, threonine, tyrosine and valine; and the organic compounds methylamine and taurine (Figure 15). As in the first experiment, glycine was the osmolyte that determined the total concentration with a proportion of 75-80 % of the total pool. The sum of all osmolytes was significantly affected by the two factors salinity (p-value < 0.001) and population origin (p-value < 0.01) separately and by the interaction term (p-value < 0.001) (appendix Table 9, Table 10).

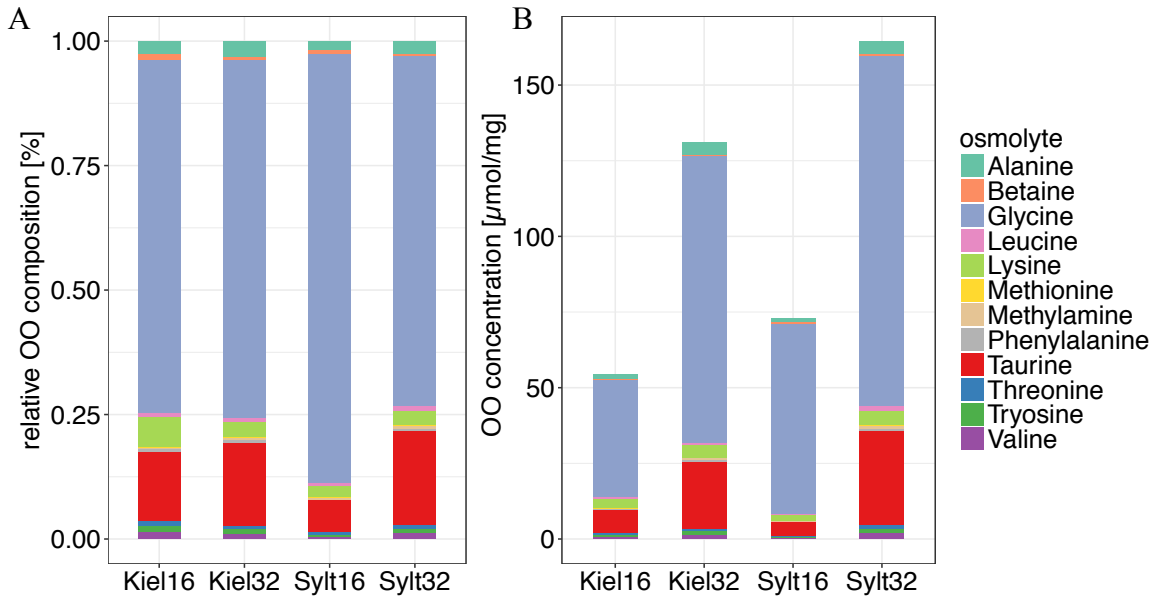

Figure 15: Composition of organic osmolytes utilized by *Asterias rubens*. Compounds quantified by ^{1}H-NMR spectroscopy. **A**: Relative composition of intracellular osmolytes (%). **B**: Absolute concentration of intracellular osmolytes per mg tissue (µmol mg^{-1}).

To visualize the difference between treatments, a PCA was conducted on osmolyte concentrations. The 12 compounds that vary with salinity were chosen for the analysis. More than 80 % of the variance can be explained by the first and second dimension of the PCA plot (Figure 16). Animals from Sylt in 32 PSU clearly differ from both populations in 16 PSU, while the latter overlap. Sea stars from Kiel in 32 PSU show a high variability and overlap with all other treatments.

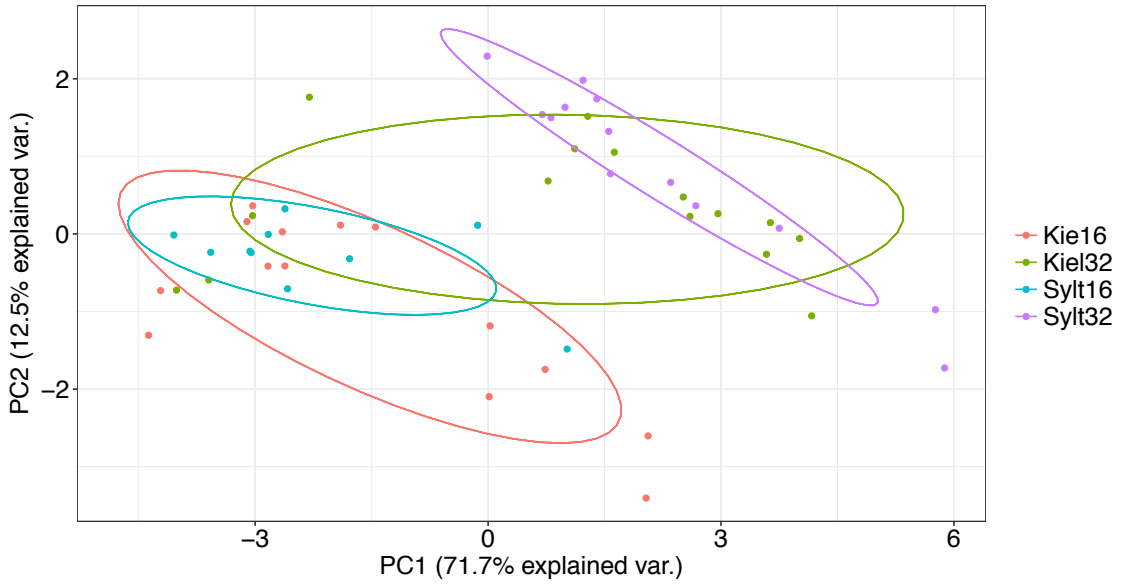

Figure 16: PCA of main organic osmolyte concentrations. Analysis based on alanine, betaine, glycine, leucine, lysine, methionine, methylamine, phenylalanine, taurine, threonine, tyrosine and valine. Colours indicate the different treatments: Kiel 16 PSU (red), Kiel 32 PSU (green), Sylt 16 PSU (turquoise), Sylt 32 PSU (purple).

3.3 Population genetics

To analyse the population structure of *A. rubens* in the North Atlantic, microsatelliltes were developed from two available transcriptomes. From 28 identified microsatellite loci (appendix Table 11), 14 could be genotyped with the designed primers, while only 7 loci were polymorphic and suitable for analyses (Table 1). We were not able to apply the previously published primer pair Ar50 (Harper and Hart 2005) to any of our samples. A total of 310 individuals from 14 populations of *A. rubens* was genotyped applying the 7 developed microsatellite markers. Due to unsuccessful DNA extraction from some individuals, 29 samples were excluded from the analyses, thus resulting in a final number of 281 genotypes used for analysis.

A deficit in heterozygosity was detected with GENEPOP over all loci and populations (p-value < 0.01), with the loci Ar 5, Ar 26 and Ar 29 being significant (p-values < 0.05). Only for locus Ar 19 a heterozygote excess was detected (p-value < 0.001) while the overall test was not significant. Linkage disequilibrium was suggested for the loci Ar 5 and Ar 17 (p-value < 0.001).

3.3.1 Population structure

A Bayesian clustering algorithm was applied to genotype data with the STRUCTURE software (Pritchard *et al.,* 2000) to reveal population subdivision. As there is no prior knowledge about the degree of admixture between *A. rubens* populations, the no-admixture model was considered appropriate for this study (Porras-Hurtado *et al.,* 2013). Furthermore, it was also described useful to detect weak population structure (Pritchard *et al.,* 2000). Nevertheless, considering the close proximity of some populations (e.g. Schilksee and Kiel), admixture is very likely to occur and thus the admixture model was applied, too. Additionally, each analysis was performed with (Figure 18) and without (Figure 17) using the LOCPRIOR setting with inferred population information (Hubisz *et al.,* 2009). This setting is expected advantageous in case of weak population structure (Porras-Hurtado *et al.,* 2013) which was confirmed by our results that were much more pronounced with inferred sampling location information. The Evanno method implemented in the online tool Structure Harvester (Earl and vonHoldt 2012, Evanno *et al.,* 2005) indicated the most increase of log-likelihood for $K = 2$ cluster for both models without given population IDs (Figure 17). Only trends of separation were visible, while the no admixture model gave slightly more information than the admixture model. A clustering of the three Swedish populations Vattenholmen shallow, Kristineberg and Tjärnö was revealed as well as a separation of the Canadian population Québec. Differentiation was much more pronounced when populations were set as prior and the Evanno method revealed $K = 2$ clusters applying the admixture model and $K = 3$ clusters for the no admixture model (Figure 18). No clear trend of isolation by distance or a division of a Baltic and a North Sea cluster is visible. The admixture model suggests that all tested individuals belong to the same two clusters while for most populations one cluster is more representative than the other. The three Swedish populations Vattenholmen shallow, Tjärnö and Kristineberg can be separated from Bear Cove, Québec, Sylt, Bergen, Oslo, Vattenholmen deep, Kattegat and Kiel. The populations Iceland, Helgoland and Schilksee can not be assigned to one of the two groups and lie in between. The no admixture model shows a similar picture with more resolution due to the division into $K = 3$ clusters (Figure 18). Bear Cove, Quèbec, Sylt, Bergen Vattenholmen deep and Kattegat are assigned to almost only one cluster, while Kristineberg belongs almost completely to a second cluster. The populations Iceland and Helgoland are a mixture of the two clusters. A third cluster reveals similarities between Kiel and Oslo and also between Vattenholmen shallow and Tjärnö. The population from Schilksee has the greatest variety and similar proportions of all three clusters. It is striking, that the deep and shallow sea star populations from Vattenholmen are clearly

different in both models and less connected than to other populations that are geographically far away.

As for the STRUCTURE analysis, the NJ tree topology calculated from allele frequencies only revealed some divisions that were supported by bootstrap values > 60 %, suggesting a generally weak population structure in *A. rubens* (Figure 19). Nevertheless, the analyses support each other and detect similar groupings. No genetic difference can be found between Sylt, Bergen, Oslo, Vattenholmen deep, Kattegat, Schilksee and Kiel, which agrees with the STRUCTURE admixture model. The tree topology reveals a small but significant differentiation of the Canadian populations Bear Cove and Québec that could not be resolved by the STRUCTURE analysis. The NJ tree also supports the strong difference between the Swedish populations Vattenholmen shallow, Tjärnö and Kristineberg from the other populations, while additionally resolving the distance within these three populations. The two populations characterized by being most far away from the continent, Helgoland and Iceland, can be clearly differentiated from the other populations. The subdivision that was found by STRUCTURE and groups Oslo and Kiel was not detected with the tree topology.

Wright's F-statistics were applied to calculate pairwise differentiation between populations. F_{st} values varied from 0-0.25814, while significant differentiation was confirmed by p-values corrected for multiple testing after Benjamini and Hochberg (1995) (Table 4). The cluster of Kristineberg, Vattenholmen shallow and Tjärnö was supported by no significant differences between those three populations, but between them and many other populations. The Canadian population Québec was clearly separated from the open ocean populations Iceland and Helgoland, the Swedish coast except Vattenholmen Deep and the Baltic population Schilksee. Sea stars sampled in Kiel differed from many sites, including Iceland, Helgoland, Vattenholmen shallow, Kristineberg and Tjärnö, but not from the Canadian populations. Interestingly, the extremely close by population of Schilksee (less than 10 km away) only differed significantly from Québec and Kristineberg. The difference between the two populations from Vattenholmen was manifested by significant differences of the deep-water population and the Swedish coast populations Vattenholmen shallow, Kristineberg and Tjärnö.

All four different Mantel test applied to analyse isolation by distance, revealed no significant correlation between genetic and geographic distance while the maximum R^2 was 2.07 %.

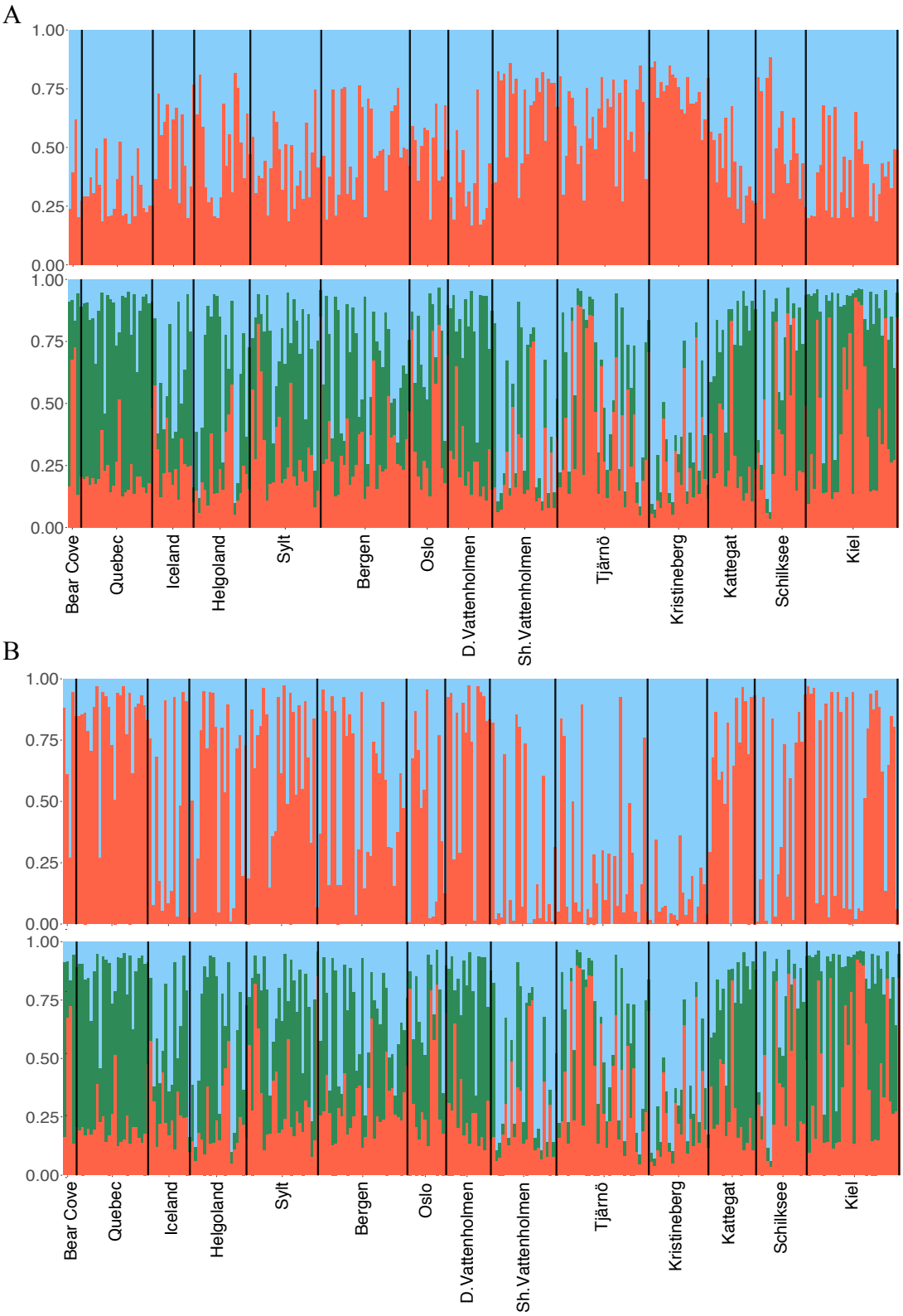

Figure 17 STRUCTURE plot of K = 2 and K = 3 for the admixture (A) and no admixture model (B) with correlated allele frequencies. No populations inferred. Each bar represents one individual sea star and displays its relative belonging to each of the two or three clusters, respectively. Colours indicate different clusters. Thicker, black bars divide the populations. Bear cove (N = 4), Quebèc (N = 24), Iceland (N = 14), Helgoland (N = 19), Sylt (N = 24), Bergen (N = 30), Oslo (N = 13), deep Vattenholmen (N = 15), shallow Vattenholmen (N = 22), Tjärnö (N = 31), Kristineberg (N = 20), Kattegat (N = 16), Schilksee (N = 17), Kiel (N = 31).

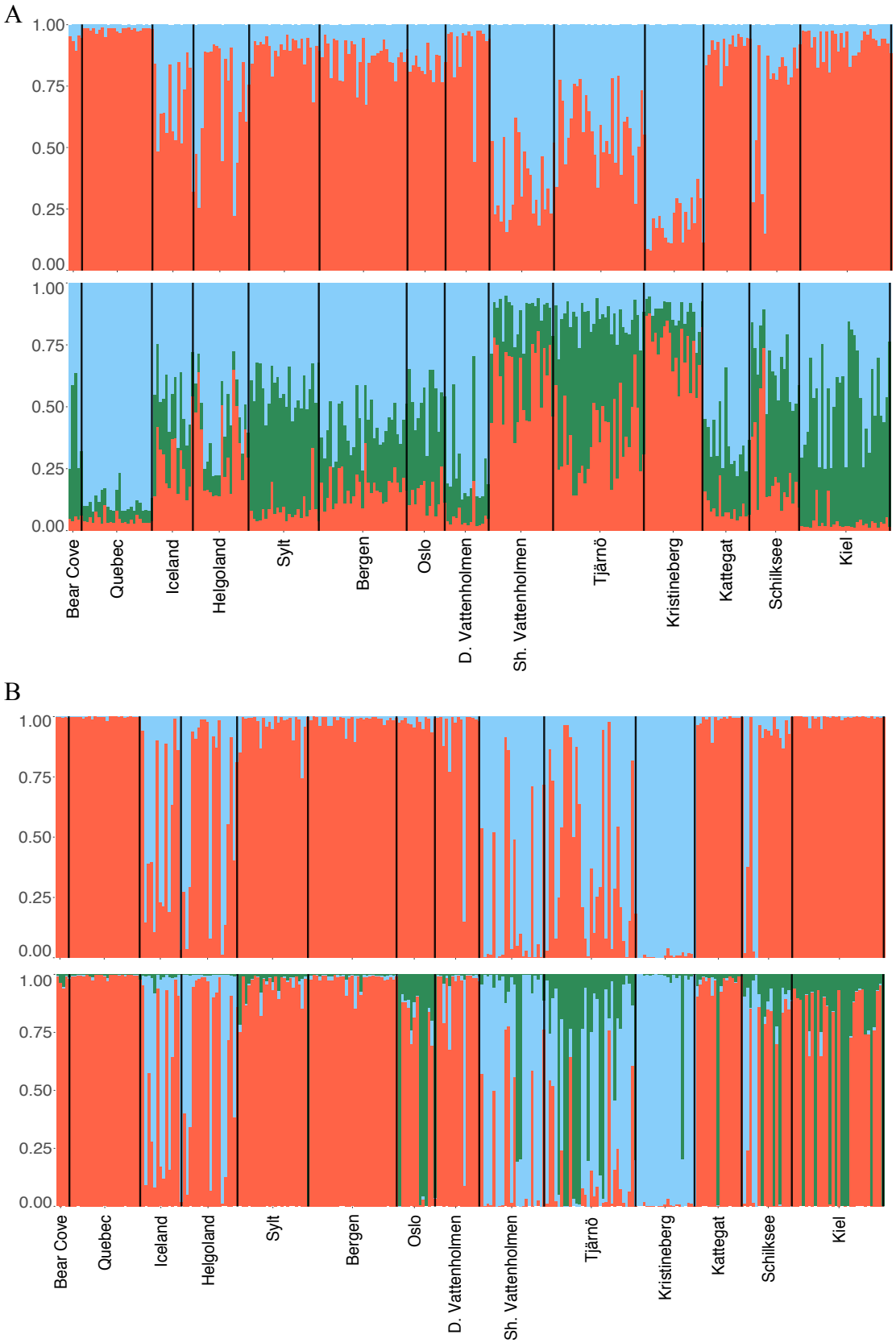

Figure 18: STRUCTURE plot of K = 2 and K = 3 for the admixture (A) and no admixture model (B) with correlated allele frequencies. Populations inferred. Each bar represents one individual sea star and displays its relative belonging to each of the two or three clusters, respectively. Colours indicate different clusters. Thicker, black bars divide the populations. Bear cove (N = 4), Quebèc (N = 24), Iceland (N = 14), Helgoland (N = 19), Sylt (N = 24), Bergen (N = 30), Oslo (N = 13), deep Vattenholmen (N = 15), shallow Vattenholmen (N = 22), Tjärnö (N = 31), Kristineberg (N = 20), Kattegat (N = 16), Schilksee (N = 17), Kiel (N = 31).

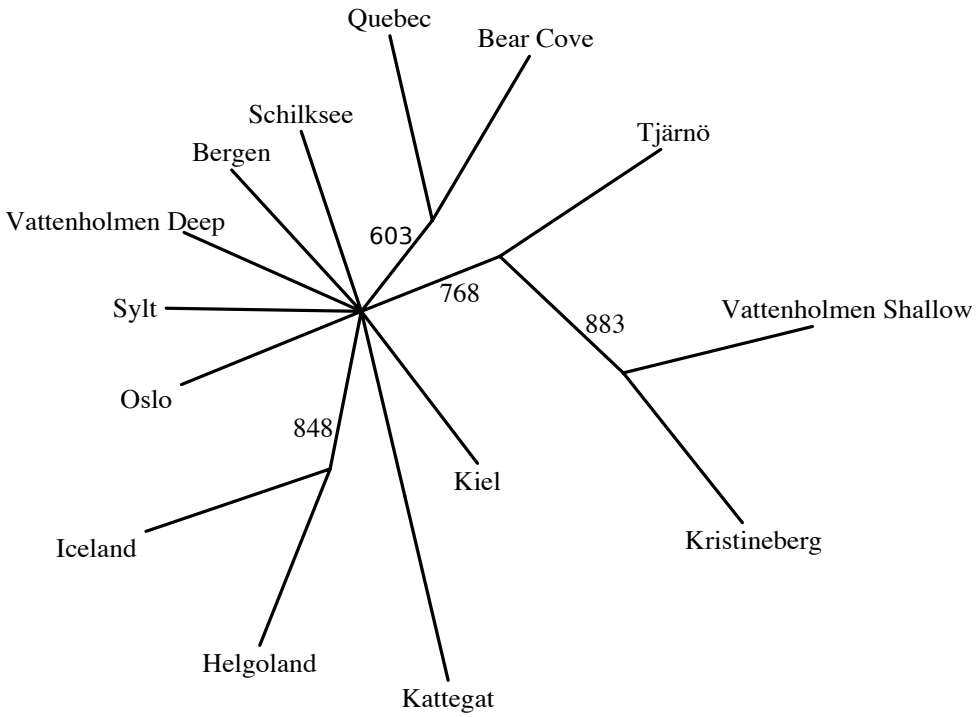

Figure 19: Neighbour-joining tree for 14 *A. rubens* populations from the North Atlantic. Analysis based on allele frequencies from 7 microsatellite loci and conducted using Cavalli-Sforza's and Edwards chord distance. Consensus type: majority rule and (mr/ml)

Table 4: Pairwise genetic differentiation of *A. rubens* populations from the North Atlantic. F_{st} values calculated after Weir and Cockerham (1984) in GENETIX (upper half of matrix), p-values calculated in GENEPOP and corrected after Hochberg *et al.,* for multiple testing (lower half of matrix). Negative F_{st} values were set to zero. For population abbreviations see **Table 2**.

	B	**Q**	**Ice**	**H**	**S**	**Be**	**O**	**D_VH**	**S_VH**	**T**	**Krist**	**Kat**	**Sch**	**K**
B		0	0,10688	0,08881	0,05623	0,02855	0,03958	0,00000	0,18090	0,07735	**0,25797**	0,16460	0,03095	0,00000
Q	0,96217		**0,12386**	**0,09308**	0,07417	0,04071	0,04976	0,00086	**0,19768**	**0,10043**	**0,25814**	0,02958	**0,05684**	0,03437
Ice	0,96217	**< 0,001**		0,00000	0,04422	0,08779	0,09271	0,06429	0,05846	**0,04443**	0,09763	0,06452	0,03941	**0,08150**
H	0,96217	**< 0,01**	0,96217		0,02338	0,06394	0,07030	0,04622	0,05679	0,03825	0,08551	0,03806	0,03236	**0,07562**
S	0,96217	0,07453	0,58800	0,96217		**0,06602**	0,06506	0,01850	**0,09428**	**0,03937**	**0,13799**	0,00071	0,02597	0,03923
Be	0,96217	0,14552	0,14490	0,47420	**< 0,05**		0,02680	0,02900	**0,11889**	**0,05537**	**0,16793**	0,05317	0,02863	**0,04716**
O	0,96217	0,96217	0,12816	0,74322	0,96213	0,96217		0,03642	0,08862	0,01913	**0,12951**	0,04561	0,00000	0,01242
D_VH	0,96217	0,96217	0,96217	0,96217	0,96217	0,96217	0,96217		**0,13859**	**0,06263**	**0,19621**	0,00750	0,02573	0,00538
S_VH	0,63307	**< 0,001**	0,47420	0,63307	**< 0,01**	**< 0,01**	0,47281	**< 0,001**		0,01886	0,00000	**0,11444**	0,03272	**0,12409**
T	0,96217	**< 0,001**	**< 0,05**	0,06618	**< 0,05**	**< 0,01**	0,96217	**< 0,05**	0,96217		0,05261	0,03911	0,00000	0,03972
Krist	**< 0,05**	**< 0,001**	0,08816	0,96217	**< 0,001**	**< 0,001**	**< 0,05**	**< 0,001**	0,96217	0,23031		**0,16843**	**0,07944**	**0,17943**
Kat	0,96217	0,96217	0,80001	0,96217	0,96217	0,96213	0,96217	0,96217	**< 0,05**	0,96217	**< 0,001**		0,01809	0,02336
Sch	0,96217	**< 0,05**	0,96217	0,18659	0,96217	0,17545	0,96217	0,96217	0,96217	0,96217	**< 0,05**	0,96217		0,01539
K	0,96217	0,74322	**< 0,01**	**< 0,001**	0,21313	**< 0,001**	0,96217	0,96217	**< 0,001**	0,11791	**< 0,001**	0,96217	0,96217	

A PCA performed on allele frequencies reveals no strong differences between populations at first glance (Figure 20). The first principle component has an explanatory power of 3.71 % while the second has a power of 2.68 %. There is no clear differentiation between populations although Kristineberg and Vattenholmen shallow are slightly separated in the second dimension. Strikingly, single individuals from different populations are obviously separated along PC1 forming three separate clusters. Analysing the loading of the different principal components it becomes apparent that only two loci with two alleles each contribute to the differentiation along the first dimension (appendix Figure 26). The involved loci are Ar5 and Ar17 which are in strong linkage disequilibrium (appendix Table 13). The second dimension is explained by a higher number of alleles (appendix Figure 27). In contrast to PC1, the most polymorphic primer Ar14 and Ar29 contribute to PC2 with two and one alleles, respectively, as well as Ar1, Ar19 and Ar27.

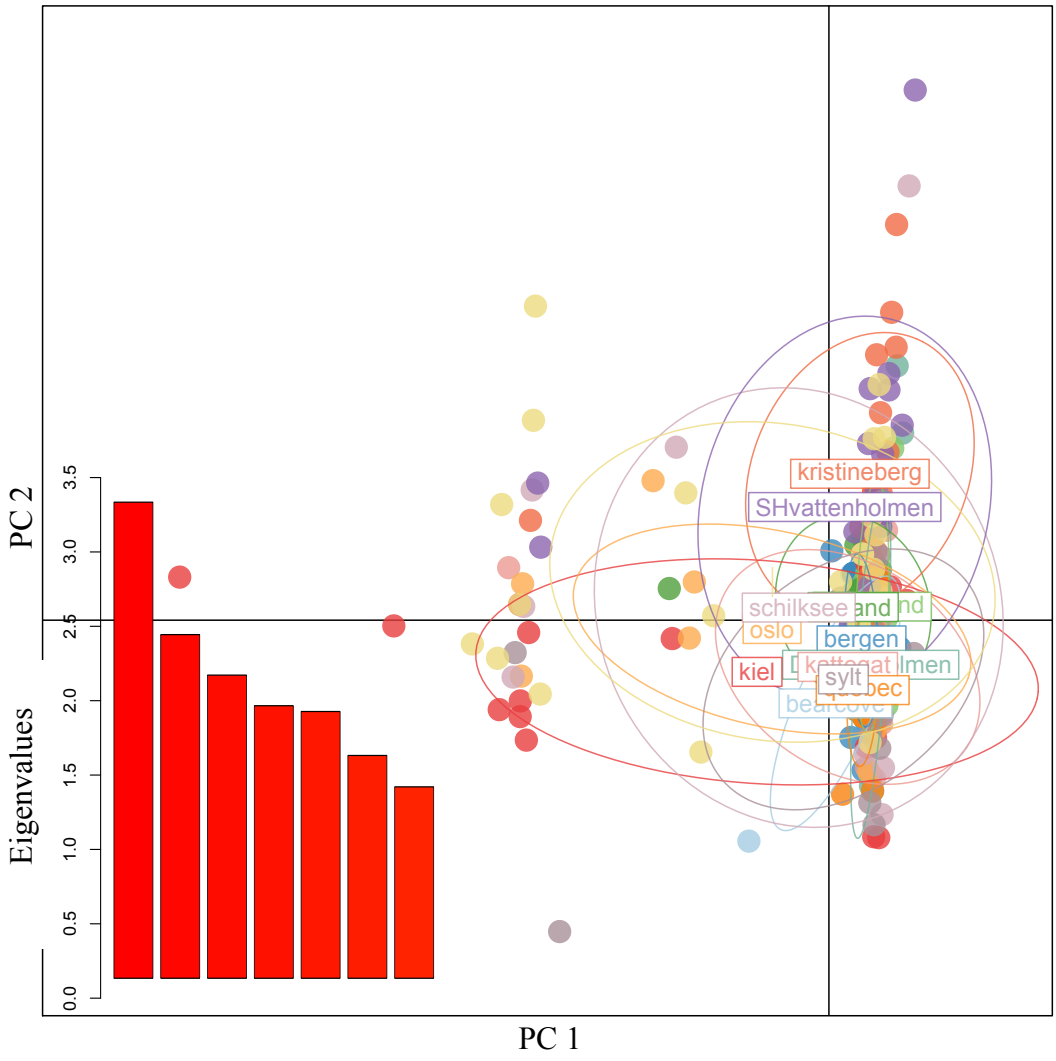

Figure 20: Principle component analysis based on allele frequencies. Eigenvalues of the principle components are displayed in the lower left corner. Loadings of PC1 and PC2 are shown in the appendix Figure 26 and Figure 27.

3.3.2 Genetic diversity

The expected and observed heterozygosity compared to Hardy-Weinberg equilibrium was calculated for each population and tested for significance (Table 5). The open ocean populations Iceland and Helgoland and the Baltic Sea populations Kiel (p-value <0.01) and Schilksee had a significant deficit in heterozygote individuals (all p-value < 0.05, except Kiel p-value < 0.01) while Kristineberg showed a heterozygote excess (p-value < 0.05). The frequency of null alleles ranged from 0-6.6 % within loci, while the most diverse markers Ar14 and Ar29 had the highest null allele frequencies (appendix Table 12). The mean allelic diversity per locus varies between 4.25 and 7 alleles for the different populations (Figure 21). The most remote populations have the least allelic diversity, with Québec (4.25) and Kiel (5). The highest diversity is visible in the deep population from Vattenholmen with a mean of 7 alleles per locus. The mean genotype number per locus shows a similar pattern but with higher differences between populations (Figure 21). Québec shows a lower mean number of genotypes (6) than all other populations (6.5-9.5). The highest genotype numbers are found in the populations of Iceland, Helgoland and Vattenholmen deep (8.5-9.5).

The Canadian populations Bear Cove and Québec revealed three unique alleles that did not appear in any of the other populations. Although, Bear Cove was only represented by five individuals, the population had one unique allele each at the loci Ar17 and Ar19. Both loci were not very polymorph and had 4 and 6 alleles in total, respectively. For sea stars from Québec, a unique allele was found at the more diverse locus Ar29 with a total of 13 alleles.

Table 5: Genetic diversity (expected and observed heterozygosity) of *A. rubens* in the North Atlantic. Numbers are based on 7 microsatellite loci. Significances assesses with GENEPOP: *heterozygote deficit **heterozygote excess.

Population	**$H_{exp.}$**	**$H_{obs.}$**
Bear Cove	0.1886	0.2286
Québec	0.1635	0.1537
Iceland*	0.2382	0.2017
Helgoland*	0.2342	0.1779
Sylt	0.2983	0.2829
Bergen	0.1919	0.2005
Oslo	0.2483	0.2679
Deep Vattenholmen	0.2354	0.2327
Shallow Vattenholmen	0.2749	0.2597

Tjärnö	0.3170	0.3284
Kristineberg**	0.2450	0.2797
Kattegat	0.2453	0.2781
Schilksee*	0.3223	0.2857
Kiel*	0.3061	0.2692

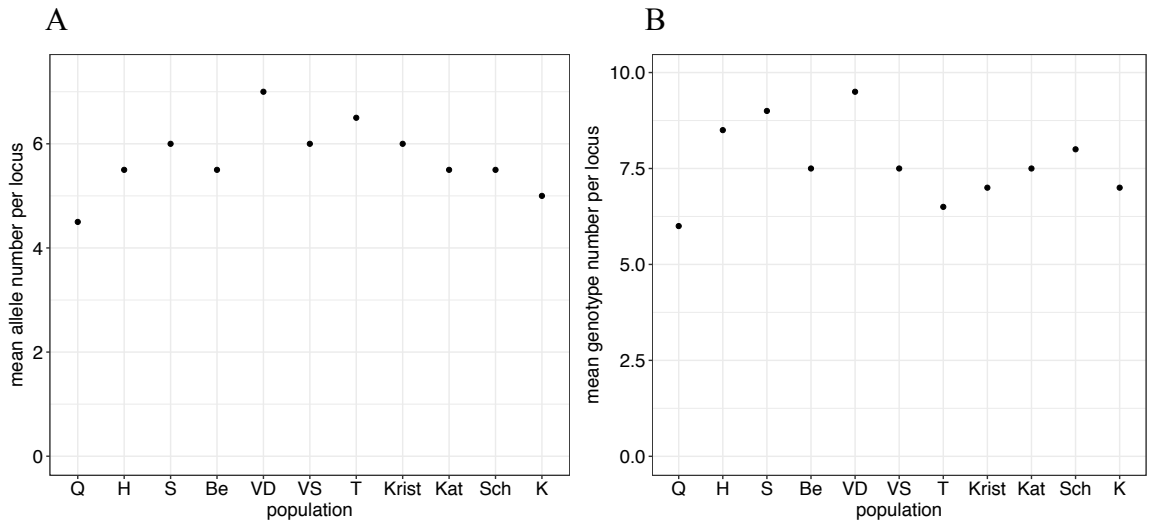

Figure 21: Mean allelic and genotypic richness in 7 loci of *A. rubens*. Populations were resampled with rarefraction to N = 15. For population abbreviations see **Table 2**.

3.3.3 Isolation by distance and environment

IBD as a correlation of genetic distance with geographic distance could neither be detected with Pearson's correlation nor with MANTEL tests (maximum $R^2 = 0.0207$) (Figure 22, appendix Table 14, appendix Table 15). Also log-transformation of one or both parameters revealed no significant correlations, neither did the correlation suggested by Rousset (1997). The correlation of genetic distance with salinity was not significant for original and also log-transformed data (Figure 22, appendix Table 14) (maximum $R^2 = -0.01$).

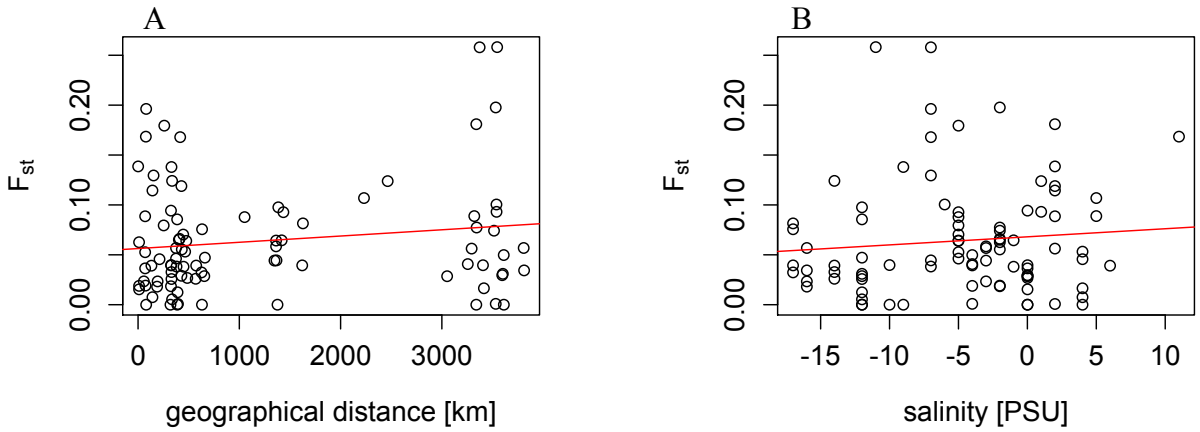

Figure 22: Correlation of genetic with geographical distance (A) and with environmental distance (B). Each dot represents a single comparison between two *A. rubens* populations. Red line indicates linear models (A: adjusted $R^2 = 0.01179$, p-value = 0.1534; B: adjusted $R^2 = -0.0105$, p-value = 0.758). Geographic distance was measured as distance in km seaway between two populations. Environmental distance was measured as the difference in salinity of two sampling sites.

4 Discussion

The aim of this study was to investigate the adaptation and acclimation potential of the common sea star, *Asterias rubens* to different salinities with the aid of physiological experiments and a population genetics approach. Previous experiments suggest that sea stars from the North Sea cannot tolerate salinities as low as experienced by animals living in the low saline Baltic Sea (Findeisen *et al.,* unpublished). With a reciprocal transplant experiment we confirmed our hypothesis of higher growth and feeding rates as well as faster righting time in 32 PSU compared to 16 PSU for both populations. Further, we expected local adaptation, manifested as higher fitness of Baltic Sea populations in low salinities compared to North Sea populations, which was also confirmed. The quantitative and qualitative analysis of organic osmolytes revealed glycine as the main OO in *A. rubens* while the composition of the OO pool was different in 16 PSU between the two populations, but the total concentration was the same. Thus, we hypothesize that sea stars from the Baltic Sea have adapted to low salinities by intracellular ion regulation rather than by increased OO concentrations. For *A. rubens* from the low saline Baltic Sea the critical salinity that can be tolerated was found to be 9.2 PSU. Furthermore, the population structure of sea stars in the North Atlantic was investigated with seven microsatellite markers developed within this study. Expected signals for isolation by distance or isolation by salinity were not found with the aid of the chosen markers. Based on F-statistics, a Bayesian clustering and a neighbour joining algorithm, our results suggest a strong influence of currents and water depth on *A. rubens* dispersal. The hypothesis of lower genetic diversity in Baltic Sea populations and a strong genetic differentiation to Atlantic populations was not completely confirmed within this study. It would be very interesting to investigate these questions further with higher resolution markers and a sampling approach taking water depth into account.

4.1 Growth, feeding rate and righting time

The results of our reciprocal transplant experiment between *A. rubens* from the Baltic and the North Sea demonstrated an advantage of animals from the Baltic Sea in low salinities, in accordance with our hypothesis. In 16 PSU, animals from Kiel increased in weight while sea stars from Sylt lost weight. Both populations showed positive feeding rates, although mussel consumption of Kiel sea stars was ~ 1.6 times higher than in animals from Sylt. Weight loss regardless of food consumption hints towards an increased energy demand of sea

stars from Sylt in low salinities and probably reduced scope for growth compared to sea stars from Kiel.

Our results demonstrate a higher fitness of sea stars from the Baltic Sea population in 32 PSU compared to animals from the North Sea. Kiel animals had more than 2 times higher growth rates than Sylt animals while having comparable feeding rates. Furthermore, righting time was measured as an indicator for activity and neuromuscular function. It was found to be overall lower for sea stars from Kiel than from Sylt. An apparently better fitness of the population from Kiel regardless of salinity can be attributed to different reasons. The sea star population in Kiel experiences extreme environmental fluctuations of different abiotic factors. Especially during summer, organisms face periods where pH already meet values predicted for 2100 (Thomsen *et al.,* 2010, 2013; Saderne *et al.,* 2013). In addition, salinity fluctuations are between ~10 and ~22 PSU and sometimes change within hours (Hiebenthal *et al.,* 2013). Those challenging conditions pose a strong selection pressure for extremely resistant genotypes resulting in an overall increased fitness compared to North Sea animals. Nevertheless, the analysed population from Sylt was collected in the intertidal zone in the Wadden Sea. The mean annual salinity of the Wadden Sea is close to 30 PSU (Diederich *et al.,* 2004). During low tide, also this population experiences fluctuations of abiotic factors. Rainfall can reduce salinity substantially, temperature can be elevated by solar radiation and periods of deoxygention can occur due to high respiration levels of organisms. Thus, the same hypothesis of selection of resistant genotypes should apply here. Nevertheless, environmental fluctuations due to the tidal cycle pose a strong stress towards organisms but fluctuations are predictable, regular and of short duration. Fluctuations in Kiel fjord however, are unpredictable and desalination or temperature increase can last much longer than a tidal cycle. Thus, we suggest an increased performance of Baltic sea stars due to their adaptation to adverse environmental conditions including low salinities. Also, the brittle star, *Ophiophragmus filograneus* is found in brackish waters down to 7.7 PSU in Florida but nevertheless, performs better under fully marine conditions (Talbot and Lawrence 2002). This finding goes along with the increased growth, feeding rates and faster righting times of sea stars sampled from the Baltic Sea in 32 PSU compared to 16 PSU. It can be hypothesized that animals selected for low salinity tolerance are generally stress resistant and thrive under conditions closer to their physiological optimum. While often the resistance to an environmental stressor comes with a trade-off and susceptibility to another stressor (additive and synergistic effects of multiple stressors), also antagonistic effects are observed (Byrne and Przeslawsi 2013; Crain *et al.,* 2008; Harvey *et al.,* 2013). Another reason for increased

performance of sea stars from Kiel compared to sea stars from Sylt can be the use of seawater from Kiel fjord. The water contains pathogens that are novel to the North Sea population and decreasing their fitness while animals from Kiel are locally adapted to those pathogens. For different species local adaptation to pathogens was already found (Bryan-Walker *et al.,* 2007; Kalbe and Kurtz 2006; Wendling *et al.,* 2017). The same home-advantage holds true for the food source *Mytilus edulis* collected from the Fjord that potentially have different nutritional values than *M. edulis* from the North Sea. UV-sterilization and filtration of seawater prior to experimental use minimized the risk of pathogen infection. Ideally, the reciprocal transplant experiment for high salinity conditions should have taken place on the island of Sylt directly, to exclude the influence of local pathogens.

Locomotion and activity of sea stars was suspected to be impaired by hyposaline conditions and this hypothesis tested by righting time measurements in the reciprocal transplant experiment. Righting time was negatively affected by decreased salinities in both populations, while animals from Kiel took approximately half the time of Sylt animals to turn around. Three animals from Sylt were not able to successfully right for the whole duration of the measurement and showed no sign of movement. Locomotion in sea stars depends on the hydrostatic pressure in the water vascular system (Smith 1947; Binyon 1964, 1972, 1976) as well as the production of adhesive molecules (Hennebert *et al.,* 2014, 2015). With contraction and relaxation of longitudinal muscles, the water pressure in water vascular system is modified and tube feet are either extended or contracted. As both muscle contraction and water content of the vascular system are influenced by external salnity, hyposaline conditions can alter the ability of tube feet to properly contract. *A. rubens* has approximately ten times more tube feet than necessary for support (Kerkut 1953) and after each contraction a single tube foot undergoes an inactive phase during which ion and water content and therefore hydrostatic pressure are probably regained (Smith 1947). When this inactive phase is prolonged due to salinity stress, it is possible that not enough tube feet are available for sufficient support. This would explain the observed detachment from aquaria walls in low salinities in our experiments. Another explanation could be that sea stars pause movement to save energy. Metabolic arrest or metabolic depression serves as a mechanism to preserve energy through minimizing metabolism (Hand and Hardewig 1996; Guppy and Withers 2007). It is a common response to adverse environmental conditions to survive until conditions change and was previously shown for invertebrates including echinoderms (Sokolova *et al.,* 2000; Yu *et al.,* 2012; Rivera-Ingraham *et al.,* 2016). It is possible that *A. rubens* is unable to alter the hydrostatic pressure in the water vascular system and synthesize

adhesive molecules under low salinities required for movement due to lack of energy and thus enters a state of metabolic arrest.

It has to be considered that experimental studies are usually biased by short duration times. For most organisms, negative effects of environmental stressors are erased after a long enough acclimation time or over a few generations (Kroeker *et al.,* 2013). It was shown that *A. rubens* from the Barents Sea (34 PSU) acclimated over one year to low salinities (24 PSU), had higher offspring survival at brackish salinities (Sarantchova 2001). Adult sea stars were found to prefer high salinities when only acclimated to low salinities for two weeks, while after one year they preferred low salinities. Nevertheless, intracellular osmoregulation is necessarily an extremely fast process as an osmolality gradient across the cell membrane would lead to net water influx, cell disruption and ultimately death. Thus, we consider a one month period of gradual salinity reduction plus a one month acclimation period to final salinity conditions sufficient as it was shown in multiple studies that the so-called "long-term response" to hyposaline conditions, the alteration of OO, happens within hours to days (Shumway 1977; Diehl and Lawrence 1985). Also, a long-term response on the ion level was found to happen within 2-4 days in the brown mussel, *Perna perna* (Rola *et al.,* 2017).

4.2 Organic osmolyte composition and concentration

Our results reveal the importance of free amino acids (FAA) and FAA derivatives such as betaine and taurine in osmoregulation. The compounds alanine, glycine, lysine and taurine had the highest contribution to the total intracellular OO pool while glycine with a relative concentration of 70-90 % is clearly the most important osmolyte in *A. rubens*. The two populations Kiel and Sylt differed in their utilization of FAA as animals from Sylt had a considerably higher concentration of glycine. Furthermore, population differences became visible under the influence of salinity as shifts in the contribution of certain FAA to the total sum. Taurine and valine increased in proportion in animals from Kiel with decreasing salinity and glycine increased in proportion in sea stars from Sylt with decreasing salinity. Sea stars from Kiel apparently do not rely on a higher total concentration of OO to decrease their critical salinity. Rather, they seem to decrease glycine concentrations faster than animals from Sylt and keep taurine and valine levels higher.

Also in other marine invertebrates alanine, glycine and taurine were among the most abundant OO correlated to salinity (Shumway *et al.,* 1977; Bishop and Burton 1993; Blank *et al.,* 2004; Kube *et al.,* 2006). The pronounced overrepresentation of a single OO in our

experiments (glycine) is rather rare and other species seem to rely on a mixture of OO. Differences in the composition of the OO pool were shown to differ between the two bivalve species *Macoma balthica* and *Mytilus sp.* but also between different regions (Kube *et al.,* 2006). In these species, the concentration of OO was negatively correlated with salinity but also fluctuated under constant salinity conditions depending on the season (Kube *et al.,* 2007). It has to be taken into account that in many studies, only FAA were measured neglecting other possible compounds contributing to osmolality adjustment.

For *Asterias rubens*, the importance of glycine and taurine in osmoregulation in the pyloric caecae has been assessed before (Jeuniaux *et al.,* 1962). *Luidia clathrata* is one of the only other asteroid species for that the contribution of amino acids and also inorganic ions to cell volume regulation was assessed in different salinities (Diehl and Lawrence 1985). When sea stars were transferred from control salinities of 25 PSU to 15 PSU, immediate efflux of Na^+ and Cl^- was observed, followed by a decrease in glycine concentrations and a decrease of ion concentrations to initial values. It was proposed that the fast response in ion regulation serves to maintain cell volume but has to be followed by adjustment of OO concentrations in order to restore ion concentrations necessary for membrane function (Diehl and Lawrence 1985; Silva and Wright 1994; Hochachka and Somero 2002). As in this study on *A. rubens*, glycine was found to account for 60-90 % of the OO pool and was the only amino acid that changed with salinity in *L. clathrata*. Other potentially important osmotically active compounds were not quantified as only FAA were analysed (Dionex Peptide/Amino Acid Analyze). It should be taken into account that in the described experiment sea stars were transferred into low salinities directly without a gradual salinity decrease and responses were measured within seven days after exposure to low salinities. Other OO might contribute to the slow acclimation to different salinities or to the long-term response to constantly decreased salinities.

As described in the introduction, strategies of adaptation to low salinities can include alteration of OO and/or ion concentrations. The hypothesized increased concentration of OO in animals from Kiel was not found. In contrast, animals from Sylt had higher concentrations regardless of salinity. Experimental results suggest, that the adaptive mechanism of animals from Kiel lies in the alteration of the ion concentrations at certain salinities. For the brown mussel, *Perna perna* it was shown that estuarine populations are able to regulate haemolymph osmolality in comparison to marine mussels (Rola *et al.,* 2017). Within approximately 4 days after exposure to hyposaline conditions, the animals were found to restore sodium, potassium

and chloride levels to control concentrations resulting in increased Na^+/K^+ ATPase activity. Another potential adaptation is the speed of response to salinity changes. Baltic Sea animals might have more ion channels, more papillae on their body surface to increase surface area and thus regulative capacities, or ion channel response and regulation might happen faster.

The increased ability to accumulate certain ions would benefit the animals in case of OO depletion to keep up the ion concentration necessary for cellular function. This could be achieved by e.g. altered expression of ion transport proteins leading to increased membrane permeability (Havird *et al.,* 2013) or higher activity of the already existing ion pumps (Lee *et al.,* 2011). An extremely increased water efflux was shown in polychaetes when transferred to low salinities (Willmer *et al.,* 2005). Another potential way to increase hyposaline tolerance of Baltic Sea populations is the regulation of the extracellular fluid in order to decrease the osmotic gradient between extra- and intracellular fluid and thus osmotic pressure (Diehl 1986; Freire *et al.,* 2011; Santos *et al.,* 2013, Stickle and Ahokas 1974, Stickle and Diehl 1987). Especially K^+ was found upregulated in ambulacral fluid but not coelomit fluid of most echinoderms (18-93 % upregulation *Echinus esculentus* Robertson, 1949, *Solaster papposus* Binyon, 1966). Ion gradients in response to salinity changes do not only depend on the study species but can be influenced by the experimental set-up. For instance, abrupt salinity changes did not result in ion gradients between coelomic fluid and seawater in the sea urchin, *Echinometra lucunter* (Freire *et al.,* 2011), while stepwise changes (2-3 PSU/h) did (Santos *et al.,* 2013). In the sea urchin *Arbacia lixula* neither stepwise nor abrupt salinity changes revealed osmotic gradients between extra- and intracellular fluids (Vidolin *et al.,* 2007, Santos *et al.,* 2013).

There are two aspects that have to be considered when interpreting the experimental results. First, it is possible that the intracellular water content of our sea stars was substantially different in the different salinities and potentially between the two populations. It was shown that water content differs between tissues as well, but the OO concentration in pyloric caecae and tube feet is similar when corrected for tissue water content (Diehl and Lawrence 1985). In the future, it is interesting to correct for cell water content. It is possible that sea stars from Sylt have a higher cell water content in low salinities than animals from Kiel due to difficulties with intracellular osmoregulation. This would lead to more dilute OO concentrations in Sylt animals than Kiel animals in contrast to the observed higher absolute OO values in the Sylt population. Second, mortality due to unresolved reasons was observed towards the end of the experiment. In total, four animals from different replicate tanks in three

different treatments died in the last two weeks of the experiment. All four animals died in the same noticeable way of first showing white lesions between the arms and following loss of single arms until total disintegration. Detached arms kept moving constantly for a few hours up to one day. As animals from the control treatments died as well, a salinity effect can be excluded. These symptoms were previously described to be associated with one of the most severe marine wildlife epizootic, the sea star wasting disease (SSWD). A SSWD epidemic was observed during 2014 on the Pacific coast of America (Menge *et al.,* 2016). Over 20 species of sea stars were affected and the SSWD caused widespread deaths. It was found associated with a densovirus of the family *Parvoviridae* (sea star associated densovirus, SSaDV), whereas the trigger of the actual outbreak was not found (Hewson *et al.,* 2014; Fahsbender *et al.,* 2015). For the pacific sea star, *Pisaster ochraceus* infection rates increased significantly with higher temperatures (Bates *et al.,* 2009; Eisenlord *et al.,* 2016) while more infected animals were found in sheltered areas (Bates *et al.,* 2009). In 2014, extremely high summer temperatures of +2-4 °C in some regions correlated with SSWD outbreaks (Eisenlord *et al.,* 2016). It seems that the virus is present as well in apparently healthy animals as in sediments and non-affected species like sea urchins which opens many ways of transmission (Hewson *et al.,* 2014). During another physiological experiment that was conducted in early summer 2016, *A. rubens* collected from the North Sea close to the Island of Sylt, presented symptoms that reminded of the SSWD in the Pacific, although, to our best knowledge, this disease was never proven to have spread to the Atlantic.

All animals were examined for signs of infection prior to measurements. Tissue for OO extraction was only taken from live individuals without white lesions.

4.3 Critical salinity for *Asterias rubens* from the Baltic Sea

The concept of the critical salinity was first proposed by Braby and Somero (2006) who studied the influence of salinity on blue mussels. They detected a certain salinity at which the heart rate and therefore performance drops significantly and termed it S_{crit}. In a study on the sea anemone *Diadumene lineata* the response on the cellular level was revealed as a depletion of OO and a fitness of zero (Podbielski *et al.,* 2016). We estimated S_{crit} in *A. rubens* from the decrease in OO with decreasing salinities and found 9.22 PSU to be the limit for the analysed population from the Baltic Sea. This result is supported by our observation of total loss of scope for activity of animals kept below 10 PSU. During the experiment, the salinity was slowly changed from control conditions to the desired treatment salinity. In the 8 PSU

treatment, we observed a sudden change in animal appearance as well as locomotive activity, when salinity was lowered from 10 to 9 PSU. The salinity in this treatment was not further decreased but kept stable at 10 PSU. Nevertheless, all five replicate animals died. It seems that once salinity falls below S_{crit}, *A. rubens* is not able to recover from hyposaline stress. When OOs are depleted, ion concentrations are altered as a consequence. This leads to destabilization of the electrochemical cell membrane gradient, water uptake with cell swelling and subsequently loss of cell integrity and cell lysis. These processes are apparently dependent on the time spend in salinities under S_{crit}. While sea stars can probably recover after minutes to hours spent in salinities lower than 9.2 PSU, there is a limit after which cell integrity cannot be maintained.

The impact of hyposaline conditions on *A. rubens* was assessed in several experimental studies. Surprisingly different tolerance and mortality levels were published, ranging from a lethal threshold of 12 PSU to 26 PSU in adult sea stars (Smith 1940, Shumway 1977, reviewed by Russel 2013). Experiments on larvae revealed 100 % mortality at 8 PSU (Saranchova *et al.,* 2006) and 9-12 PSU depending on the developmental stage (Casties *et al.,* 2015). The duration of the experiments and the acclimation time definitely play an important role in assessing tolerance levels of *A. rubens*, as well as the sampled population. For a North Sea population that experiences minimal salinity levels of 28.7 PSU, the LD 50 was found to be 23 PSU when transferred directly to low salinities (Binyon 1961) while for a population from a fluctuating salinity habitat with values as low as 14 PSU, mortality only occurred at 12 PSU (Smith 1940). This study will add to the literature with tolerance levels of a North Sea population around 12 PSU and for a Baltic Sea population around 10 PSU. It should be noticed that those levels are tolerated but cannot be viable in the long-term. Although, North Sea animals were found alive at 12 PSU, they were not observed feeding after a long starvation period. When salinity was slowly increased to 16 PSU, 2 of 10 replicate sea stars started feeding. Furthermore, North Sea animals probably went to a state of metabolic arrest (discussed before) and were not found to attach to aquaria walls in 12 PSU while animals from the Baltic Sea were observed to maintain locomotion in 12 PSU.

Nevertheless, the survival of a species is not only dependent on physiological constraints in adults, but also during development. As many marine species, sea stars possess a planktonic developmental phase during which the species are mostly distributed in contrast to their sessile adult life. The limit for successful reproduction and larval development of *A. rubens* was found to be 15 PSU (Casties *et al.,* 2015). This meets the current distribution of

sea stars in the Baltic Sea where they are almost absent below 10 PSU and rarely occur east of Kiel Fjord with an annual salinity of 16 PSU. It was suggested that recruitment in Kiel fjord only occurs in years with stable salinities above 15 PSU during larval season, which was only met in 2014 between the years 2009-2014. Furthermore, salinity tolerance in *A. rubens* seems to increase with developmental stage from egg to grown sea star (Saranchova and Flyachinskaya 2001).

Our study supports the proposed concept of critical salinity S_{crit} by Podbielski *et al.,* (2016) as the salinity at which the OO concentration and therefore fitness become zero.

4.4 Population structure

The microsatellite analysis of 14 populations of *A. rubens* in the North Atlantic revealed a population structure that cannot be explained simply by distance nor differences in salinity. In the STRUCTURE analysis, most individuals are assigned to a mixture of genetic groups with different proportions rather than to distinct clusters. There is no statistically significant difference between Baltic Sea and Atlantic populations although sea stars from the Baltic are both geographically and abiotically separated. Also, the allelic and genotypic richness expressed as mean number of alleles or genotypes per locus, respectively, revealed no differentiation between Baltic and North Sea populations. Nevertheless, the population from Kiel showed, next to Kristineberg, the highest F_{st} values with differentiation from Iceland and Helgoland as well as from Bergen, Vattenholmen shallow and Kristineberg. Surprisingly, the sea stars from Schilksee that were sampled approximately 10 km away from the sampling location of the Kiel population, only differ significantly from Québec and Kristineberg. It was unclear whether such close sampling sites should be considered different populations but our analyses reveal differences even on this small sampling scale.

Heterozygote deficit as a sign for inbreeding was detected in the remote populations of Helgoland, Iceland as well as the Baltic populations Schilksee and Kiel. This would agree with an eventual geographical isolation leading to increased inbreeding. Nevertheless, inbreeding is hard to assess from a few microsatellite markers and thus no predictions can be made for this study (Balloux *et al.,* 2004). Furthermore, heterozygote deficit can be due to selection of advantageous alleles, which would be a hint towards selection pressure in the low saline Baltic Sea. Kristineberg on the other hand was the only population that showed heterozygote excess implicating increased outbreeding. For the future, a more comprehensive

sampling approach along the coast of the Baltic Sea could reveal whether all Baltic populations lack signs of population differentiation to North Sea and Atlantic populations.

The lack of evidence for population difference of Baltic sea stars could be attributed to the relatively young age of the Baltic Sea. Reports of echinoderms invading brackish seas show that in the Baltic Sea (10,000-15,000 yrs, Ojaveer *et al.,* 2010) only one species occurs (*A. rubens*), while in the much older Black Sea (50 million yrs, Kazmin *et al.,* 2007) seven echinoderm species are recorded (Russel 2013). Thus, selection towards low salinity tolerance might take longer than the Baltic Sea exists leading to the hypothesis that *A. rubens* is not fully adapted but shows high phenotypic plasticity towards low salinities. Nevertheless, the magnitude of F_{st} values despite insignificant p-values has to be considered. In this study, F_{st} values of 0.01-0.179 suggest population differentiation between North and Baltic Sea but are statistically insignificant. For comparison, significant differentiation between North and Baltic Sea populations were found in eelgrass, *Zostera marina* with F_{st} values of 0.26-0.38 (Reusch *et al.,* 2000), in Atlantic cod, *Gadus morhua* with F_{st} values as low as 0.0039-0.0221 (Nielsen *et al.,* 2003) and in the diatom, *Skeletonema marinoi* with F_{st} between 0.15-0.25 (Sjöqvist *et al.,* 2015). Probably due to partially low allele numbers or sample size in this study the statistical power was too low to detect significant differences. A whole genome SNP analysis would reveal the population structure on a finer scale with much higher statistical power.

The initial hypothesis of isolation by environment (salinity) was rejected. Furthermore, we could not detect isolation by geographic distance. The strong differentiation between populations from the same location but from different depth at Vattenholmen suggests the influence of water depth on population structure. *A. rubens* has a relatively long planktonic larval phase of ~90 days (Barker and Nichols 1983). During this period, sea stars are prone to dispersal while adult animals have a benthic lifestyle with limited movement. Additionally, the larval period can be prolonged under unfavourable conditions for settlement allowing for even longer dispersal time (Barker and Nichols 1983). While larvae from most benthic invertebrates including sea stars are able to actively move in the water column, stratification can often not be passed (Mileikovsky 1973). Next to temperature, salinity accounts for water stratification separating deeper cold and saline water from warmer hyposaline surface water as it is found in the Baltic Sea and transition to the North Sea. For *A. rubens*, the salinity threshold at which a halocline could not be crossed was found to be 24 PSU in the surface layer (Sameoto and Metaxas 2008) preventing transport of *A. rubens* larvae over the halocline

in most regions of the Baltic Sea and Kattegat. In the Kattegat and Skagerrak region the shallow Norwegian coastal current flows northwards and carries low salinity water from the Baltic Sea and rivers (Norwegian Ministry of the Environment 2012). Higher saline, deep water is introduced from the North Atlantic current, flowing south along the Norwegian coast until the Skagerrak region (Figure 23). The two directions of those major currents would disperse sea star larvae from certain depth into different directions, connecting different populations. *A. rubens* larvae can withstand much higher water pressure than adult animals making them suitable for distribution by deep currents (Villalobos *et al.,* 2006). Additionally to the effect of depth and salinity, local fjord circulation is shaped by ocean floor topography creating constraints for dispersal. With field measurements and a modelling approach the salinity distribution of a Swedish fjord, close to the sampling site Kristineberg, was found to fluctuate within a few days (Figure 24, Svenningsson 2010). All Swedish and Norwegian sea stars in this study were sampled from fjord regions from more or less sheltered coastal areas. Depending on topography, wind speed and access to open ocean, salinity and halocline depth can differ significantly between those neighbouring fjords. For sea stars from a fjord region in New Zealand, population differences between fjords were found, attributed to salinity stratification and local water circulation (Perrin *et al.,* 2004).

As early as 1927, it was reported that the green sea urchin, *Psammechinus miliaris* from the East Atlantic occurs in two different ecotypes; one in shallow, warmer water with low, fluctuating salinities and one in colder, fully marine, deep water (Lindahl and Runnström, 1929). The shallow/intertidal and deep/subtidal forms show differences in colour, size, behaviour and fatty acid composition (Lindahl and Runnström, 1929; Hughes *et al.,* 2005; Gezelius 1963). Also at our sample site Vattenholmen at the Swedish coast phenotypic population differences were already detected (Enge *et al.,* unpublished). For example, shallow sea stars show no avoidance of the predatory sunflower sea star that only occurs in deeper waters. In our results, populations that were sampled by diving or dredging and not from surface water are Sylt, Bergen, Vattenholmen deep and Kattegat. In the STRUCTURE analysis those populations show definitely similarities and differences to the other sampling sites except the Canadian populations. Unfortunately, we cannot record the sampling depth for those populations and also not for Helgoland. Additionally, samples from Iceland were taken in an intertidal area at low tide making it hard to assign a sampling depth. We suggest a sampling approach for the future that takes into account the sampling depth as well as ocean currents and proximity to open ocean access.

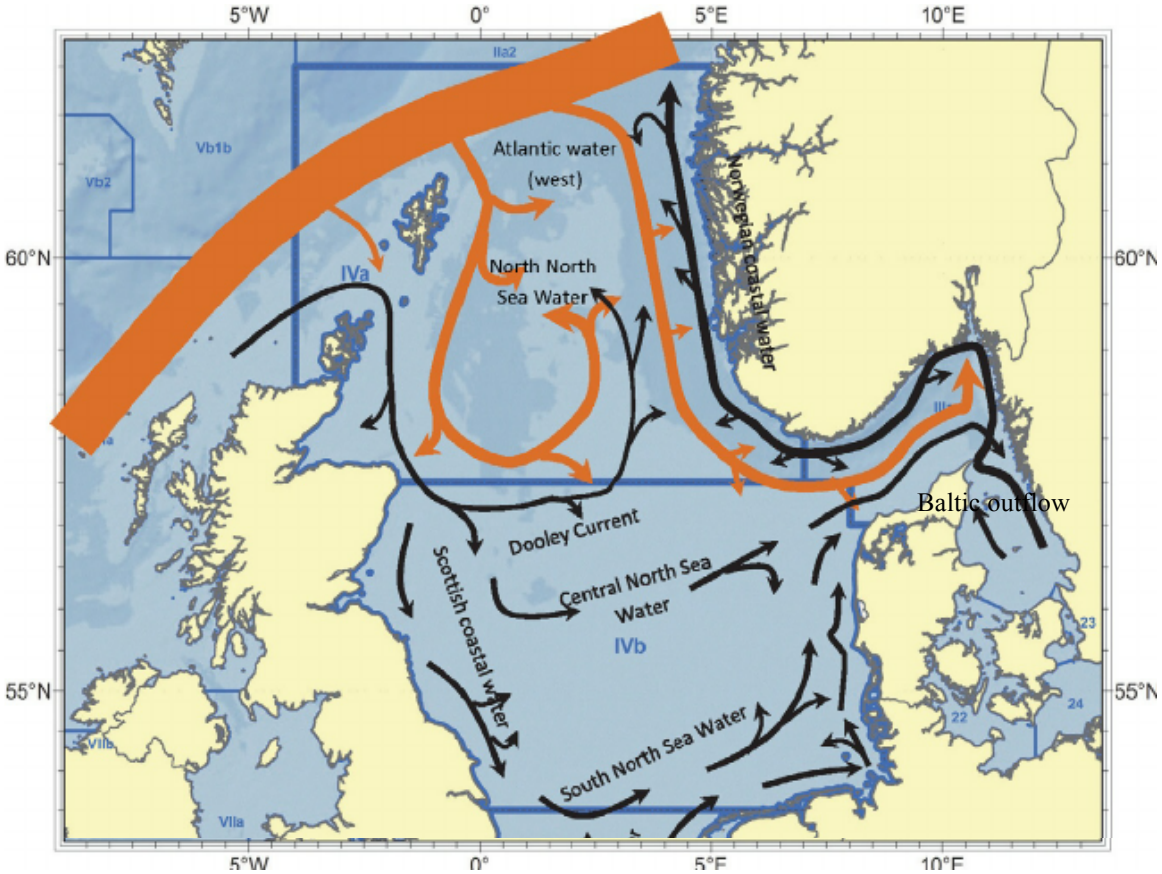

Figure 23: Currents in the North Sea (modified from Caveen *et al.*, 2014).

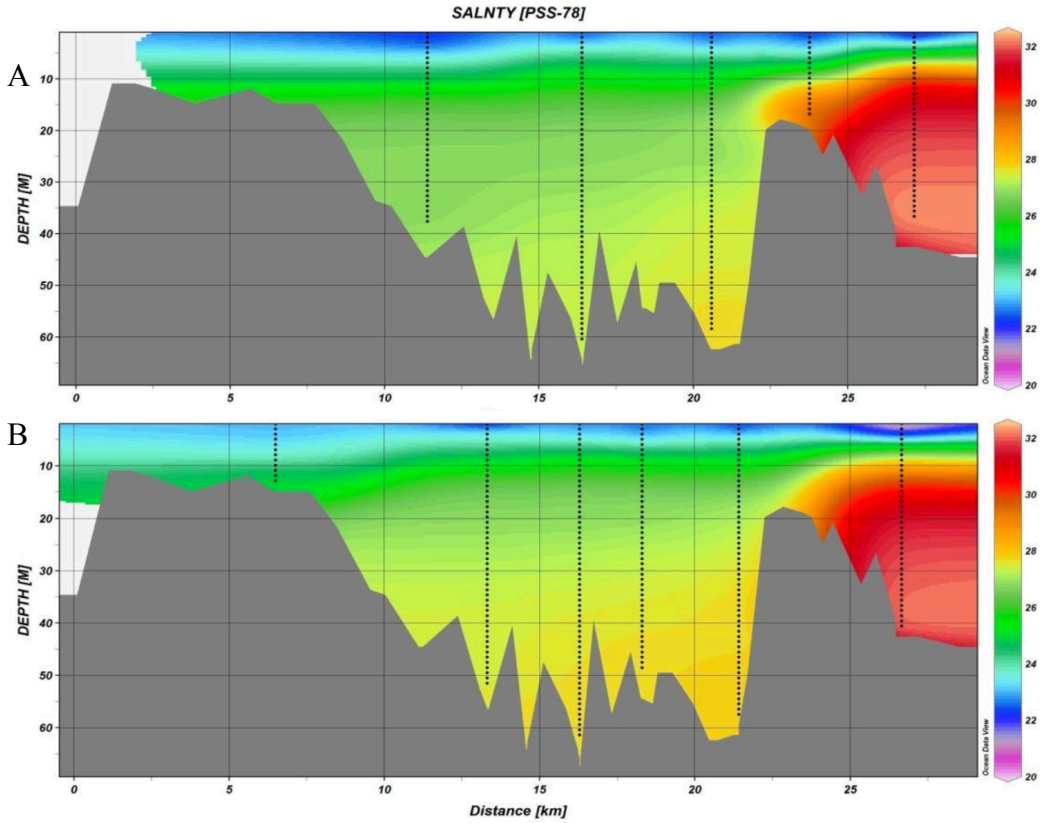

Figure 24: Salinity variation in Orust-Tjörns fjord on the Swedish coast on two separate days in December 2008 (A and B). (Svenningsson 2010)

The dispersal capacity of an organism determines population structure extremely. Sea stars with benthic larvae were found to show population structure even between tide pools while sea stars with planktonic larvae only had population difference on the larger geographical scale (Barbosa *et al.,* 2013). For 16 benthic species it was shown that only the dispersal ability determined connectivity between populations (Josefson *et al.,* 2016). Salinity gradients only affected the population structure of organisms with high dispersal ability, resulting in sorting along the gradient according to salinity tolerances. Additionally, the exposure of populations to the open ocean determines connectivity (Robins *et al.,* 2013). Larval shellfish were dispersed further starting from exposed areas than from fjords, while mesoscale currents were important for offshore dispersal. As our samples come from both exposed and fjord regions as well as the geographically remote Baltic Sea, make it difficult to assess population connectivity due to currents and geographic properties in detail. A modelling approach that takes depth into account could help to resolve the main mechanism shaping *A. rubens* dispersal.

Another important factor connecting distant populations is ship traffic as an additional vector to natural dispersal (Baguette *et al.,* 2013). In our analysis, the populations from Kiel and Oslo show certain similarities in the STRUCTURE analysis that can be attributed to the daily ferry traffic between these two sites. Animals from both populations were sampled in direct proximity to the port area.

The two Canadian populations show a difference from all other populations in the Neighbour-joining analysis while they do not show differences in the STRUCTURE analysis. Animals from Québec revealed one unique allele and in the extremely low sample size of 5 individuals from Bear Cove two unique alleles were identified. Additionally, Québec had lower genotypic and allelic diversity compared to all other populations while Bear cove was not considered for the allelic diversity analysis due to low sample size. Based on those findings, we suggest a separation of North American from European populations due to oceanographic constraints. This would support the previously published hypothesis of the reinvasion of America by *A. rubens* after warming of the ocean ~ 20,000 BP (Wares 2001). A more comprehensive picture and the estimation of population divergence could be revealed with the help of more samples from North America in comparison with European populations.

Microsatellites as genetic markers have the advantage of high mutation rates and thus usually high polymorphism. Therefore, they are considered a good marker choice to reveal recent population substructures. Nevertheless, they sometimes reveal a different pattern than

other markers. For example, results of microsatellites, allozyme and mitochondrial DNA markers showed different results in Atlantic herring (Shaw *et al.,* 1999). The Pacific sea star *Patiria miniata* revealed a clear population structure and division into 2 distinct clades with the aid of 7 microsatellites and a similar allelic richness found in our study of 3.9-5.5 alleles per locus (Keever *et al.,* 2009). Another study on herring on the other hand revealed that the difference in allozyme and microsatellite data was dependent on only one microsatellite marker (Larsson *et al.,* 2007). This locus had two extremely overrepresented alleles in Baltic Sea herring compared to North Sea herring and was interpreted as selection at or close to that locus. There is also evidence for similar patterns of microsatellite data and fragment length polymorphism analysis as found (Mikheyev *et al.,* 2010).

Nevertheless, it has to be discussed that the microsatellites used in this study were designed from transcriptome data. Thus, the markers were located in coding regions of the sea star genome and expected to differ less than microsatellites in non-coding regions. They might also be situated in regions of the genomes or linked to those under selection and thus show less difference than neutral sites. Nevertheless, a recent and elaborate study found no differences between microsatellites from expressed and neutral regions of the genome (Khimoun *et al.,* 2016). In contrary, microsatellites from expressed regions had an even higher resolution of weak population structure. We only found two dinucleotide repeat regions from the two analysed transcriptome data sets. This can be expected from coding regions as duplication or deletion of two base pairs would lead to a reading-frame shift. Contradicting this hypothesis, tetra-nucleotide repeats were very common and also used in this study. The second most polymorphic microsatellite Ar14 was a tetranucleotide repeat.

4.5 Conclusion: Adaptation of *A. rubens* to different salinities?

This study aimed to understand whether certain populations of the common sea star *A. rubens* are adapted to low salinities and if this is reflected in the genetic population structure.

A higher fitness in low salinities was found for the Baltic sea population from Kiel in comparison to the marine population from Sylt and suggests an adaptive response and selection to low salinities. From the OO measurements, it can be concluded that the composition of the OO pool might be under selection in low salinities while the total concentration is unaffected. The understanding of the underlying mechanisms of adaptation towards low salinities needs more experimental work, starting with measurements of

intracellular and extracellular ion concentrations. Furthermore, critical salinity S_{crit} should be determined for several populations along the Baltic coast to test the hypothesis that S_{crit} is shifted towards higher salinities with rising habitat salinity. Comparing different populations in low and high salinities and a combination of OO and ion measurements, will give a complete picture of the osmoregulative mechanisms that allow *A. rubens* to adjust to different salinities.

Nevertheless, the general higher fitness of sea stars from Kiel also in high salinities has to be investigated further. It would be interesting to conduct a "real" common garden experiment, where the high salinity experiments are performed with seawater directly on Sylt, to rule out effect of seawater and pathogens on experimental results. Additionally, despite higher fitness of Baltic sea stars in all salinities for the measurements taken in this experiment, crucial traits like fertility as well as hatching and developmental success were not determined. Reproductive traits should be considered in future studies to make predictions of reproductive fitness for those populations crucial for survival.

The population structure of *A. rubens* revealed neither isolation by distance nor isolation by salinity based on the seven microsatellite markers developed for this study. But we suggest a connection to salinity as isolation by water stratification. Due to salinity differences of water masses that cannot be passed by the motile *A. rubens* larvae, populations in different depth seem to be genetically isolated. A more comprehensive sampling approach taking depth into account could complete the population structure of *A. rubens* in more detail. Furthermore, working together with physical oceanographers and combining currents, water stratification and larval dispersal capacity into oceanographic models would be a promising approach to understand population structure and migration of *A. rubens*. Based on this, more comprehensive sampling approaches could be designed to confirm theoretical models in the field. Comparatively high F_{st} values despite statistical insignificance in this study suggest genetically separated populations. This could be proven with high resolution markers, for example genomic SNP's. Alternatively, higher sample sizes could account for low marker number but nevertheless, it would be interesting to apply markers from non-coding regions as well to compare to the used coding region markers.

With the predicted desalination of the Baltic Sea, the distribution boarder of *A. rubens* will probably be shifted west- and northwards. Nevertheless, the population differences between Baltic and North Sea sea stars suggest adaptation to low salinities is possible in

A. rubens while the underlying mechanisms still have to be investigated further but are probably involving both OO and ion regulation.

5 References

Adamack, A. T., and B. Gruber. 2014. PopGenReport: Simplifying basic population genetic analyses in R. Methods Ecol. Evol. 5:384–387.

Andrén, T., S. Björck, E. Andrén, D. Conley, L. Zillén, and J. Anjar. 2011. The Development of the Baltic Sea Basin During the Last 130 ka. The Baltic Sea Basin. Pp. 75–97.

Baguette, M., S. Blanchet, D. Legrand, V. M. Stevens, and C. Turlure. 2013. Individual dispersal, landscape connectivity and ecological networks. Biol. Rev. 88:310–326.

Balloux, F., W. Amos, and T. Coulson. 2004. Does heterozygosity estimate inbreeding in real populations? Mol. Ecol. 13:3021–3031.

Barbosa, S. S., S. O. Klanten, J. B. Puritz, R. J. Toonen, and M. Byrne. 2013. Very fine-scale population genetic structure of sympatric asterinid sea stars with benthic and pelagic larvae: influence of mating system and dispersal potential. Biol. J. Linn. Soc. 108:821–833.

Barker, M. F., and D. Nichols. 1983. Reproduction, recruitment and juvenile ecology of the starfish, *Asterias rubens* and *Marthasterias glacialis*. J. Mar. Biol. Assoc. United Kingdom 63:745–765.

Bates, A. E., B. J. Hilton, and C. D. G. Harley. 2009. Effects of temperature, season and locality on wasting disease in the keystone predatory sea star *Pisaster ochraceus*. Dis. Aquat. Organ. 86: 245–251.

Beldowski, J., A. Löffler, B. Schneider, L. Joensuu. 2010. Distribution and biogeochemical control of total CO_2 and total alkalinity in the Baltic Sea. J. Mar. Sci. 81:252-259.

Belkhir, K., Borsa, P., Goudet, J., Chikhi, L., and Bonhomme, F. 1998. GENETIX, logiciel sous Windows TM pour la genetique des populations. Laboratoire Genome et Populations. CNRS UPR 9060, Universite de Montpellier II, Montpellier, France

Bell, G., and A. Gonzalez. 2009. Evolutionary rescue can prevent extinction following environmental change. Ecol. Lett. 12:942–948.

Benjamini, Y., and Y. Hochberg. 1995. Controlling the False Discovery Rate: A Practical and Powerful Approach to Multiple Testing. J. R. Stat. Soc. Ser. B 57:289–300.

Benson, G. 1999b. Tandem repeats finder: a program to analyze DNA sequences. Nucleic Acids Res. 27:573–80.

Berg, P. R., S. Jentoft, B. Star, K. H. Ring, H. Knutsen, S. Lien, K. S. Jakobsen, and C. André 2015. Adaptation to low salinity promotes genomic divergence in Atlantic Cod (*Gadus morhua* L.). Genome Biol. Evol. 7(6):1644–1663.

Bergstrom, L., A. Tatarenkov, K. Johannesson, R. B. Jonsson, and L. Kautsky. 2005. Genetic and morphological identification of *Fucus radicans sp. nov.* (Fucales, Phaeophyceae) in the brackish Baltic Sea. J. Phycol. 41:1025–1038.

Beyenbach, K. W. 2006. The V-type H^+ ATPase: molecular structure and function, physiological roles and regulation. J. Exp. Biol. 209, 577-589.

Binyon, J. 1962. Ionic Regulation and Mode of adjustment to Reduced Salinity of the Starfish *Asterias Rubens* L. J. Mar. Biol. Assoc. United Kingdom 42:49.

Binyon, J. 1964. On the mode of functioning of the water vascular system of *Asterias rubens* L. J. Mar. Biol. Assoc. United Kingdom 44:577–588.

Binyon, J. 1961. Salinity Tolerance and Permeability to Water of the Starfish *Asterias Rubens* L. J. Mar. Biol. Assoc. United Kingdom 41:161.

Binyon, J. 1972. The effects of diluted sea water upon podial tissues of the starfish *Asterias rubens* L. Comp. Biochem. Physiol. Part A Physiol. 41:1–6.

Binyon, J. 1976. The permeability of the asteroid podial wall to water and potassium ions. J. Mar. Biol. Assoc. United Kingdom 56:639–647.

Bishop, J. S., and R. S. Burton. 1993. Amino acid synthesis during hyperosmotic stress in *Penaeus aztecus* postlarvae. Comp. Biochem. Physiol. Part A Physiol. 106:49–56.

Blank, M., R. Bastrop, M. Röhner, and K. Jürss. 2004. Effect of salinity on spatial distribution and cell volume regulation in two sibling species of *Marenzelleria* (Polychaeta: Spionidae). Mar. Ecol. Prog. Ser. 271:193–205.

Brattström, H. 1941. Studien über die Echinodermen des Gebietes zwischen Skaggerak und Ostsee, besonders des Öresundes mit einer Übersicht über die physische Geographie. Undersöksnigar over Öresund 27. Integr Comp Biol 53:582-596.

Bryan-Walker, K., Leung, T.L.F. & Poulin, R. 2007. Local adaptation of immunity against a trematode parasite in marine amphipod populations. Mar Biol 152: 687.

Byrne, M., Przeslawski, R. 2013. Multistressor Impacts of Warming and Acidification of the Ocean Marine Invertebrates' Life Histories. Integr Comp Biol. 53:582-96.

Cameron, R. A., M. Samanta, A. Yuan, D. He, and E. Davidson. 2009. SpBase: the sea urchin genome database and web site. Nucleic Acids Res. 37:D750-4.

Caren E. Braby, George N. Somero. 2006. Following the heart: temperature and salinity effects on heart rate in native and invasive species of blue mussels (genus Mytilus), Journal of Experimental Biology 209: 2554-2566.

Casties, I., C. Clemmesen, F. Melzner, and J. Thomsen. 2015. Salinity dependence of recruitment success of the sea star *Asterias rubens* in the brackish western Baltic Sea. Helgol. Mar. Res. 69:169–175.

Caveen, A., Fitzsimmons, C., Pieraccini, M., Dunn, E., Sweeting, C. J., Johnson, M. L., Bloomfield, H., Jones, E. V., Lightfoot, P., Gray, T. S., Stead, S. M., Polunin, N. V. C. 2014. Diverging Strategies to Planning an Ecologically Coherent Network of MPAs in the North Sea: The Roles of Advocacy, Evidence and Pragmatism in the Face of Uncertainty. In: Magnus L. Johnson and Jane Sandell. 2014. Advances in Marine Biology. Oxford Academic Press. 69:325-370.

Cognetti, G., and F. Maltagliati. 2000. Biodiversity and Adaptive Mechanisms in Brackish Water Fauna. Mar. Poll. Bull. 40:7-14.

Conley, D. J., C. Humborg, L. Rahm, O. P. Savchuk, and F. Wulff. 2002. Hypoxia in the Baltic sea and basin-scale changes in phosphorus biogeochemistry. Environ. Sci. Technol. 36:5315–5320.

Crain, C. M., Kroeker, K. and Halpern, B. S. 2008. Interactive and cumulative effects of multiple human stressors in marine systems. Ecology Letters. 11: 1304–1315.

Crutzen, P. J. 2002. Geology of mankind. Nature 415:23.

De Wit, P., M. Pespeni, and S. Palumbi. 2015. SNP genotyping and population genomics from expressed sequences – current advances and future possibilities. Mol. Ecol. 24:2310–2323.

Diederich, S., G. Nehls, J. E. E. Van Beusekom, and K. Reise. 2004. Introduced Pacific oysters (*Crassostrea gigas*) in the northern Wadden Sea: invasion accelerated by warm summers? Helgol. Mar. Res. 59.

Diehl, W. J. 1986. Osmoregulation in echinoderms. Comp. Biochem. Physiol. Part A Mol. Integr. Physiol. 84:199–205.

Diehl, W. J., and J. M. Lawrence. 1985. Effect of salinity on the intracellular osmolytes in the pyloric caeca and tube feet of *Luidia clathrata* (say) (Echinodermata: Asteroidea). Comp. Biochem. Physiol. Part A Physiol. 82:559–566.

Dutilleul, P., J. D. Stockwell, D. Frigon, and P. Legendre. 2000. The Mantel Test versus Pearson's Correlation Analysis: Assessment of the Differences for Biological and Environmental Studies. J. Agric. Biol. Environ. Stat. 5:131.

Earl, D. A., and B. M. VonHoldt. 2012. STRUCTURE HARVESTER: a website and program for visualizing STRUCTURE output and implementing the Evanno method. Conserv. Genet. Resour. 4:359–361.

Eisenlord, M. E., M. L. Groner, R. M. Yoshioka, J. Elliott, J. Maynard, S. Fradkin, M. Turner, K. Pyne, N. Rivlin, R. Van Hooidonk, and C. D. Harvell. 2016. Ochre star mortality during the 2014 wasting disease epizootic: role of population size structure and temperature. Philos. Trans. R. Soc. Lond. B. Biol. Sci. 371.

Evanno, G., S. Regnaut, and J. Goudet. 2005. Detecting the number of clusters of individuals using the software structure: a simulation study. Mol. Ecol. 14:2611–2620.

Fahsbender, E., I. Hewson, K. Rosario, A. D. Tuttle, A. Varsani, and M. Breitbart. 2015. Discovery of a novel circular DNA virus in the Forbes sea star, *Asterias forbesi*. Arch. Virol. 160(9):2349-51.

Fan, H., and J.-Y. Chu. 2007. A Brief Review of Short Tandem Repeat Mutation. Genomics. Proteomics Bioinformatics 5:7–14.

Feistel, R., S. Weinreben, H. Wolf, S. Seitz, P. Spitzer, B. Adel, G. Nausch, B. Schneider, and D. G. Wright. 2010. Density and Absolute Salinity of the Baltic Sea. Ocean Sci 6:3–24.

Freire, C. a, I. a Santos, and D. Vidolin. 2011. Osmolality and ions of the perivisceral coelomic fluid of the intertidal sea urchin *Echinometra lucunter* (Echinodermata: Echinoidea) upon salinity and ionic challenges. Zool. Curitiba, Impresso 28:479–487.

Gezelius, G. 1963. Adaptation of the sea urchin *Psammechinus miliaris* to different salinities. Zool. Bidrag Fran Upp. 35, 329-337.

Gräwe, U., R. Friedland, and H. Burchard. 2013. The future of the western Baltic Sea: Two possible scenarios. Ocean Dyn. 63:901–921.

Guichoux, E., L. Lagache, S. Wagner, P. Chaumeil, P. Léger, O. Lepais, C. Lepoittevin, T. Malausa, E. Revardel, F. Salin, and R. J. Petit. 2011. Current trends in microsatellite genotyping. Mol. Ecol. Resour. 11:591–611.

Guppy, M., and P. Withers. 2007. Metabolic depression in animals: physiological perspectives and biochemical generalizations. Biol. Rev. 74:1–40.

Halpern, B. S. 2010. A Global Map of Human Impact on. Science. 319:948–953.

Hand, S. C., and I. Hardewig. 1996. Downregulation of cellular metabolousm during environmental stress: Mechanisms and Implications. Annu. Rev. Inc. 58:539–63.

Hansson, D., and E. Gustafsson. 2011. Salinity and hypoxia in the Baltic Sea since A.D. 1500. J. Geophys. Res. Ocean. 116:1–9.

Harley, C. D. G., A. R. Hughes, K. M. Hultgren, B. G. Miner, C. J. B. Sorte, C. S. Thornber, L. F. Rodriguez, L. Tomanek, and S. L. Williams. 2006. The impacts of climate change in coastal marine systems. Ecol. Lett. 9:228–241.

Harper, F. M., J. A. Addison, and M. W. Hart. 2007. Introgression versus immigration in hybridizing high-dispersal echinoderms. Evolution (N. Y). 61:2410–2418.

Harper, F. M., and M. W. Hart. 2005. Gamete Compatibility and Sperm Competition Affect Paternity and Hybridization Between Sympatric *Asterias* Sea Stars. Biol. Bull. 209:113–126.

Harper, F. M., and M. W. Hart. 2007. Morphological and phylogenetic evidence for hybridization and introgression in a sea star secondary contact zone. Invertebr. Biol. 126:373–384.

Harvey, B.P., Gwynn-Jones, D., Moore, P.J. 2013. Meta-analysis reveals complex marine biological responses to the interactive effects of ocean acidification and warming. Ecology and Evolution 2013; 3(4): 1016–1030.

Havird, J. C., R. P. Henry, and A. E. Wilson. 2013. Altered expression of Na^+/K^+–ATPase and other osmoregulatory genes in the gills of euryhaline animals in response to salinity transfer: A meta-analysis of 59 quantitative PCR studies over 10 years. Comp. Biochem. Physiol. Part D Genomics Proteomics 8:131–140.

Hennebert, E., B. Leroy, R. Wattiez, and P. Ladurner. 2015. An integrated transcriptomic and proteomic analysis of sea star epidermal secretions identifies proteins involved in defense and adhesion. J. Proteomics 128:83–91.

Hennebert, E., R. Wattiez, M. Demeuldre, P. Ladurner, D. S. Hwang, J. H. Waite, and P. Flammang. 2014. Sea star tenacity mediated by a protein that fragments, then aggregates. Proc. Natl. Acad. Sci. 111:6317–6322.

Henry, R. P., E. E. Garrelts, M. M. McCarty, and D. W. Towle. 2002. Differential induction of branchial carbonic anhydrase and Na^+/K^+ ATPase activity in the euryhaline crab, *Carcinus maenas*, in response to low salinity exposure. J. Exp. Zool. 292:595–603.

Hewson, I., J. B. Button, B. M. Gudenkauf, B. Miner, A. L. Newton, J. K. Gaydos, J. Wynne, C. L. Groves, G. Hendler, M. Murray, S. Fradkin, M. Breitbart, E. Fahsbender, K. D. Lafferty, A. M. Kilpatrick, C. M. Miner, P. Raimondi, L. Lahner, C. S. Friedman, S. Daniels, M. Haulena, J. Marliave, C. A. Burge, M. E. Eisenlord, and C. D. Harvell. 2014. Densovirus associated with sea-star wasting disease and mass mortality. Proc. Natl. Acad. Sci. U. S. A. 111:17278–83.

Hickling, R., D. B. Roy, J. K. Hill, R. Fox, and C. D. Thomas. 2006. The distributions of a wide range of taxonomic groups are expanding polewards. Glob. Chang. Biol. 12:450–455.

Hiebenthal, C., E. E. R. Philipp, A. Eisenhauer, and M. Wahl. 2013. Effects of seawater pCO2 and temperature on shell growth, shell stability, condition and cellular stress of Western Baltic Sea *Mytilus edulis* (L.) and *Arctica islandica* (L.). Mar. Biol. 160:2073–2087.

Hochachka, P. W., and G. N. Somero. 2002. Biochemical Adaptation: Mechanism and Process in Physiological Evolution. Oxford University Press.

Hubisz, M. J., D. Falush, M. Stephens, and J. K. Pritchard. 2009. Inferring weak population structure with the assistance of sample group information. Mol. Ecol. Resour. 9:1322–32.

Hughes, A. D., A. I. Catarino, M. S. Kelly, D. K. A. Barnes, and K. D. Black. 2005. Gonad fatty acids and trophic interactions of the echinoid *Psammechinus miliaris*. Mar. Ecol. Prog. Ser. 305:101–111.

IPCC. 2014. IPCC, 2014: Climate Change 2014: Synthesis Report. Contribution of Working Groups I, II and III to the Fifth Assessment Report of the Intergovernmental Panel on Climate Change [Core Writing Team, R.K. Pachauri and L.A. Meyer (eds.)]. IPCC, Geneva, Switzer.

Jeuniaux, S., S. Bricteux-Grégoire, and M. Florkin. 1962. Régulation osmotique intracellulaire chez *Asterias rubens* - Rôle du glycocolle et de la taurine. Cah. Biol. Mar. 3:107–113.

Johannesson, K., and C. André. 2006. Life on the margin: Genetic isolation and diversity loss in a peripheral marine ecosystem, the Baltic Sea. Mol. Ecol. 15:2013–2029.

Johannesson, K., K. Smolarz, M. Grahn, and C. André. 2011. The future of Baltic sea populations: Local extinction or evolutionary rescue? Ambio 40:179–190.

Jombart, T., and A. Bateman. 2008. adegenet: a R package for the multivariate analysis of genetic markers. 24:1403–1405.

Josefson, A. B., C. Higgins, M. Willig, F. Jeltsch, R. Virtanen, and T. Muotka. 2016. Species Sorting of Benthic Invertebrates in a Salinity Gradient - Importance of Dispersal Limitation. PLoS One 11:e0168908.

Kalbe M, Kurtz J. 2006. Local differences in immunocompetence respect resistance of sticklebacks against the eye fluke Diplostomum pseudospathaceum. Parasitology 132:105–116.

Kappel, C. V. 2005. Losing pieces of the puzzle: threats to marine, estuarine, and diadromous species. Front. Ecol. Environ. 3:275–282.

Karhan, S. Ü., E. Kalkan, and M. B. Yokes. 2008. First record of the Atlantic starfish, *Asterias rubens* (Echinodermata: Asteroidea) from the Black Sea. Mar. Biodivers. Rec. 1:1-3.

Kazmin, V.G., Shreider, A.A., Shreider, A.A.. 2007. Age of the western Black Sea basin according to an analysis of the anomalous magnetic field and geological data. Oceanology 47, 571-578.

Keever, C. C., J. Sunday, J. B. Puritz, J. a. Addison, R. J. Toonen, R. K. Grosberg, and M. W. Hart. 2009. Discordant Distribution of Populations and Genetic Variation in a Sea Star With High Dispersal Potential. Evolution (N. Y). 63:3214–3227.

Kerkut, G. A. 1953. The forces exerted by the tube feet of the starfish during locomotion. J. Exp. Biol. 30, 575-583.

Khimoun, A., A. Ollivier, B. Faivre, and S. Garnier. 2016. Level of genetic differentiation affects relative performances of EST- and genomic SSRs. Mol. Ecol. Resour.

Koressaar, T., and M. Remm. 2007. Enhancements and modifications of primer design program Primer3. Bioinformatics 23:1289–1291.

Koster, E. A. 2005. The Physical Geography of Western Europe. Oxford University Press. 1:472.

Kowalski, R. 1955. Untersuchungen zur Biologie des Seesternes *Asterias rubens* L. in Brackwasser. Kieler Meeresforschungen 11:201–213.

Kroeker, K. J., R. L. Kordas, R. Crim, I. E. Hendriks, L. Ramajo, G. S. Singh, C. M. Duarte, and J.-P. Gattuso. 2013. Impacts of ocean acidification on marine organisms: quantifying sensitivities and interaction with warming. Glob. Chang. Biol. 19:1884–96.

Kube, S., A. Gerber, J. M. Jansen, and D. Schiedek. 2006. Patterns of organic osmolytes in two marine bivalves, *Macoma balthica*, and *Mytilus spp*., along their European distribution. Mar. Biol. 149:1387–1396.

Kube, S., A. Sokolowski, J. M. Jansen, and D. Schiedek. 2007. Seasonal variability of free amino acids in two marine bivalves, *Macoma balthica* and *Mytilus spp*., in relation to environmental and physiological factors. Comp. Biochem. Physiol. - A Mol. Integr. Physiol. 147:1015–1027.

Lamichhaney, S., A. Martinez Barrio, N. Rafati, G. Sundström, C.-J. Rubin, E. R. Gilbert, J. Berglund, A. Wetterbom, L. Laikre, M. T. Webster, M. Grabherr, N. Ryman, and L. Andersson. 2012. Population-scale sequencing reveals genetic differentiation due to local adaptation in Atlantic herring. Proc. Natl. Acad. Sci. U. S. A. 109:19345–50.

Larsson, L. C., L. Laikre, S. Palm, C. André, G. R. Carvalho, and N. Ryman. 2007. Concordance of allozyme and microsatellite differentiation in a marine fish, but evidence of selection at a microsatellite locus. Mol. Ecol. 16:1135–1147.

Lee, C. E., M. Kiergaard, G. W. Gelembiuk, B. D. Eads, and M. Posavi. 2011. Pumping Ions: Rapid Parallel Evolution of Ionic Regulation Following Habitat Invasions. Evolution (N. Y). 65:2229–2244.

Leppäranta, M., and K. Myrberg. 2009. Physical Oceanography of the Baltic Sea. Springer.

Lindahl, P. E., and J. Runnström. 1929. Variation und Ökologie von *Psammechinus miliaris*. Acta Zool. 10:401–484.

Lucu, Č., M. Devescovi, B. Skaramuca, and V. Kožul. 2000. Gill Na^+-K^+ ATPase in the spiny lobster *Palinurus elephas* and other marine osmoconformers: Adaptiveness of enzymes from osmoconformity to hyperregulation. J. Exp. Mar. Bio. Ecol. 246:163–178.

Lv, J., D. Zhang, P. Liu, and J. Li. 2016. Effects of salinity acclimation and eyestalk ablation on Na^+, K^+, 2 Cl^- cotransporter gene expression in the gill of *Portunus trituberculatus*: a molecular correlate for salt-tolerant trait. Cell Stress Chaperones. 1(5): 829–836.

Maar, M., C. Saurel, A. Landes, P. Dolmer, and J. K. Petersen. 2015. Growth potential of blue mussels (*M. edulis*) exposed to different salinities evaluated by a Dynamic Energy Budget model. J. Mar. Syst. 148:48–55.

Meier, H. E. M., K. Eilola, B. G. Gustafsson, I. Kuznetsov, T. Neumann, and O. P. Savchuk. 2012. Uncertainty assessment of projected ecological quality indicators in future climate. Oceanography. 12:1-22.

Menge, B. A., E. B. Cerny-Chipman, A. Johnson, J. Sullivan, S. Gravem, and F. Chan. 2016. Sea Star Wasting Disease in the Keystone Predaror *Pisaster ochraceus* in Oregon: Insights into Differential Population Impacts, Recovery, Predation Rate, and Temperature Effects from Long-Term Research. PLoS One. 1-28.

Mikheyev, A. S., T. Vo, B. Wee, M. C. Singer, and C. Parmesan. 2010. Rapid Microsatellite Isolation from a Butterfly by De Novo Transcriptome Sequencing: Performance and a Comparison with AFLP-Derived Distances. PLoS One 5:e11212.

Mileikovsky, S. A. 1973. Speed of active movement of pelagic larvae of marine bottom invertebrates and their ability to regulate their vertical position. Mar. Biol. 23:11–17.

Mortensen, T. 1927. Handbook of the echinoderms of the British Isles. Oxford University Press, London.

Nakićenović, N., R. Swart, G. D. Alcamo, and B. de Vries. 2000. Special report on emissions scenarios : a special report of Working Group III of the Intergovernmental Panel on Climate Change. Cambridge University Press.

Nielsen, E. E., M. M. Hansen, D. E. Ruzzante, D. Meldrup, and P. Gronkjaer. 2003. Evidence of a hybrid-zone in Atlantic cod (*Gadus morhua*) in the Baltic and the Danish Belt Sea revealed by individual admixture analysis. Mol. Ecol. 12:1497–1508.

Nikula, R., P. Strelkov, and R. Väinölä. 2008. A broad transition zone between an inner Baltic hybrid swarm and a pure North Sea subspecies of *Macoma balthica* (Mollusca, Bivalvia). Mol. Ecol. 17:1505–1522.

Norwegian Ministry of the Environment. 2012. Integrated Management of the Marine Environment of the North Sea and Skagerrak (Management Plan).

Ojaveer, H., A. Jaanus, B. R. Mackenzie, G. Martin, S. Olenin, T. Radziejewska, I. Telesh, M. L. Zettler, and A. Zaiko. 2010. Status of biodiversity in the Baltic sea. PLoS One 5:1–19.

Pawlak, J. F., H. Paulomaki, M. Laamanen, and U. L. Zweifel. 2009. HELCOM 2009 Biodiversity in the Baltic Sea- An integrated thematic assessment on biodiversity and nature conservation in Baltic Sea: Executive Summary. Balt. Sea Environ. Proc. 116A:24.

Pereyra, R. T., L. Bergström, L. Kautsky, and K. Johannesson. 2009. Rapid speciation in a newly opened postglacial marine environment, the Baltic Sea. BMC Evol. Biol. 9:70.

Perrin, C., S. R. Wing, and M. S. Roy. 2004. Effects of hydrographic barriers on population genetic structure of the sea star *Coscinasterias muricata* (Echinodermata, Asteroidea) in the New Zealand fiords. Mol. Ecol. 13:2183–2195.

Podbielski, I., C. Bock, M. Lenz, and F. Melzner. 2016. Using the critical salinity (Scrit) concept to predict invasion potential of the anemone *Diadumene lineata* in the Baltic Sea. Mar. Biol. 163:1–15.

Porras-Hurtado, L., Y. Ruiz, C. Santos, C. Phillips, Ángel Carracedo, and M. V. Lareu. 2013. An overview of STRUCTURE: applications, parameter settings, and supporting software. Front. Genet. 4:98.

Pritchard, J. K., M. Stephens, and P. Donnelly. 2000. Inference of population structure using multilocus genotype data. Genetics 155:945–59.

Reusch, T. B. H., and A. R. O. Chapman. 1997. Persistence and Space Occupancy by Subtidal Blue Mussel Patches. Ecol. Monogr. 67:65–87.

Reusch, T. B. H., W. T. Stam, and J. L. Olsen. 2000. A microsatellite-based estimation of clonal diversity and population subdivision in *Zostera marina*, a marine flowering plant. Mol. Ecol. 9:127–140.

Richardson, M. F., A. M. Stanley, and C. D. H. Sherman. 2012. Development of novel microsatellite markers for the invasive Northern Pacific seastar, *Asterias amurensis*. Conserv. Genet. Resour. 4:327–330.

Ridgway, G., and G. Naevdal. 2004. Genotypes of *Mytilus* from waters of different salinity around Bergen, Norway. Helgol Mar Res 58:104–109.

Riginos, C., and C. W. Cunningham. 2005. Local adaptation and species segregation in two mussel (*Mytilus edulis* × *Mytilus trossulus*) hybrid zones. Mol. Ecol. 14:381–400.

Rivera-Ingraham, G. A., K. Barri, M. Boël, E. Farcy, A.-L. Charles, B. Geny, and J.-H. Lignot. 2016. Osmoregulation and salinity-induced oxidative stress: is oxidative adaptation determined by gill function? J. Exp. Biol. 219.

Rivera-Ingraham, G. A., and J.-H. Lignot. 2017. Osmoregulation, bioenergetics and oxidative stress in coastal marine invertebrates: raising the questions for future research. J. Exp. Biol. 220:1749–1760.

Robertson J. D. 1949. Ionic regulation in some marine invertebrates. J. exp. Biol. 26, 182-200.

Robins, P. E., S. P. Neill, L. Giménez, S. R. Jenkins, and S. K. Malham. 2013. Physical and biological controls on larval dispersal and connectivity in a highly energetic shelf sea. Limnol. Oceanogr. 58:505–524.

Rola, R. C., M. M. Souza, and J. Z. Sandrini. 2017. Hypoosmotic stress in the mussel *Perna perna* (Linnaeus, 1758): Is ecological history a determinant for organismal responses? Estuar. Coast. Shelf Sci. 189:216–223.

Rousset, F. 2008. genepop'007: a complete re-implementation of the genepop software for Windows and Linux. Mol. Ecol. Resour. 8:103–106.

Rousset, F. 1997. Genetic Differentiation and Estimation of Gene Flow from FStatistics Under Isolation by Distance. Genet. Soc. Am. 145:1219–1228.

Russell, M. P. 2013. Echinoderm Responses to Variation in Salinity. Adv. Mar. Biol. 66:171-212.

Saderne, V., P. Fietzek, and P. M. J. Herman. 2013. Extreme Variations of pCO_2 and pH in a Macrophyte Meadow of the Baltic Sea in Summer: Evidence of the Effect of Photosynthesis and Local Upwelling. PLoS One 8:2–9.

Sameoto, J. A., and A. Metaxas. 2008. Can Salinity-Induced Mortality Explain Larval Vertical Distribution With Respect to a Halocline ? Biol. Bull. 214:329–338.

Sanford, E., and M. W. Kelly. 2011. Local Adaptation in Marine Invertebrates. Ann. Rev. Mar. Sci. 3:509–535.

Santos, I. a., G. C. Castellano, and C. a. Freire. 2013. Direct relationship between osmotic and ionic conforming behavior and tissue water regulatory capacity in echinoids. Comp. Biochem. Physiol. - A Mol. Integr. Physiol. 164:466–476.

Sarà, G., C. Romano, J. Widdows, and F. J. Staff. 2008. Effect of salinity and temperature on feeding physiology and scope for growth of an invasive species (*Brachidontes pharaonis* – Mollusca: Bivalvia) within the Mediterranean sea. J. Exp. Mar. Bio. Ecol. 363:130–136.

Saranchova, O. L., and L. P. Flyachinskaya. 2001. The Influence of Salinity on Early Ontogeny of the Mussel *Mytilus edulis* and the Starfish *Asterias rubens* from the White Sea. Russ. J. Mar. Biol. 27:87–93.

Sarantchova, O. L. 2001. Research into tolerance for the environment salinity in sea starfish *Asterias rubens* L . from populations of the White Sea and Barentz Sea. J. Exp. Mar. Bio. Ecol. 264:15–28.

Schlieper, C. 1957. Comparative study of *Asterias rubens* and *Mytilus edulis* from the North Sea (30 per 1,000 S) and the western Baltic Sea (15 per 1,000 S). Annu. Biol. 33:117–127.

Selkoe, K. A., and R. J. Toonen. 2006. Microsatellites for ecologists: A practical guide to using and evaluating microsatellite markers. Ecol. Lett. 9:615-629.

Shaw, P. W., C. Turan, J. M. Wrightà, M. O 'connellà, and G. R. Carvalho. 1999. Microsatellite DNA analysis of population structure in Atlantic herring (*Clupea harengus*), with direct comparison to allozyme and mtDNA RFLP analyses. Heredity (Edinb). 83:490–499.

Shin, Y.-K., J.-C. Jun, J.-H. Im, D.-W. Kim, M.-H. Son, and E.-O. Kim. 2011. Physiological Responses in Abalone *Haliotis discus hannai* with Different Salinity. Korean J. Malacol. 27:283–289.

Shumway, S. 1977. The effects of fluctuating salinities on four species of asteroid echinoderms. Comp. Biochem. Physiol. - A Mol. Integr. Physiol. 58:177–179.

Shumway, S. E., P. A. Gabbott, and A. Youngson. 1977. The effect of fluctuating salinity on the concentrations of free amino acids and ninhydrin- positive substances in the

adductor muscles of eight species of bivalve mollusks. J. exp. mar. Biol. Ecol 29:131–150.

Silva, A. L., and S. H. Wright. 1994. Short-term cell volume regulation in *Mytilus californianus* gill. J. exp. Biol 194:47–68.

Sjöqvist, C., A. Godhe, P. R. Jonsson, L. Sundqvist, and A. Kremp. 2015. Local adaptation and oceanographic connectivity patterns explain genetic differentiation of a marine diatom across the North Sea-Baltic Sea salinity gradient. Mol. Ecol. 24:2871-2885.

Slater, C., and E. Birney. 2005. Automated generation of heuristics for biological sequence comparison. BMC Bioinformatics. 6:31

Smith, J. E. 1947. The Activities of the Tube Feet of *Asterias rubens* L. J. Cell Sci. 3:1–14.

Sokolova, I. M., C. Bock, and H. O. Pörtner. 2000. Resistance to freshwater exposure in White Sea *Littorina spp*. I: Anaerobic metabolism and energetics. J. Comp. Physiol. B. 170:91–103.

Sommer, U., B. Meusel, and C. Stielau. 1999. An experimental analysis of the importance of body-size in the seastar-mussel predator-prey relationship. Acta Oecologica. 20:81-86.

Stickle, B., and R. Ahokas. 1974. The effects of tidal fluctuation of salinity on the perivisceral fluid composition of several echinoderms. Comp. Biochem. Physiol. - A Mol. Integr. Physiol. 47:469–476.

Stickle, W.B. & W.J. Diehl. 1987. Effects of salinity on echinoderms, In: M. Jangoux & J.M. Lawrence (Eds). Echinoderm Studies 2.Rotterdam, AA Balkema. p. 235-285.

Stuckas, H., K. Stoof, H. Quesada, and R. Tiedemann. 2009. Evolutionary implications of discordant clines across the Baltic Mytilus hybrid zone (*Mytilus edulis* and *Mytilus trossulus*). Heredity (Edinb). 103:146–156.

Svenningsson, L. 2010. A Snapshot of a Deep Water Renewal Event in the Koljö Fjord System. http://kultur.gu.se/digitalAssets/1322/1322959_b610-klar---kopia.pdf. Accessed 19/07/2017.

Takezaki, N., and M. Nei. 1996. Genetic distances and reconstruction of phylogenetic trees from microsatellite DNA. Genetics 144:389–99.

Talbot, T. D., and J. M. Lawrence. 2002. The effect of salinity on respiration, excretion, regeneration and production in *Ophiophragmus filograneus* (Echinodermata : Ophiuroidea). J. Exp. Mar. Bio. Ecol. 275:1–14.

Tatarenkov, A., L. Bergström, R. B. Jönsson, E. A. Serrão, L. Kautsky, and K. Johannesson. 2005. Intriguing asexual life in marginal populations of the brown seaweed *Fucus vesiculosus*. Mol. Ecol. 14:647–651.

Thomsen, J., I. Casties, C. Pansch, A. Körtzinger, and F. Melzner. 2013. Food availability outweighs ocean acidification effects in juvenile *Mytilus edulis*: laboratory and field experiments. Glob. Chang. Biol. 19:1017–1027.

Thomsen, J., M. a. Gutowska, J. Saphörster, a. Heinemann, K. Trübenbach, J. Fietzke, C. Hiebenthal, a. Eisenhauer, a. Körtzinger, M. Wahl, and F. Melzner. 2010. Calcifying invertebrates succeed in a naturally CO_2-rich coastal habitat but are threatened by high levels of future acidification. Biogeosciences 7:3879–3891.

Untergasser, A., I. Cutcutache, T. Koressaar, J. Ye, B. C. Faircloth, M. Remm, and S. G. Rozen. 2012. Primer3—new capabilities and interfaces. Nucleic Acids Res. 40:115–115.

Vidolin, D, Santos-Gouvea IA, Freire CA. 2007. Differences in ion regulation in the sea urchin *Lytechinus variegatus* and *Arbacia lixula* (Echinodermata: Echinoidea). J. Mar. Biol. Ass. UK. 87:769-775.

Villalobos, F. B., P. A. Tyler, and C. M. Young. 2006. Temperature and pressure tolerance of embryos and larvae of the Atlantic sea stars *Asterias rubens* and *Marthasterias glacialis* (Echinodermata: Asteroidea): potential for deep-sea invasion. Mar. Ecol. Prog. Ser. Mar Ecol Prog Ser 314:109–117.

Wares, J. P. 2001. Biogeography of Asterias: North Atlantic climate change and speciation. Biol. Bull. 201:95–103.

Weber, A. A., and S. Holmes. 2010. The role of salinity in starfish (*Asterias rubens*) colouration. VANN 4:459–466.

Weir, B. S., and C. C. Cockerham. 1984. Estimating F-Statistics for the Analysis of Population Structure. Evolution (N. Y). 38:1358.

Wendling CC, Fabritzek AG, Wegner KM. Population-specific genotype x genotype x environment interactions in bacterial disease of early life stages of Pacific oyster larvae. Evol Appl. 2017;10:338–347.

Wennerström, L., L. Laikre, N. Ryman, F. M. Utter, N. I. Ab Ghani, C. André, J. DeFaveri, D. Johansson, L. Kautsky, J. Merilä, N. Mikhailova, R. Pereyra, A. Sandström, A. G. F. Teacher, R. Wenne, A. Vasemägi, M. Zbawicka, K. Johannesson, and C. R. Primmer. 2013. Genetic biodiversity in the Baltic Sea: Species-specific patterns challenge management. Biodivers. Conserv. 22:3045–3065.

Wheeler, D. L., D. M. Church, S. Federhen, A. E. Lash, T. L. Madden, J. U. Pontius, G. D. Schuler, L. M. Schriml, E. Sequeira, T. A. Tatusova, and L. Wagner. 2003. Database resources of the National Center for Biotechnology. Nucleic Acids Res. 31:28–33.

Willmer, P. G. 1978a. Sodium Fluxes and Exchange Pumps: Further Correlates of Osmotic Conformity in the Nerves of an Estuarine Bivalve (*Mytilus Edulis*). J. Exp. Biol. 77:207–223.

Willmer, P. G. 1978b. Volume Regulation and Solute Balance in the Nervous Tissue of an Osmoconforming Bivalve (*Mytilus Edulis*). J. Exp. Biol. 77:157.

Willmer, P., G. Stone, and I. Johnston. 2005. Shorelines and Estuaries. Environmental Physiology of Animals. 444–486

Wood, H. L., G. Nylund, and S. P. Eriksson. 2014. Physiological plasticity is key to the presence of the isopod *Idotea baltica* (Pallas) in the Baltic Sea. J. Sea Res. 85:255–262.

Woodland, R. J., J. R. Thomson, R. Mac Nally, P. Reich, V. Evrard, F. Y. Wary, J. P. Walker, and P. L. M. Cook. 2015. Nitrogen loads explain primary productivity in estuaries at the ecosystem scale. Limnol. Oceanogr. 60:1751–1762.

Worley, E. K., and D. R. Franz. 1983. A comparative study of selected skeletal structures in the seastars *Asterias forbesi* (Desor), *A. vulgaris* Verrill, and *A. rubens* L., with a discussion of possible relationships. Proc. Biol. Soc. Washingt. 96:524–547.

Yancey, P. H. 2005. Organic osmolytes as compatible, metabolic and counteracting cytoprotectants in high osmolarity and other stresses. J. Exp. Biol. 208:2819–2830.

Yancey, P. H. 2001. Water stress, osmolytes and proteins. Am. Zool. 41:699–709.

Yu, Z., Z. Qi, C. Hu, W. Liu, and H. Huang. 2012. Effects of salinity on ingestion, oxygen consumption and ammonium excretion rates of the sea cucumber *Holothuria leucospilota.* Aquac. Res. 11:1760-1767.

6 Acknowledgements

Thank you very much, Frank Melzner and Thorsten Reusch, for the opportunity to develop and realize my master thesis project, the friendly support and help. Thank you, Frank, for the chance to conduct different experiments and learn a lot about experimental design.

Thank you, Christian Bock for the friendly welcome at the AWI in Bremerhaven and to teach me how to analyse osmolytes.

I would like to thank my colleagues and friends: Jennifer Nascimento Schulze, Kirti Ramesh, Trystan Sanders and short and long-term office mates for all advices, help, motivation and fun. Ulrike Panknin for your help with my sea stars (both dead and alive). Diana Gill for advice in and around the lab. The computer crew: Moritz Ehrlich, Kosmas Hench and Till Bayer for many ideas and solutions.

Thanks a lot to all the people that provided and collected samples from many places and put a lot of effort: Felix Mittermayer, Isabel Casties, Kirti Ramesh, Trystan Sanders, Josephine Watson, Fiona Harper, Ulrike Findeisen, David Thor, the AWI on Helgoland and on Sylt. Special thanks also to Fabian Wolf and Isabel Grievson, for your help and interest during the practical course last year.

I had a great time in Kiel and Geomar in the last 2.5 years due to my great friends and colleagues! Thank you very much for all the fun during and after work and the extremely good working atmosphere. Thanks also to my good friends from far away for being there for me. And thank you, Felix, for everything.

Finally, a great thank you to my parents, for all your support and love.

7 Appendix

Table 6: Reference list for mean annual salinity values taken for isolation by environment analysis.

Population	Salinity	Source	Last accessed
Kiel, Germany	15.89 PSU	Feistel *et al.,* 2010	12/07/2017
Schilksee, Germany	15.89 PSU	Feistel *et al.,* 2010	12/07/2017
Sylt, Germany	30 PSU?	Koster 2005	12/07/2017
Kattegat	32 PSU	Leppäranta and Myrberg 2009, Lindberg 2016	12/07/2017
Helgoland, Germany	32 PSU	http://www.st.nmfs.noaa.gov/copepod/time-series/de-30201/	12/07/2017
Bear cove (Nova Scotia) Canada	31 PSU	http://oceanviewer.org/south-nova-scotia/salinity/global-rtofs/test604	12/07/2017
Quebec, Canada	32 PSU	http://www.bio.gc.ca/science/data-onnees/archive/tsc/gsl/gslmap-en.php	12/07/2017
Reykjavik, Iceland	35 PSU	https://www.nodc.noaa.gov/OC5/regional_climate/arctic/	12/07/2017
Kristineberg, Schweden	24 PSU	Feistel *et al.,* 2010	12/07/2017
Oslo, Norway	25.2 PSU	Feistel *et al.,* 2010	12/07/2017
Tjärnö, Norway	26.23 PSU	Feistel *et al.,* 2010	12/07/2017
Bergen, Norway	22 PSU	Ridgway and Naevdal 2004	12/07/2017
Vattenholmen Deep, Sweden	26-32?		
Vattenholmen Shallow, Sweden	26.23 PSU	Feistel *et al.,* 2010	12/07/2017

Table 7: ANOVA results of influence of salinity treatments on concentrations of substances classified as organic osmolytes. Only results of substances that were significantly affected are displayed here.

		Df	Sum Sq	Mean Sq	F-value	Pr(>F)
Alanine	Salinity	1	2.174	2.1744	4.695	0.0432 *
	Residuals	19	8.799	0.4631		
Betaine	Salinity	1	0.8016	0.8016	8.766	0.00803 **
	Residuals	19	1.7375	0.0914		
Glycine	Salinity	1	18.193	18.193	105.7	3.37e-09 ***
	Residuals	19	3.272	0.172		
Phenylalanine	Salinity	1	0.0987	0.09873	5.307	0.0327 *
	Residuals	19	0.3535	0.01860		

Taurine	Salinity	1	42.04	42.04	8.751	0.00808 **
	Residuals	19	91.28	4.80		
Sum of all	Salinity	1	15.170	15.170	98.06	6.16e-09 ***
	Residuals	19	2.939	0.155		

Table 8: Two-way ANOVA results of the effect of salinity (16 and 32 PSU), population origin (Kiel and Sylt) and their interaction term on weight change, feeding rate and righting time. All dependent variables were divided by wet weight of sea stars to correct for animal size.

Weight change (FW – AAW) / FW					
Factor	Df	Sum Sq	Mean Sq	F-value	Pr(>F)
Population	1	0.01274	0.012735	7.805	0.00712 **
Salinity	1	0.01334	0.013337	8.174	0.00596 **
Population:Salinity	1	0.00011	0.000105	0.064	0.80058
Residuals	56	0.09138	0.001632		
Feeding rate / FW					
Factor	Df	Sum Sq	Mean Sq	F-value	Pr(>F)
Population	1	57.1	57.07	3.809	0.06103
Salinity	1	189.6	189.59	12.655	0.00136 **
Population:Salinity	1	1.9	1.87	0.125	0.72640
Residuals	28	419.5	14.98		
Righting time / FW					
Factor	Df	Sum Sq	Mean Sq	F-value	Pr(>F)
Population	1	6.286	6.286	21.778	0.0000746 ***
Salinity	1	2.248	2.248	7.788	0.00954 **
Population:Salinity	1	0.100	0.100	0.345	0.56192
Residuals	27	7.794	0.289		

Table 9: Two-way ANOVA results of the effect of salinity (16 and 32 PSU), population origin (Kiel and Sylt) and their interaction term on concentration of substances classified as organic osmolytes. Only results of substances that were significantly affected are displayed here.

		Df	**Sum Sq**	**Mean Sq**	**F-value**	**Pr(>F)**
Alanine	Salinity	1	2.484	2.4844	16.698	0.000167***
	Population	1	0.008	0.0075	0.051	0.822831
	Salinity:Population	1	0.007	0.0071	0.048	0.827522
	Residuals	48	7.142	0.1488		
Glutamate	Salinity	1	0.012	0.012	0.040	0.84172
	Population	1	4.036	4.036	13.065	0.00072 ***
	Salinity:Population	1	0.304	0.304	0.983	0.32653
	Residuals	48	14.826	0.309		
Leucine	Salinity	1	11.67	11.670	16.260	0.00020***
	Population	1	0.47	0.473	0.659	0.420769
	Salinity:Population	1	0.84	0.844	1.176	0.283657
	Residuals	48	34.45	0.718		
Lysine	Salinity	1	0.826	0.8264	9.839	0.00292 **
	Population	1	0.037	0.0366	0.436	0.51212
	Salinity:Population	1	0.548	0.5485	6.530	0.01383 *
	Residuals	48	4.032	0.0840		
Methionine	Salinity	1	1.731	1.7306	4.866	0.0322 *
	Population	1	0.317	0.3166	0.890	0.3502

	Salinity:Population	1	0.248	0.2479	0.697	0.4079
	Residuals	48	17.070	0.3556		
Phenylalanine	Salinity	1	17.94	17.939	16.648	0.00017 ***
	Population	1	0.43	0.430	0.399	0.530620
	Salinity:Population	1	0.75	0.755	0.700	0.406769
	Residuals	48	51.72	1.078		
Tyrosine	Salinity	1	18.85	18.845	16.215	0.0002 ***
	Population	1	0.06	0.059	0.050	0.8232
	Salinity:Population	1	1.90	1.905	1.639	0.2066
	Residuals	48	55.79	1.162		

Table 10: Non-parametric two-way ANOVA (Kruskal-Wallis rank sum test) results of the effect of salinity (16 and 32 PSU), population origin (Kiel and Sylt) and their interaction term on concentration of substances classified as organic osmolytes. Only results of substances that were significantly affected are displayed here.

		df	**Chi-squared**	**p-value**
Glycine[1]	Salinity	1	29.321	6.13e-08***
	Population	1	8.9637	0.002754**
	Salinity:Population	3	37.06	4.47e-08***
	Residuals			
Methylamine[1]	Salinity	1	25.491	4.45e-07***
	Population	1	3.6028	0.05768
	Salinity:Population	3	31.456	6.81e-07***
	Residuals			
Taurine[1]	Salinity	1	29.123	6.79e-08***
	Population	1	0.79848	0.3715
	Salinity:Population	3	35.726	8.56e-08***
	Residuals			
Threonine[1]	Salinity	1	9.8521	0.001696**
	Population	1	0.70275	0.4019
	Salinity:Population	3	11.039	0.01152*
	Residuals			
Valine[1]	Salinity	1	10.437	0.001235**
	Population	1	0.07137	0.7894
	Salinity:Population	3	12.04	0.007247**
	Residuals			
Sum of all[1]	Salinity	1	26.605	2.50e-07 ***
	Population	1	7.4357	0.006394 **
	Salinity:Population	3	32.825	3.51e-07 ***
	Residuals			

Table 11: Microsatellite primer names and sequences for *Asterias rubens*. Expected product length, amplified motif and suggested fluorescent dye are listed.

Name forward	Primer forward	Name reverse	Primer reverse	Product length	Motif	Fluorescent dye	Source
Ar50A	ATTGAATGTTCACTTATTGTG	Ar50B	TTTGAAAGGCTCTAATGAG		[GTT]15	FAM	Harper and Hart 2005
Ar50A	ATTGAATGTTCACTTATTGTG				[GTT]15		Harper and Hart 2005
Ar1F	TGACAAGCTTCAACGGTGTT	Ar1R	TGACGAGGAATTGGAGTGTG	122	[CAG]16	FAM	Lara Schmittmann
Ar2F	CCTCCATGGATACACCAACTG	Ar2R	CATTCCTGTTCTACAACCATTCG	153	[TAA]10	FAM	Lara Schmittmann
Ar3F	CGGTTGCTTATGGGAGAAAT	Ar3R	TGGAACACCAATCAAACCTG	183	[CTA]11	FAM	Lara Schmittmann
Ar3.2F	ACTTGGATTCGTGCCGTTG	Ar3.2R	GGTAGAAACTTCATCATGTCCCA	90	[CTA]11	FAM	Lara Schmittmann
Ar4F	CCTGCTGCTGCTGTGAACTA	Ar4R	AGGAACCTGCAGCTCCTTCT	100	[CAG]14	HEX	Lara Schmittmann
Ar5F	TTTGTACAGCAGAAACATTAAGAGC	Ar5R	TATAACCCCTTTCCCACACC	151	[TGTC]13	HEX	Lara Schmittmann
Ar6F	TACAATGGTCAACCCCGAGT	Ar6R	CAATTGGAATTCGCCTTTTC	186	[TAA]13	HEX	Lara Schmittmann
Ar7F	GGGGGATTAGAAGCAGCATA	Ar7R	GCTCACTTTGCAGCTCTGTG	128	[TAA]14	FAM	Lara Schmittmann
Ar8F	ATCCACAATGCAAAGCTTGA	Ar8R	GCCATAGACATTGATAGAAGATATTTG	182	[ATA]12	FAM	Lara Schmittmann
Ar9F	GTTCCTCCATCACTGGCATT	Ar9R	TTGCCAAAAAGATGAAGCTG	105	[CAT]10	HEX	Lara Schmittmann
Ar10F	AAAGGCGTTCATCTGGTTCA	Ar10R	ACAGGGTATTCCCCAGGCTA	151	[TGT]13	HEX	Lara Schmittmann
Ar11F	GCTGTGTGACTGGGTGAAGA	Ar11R	AGCAACTGCGACAGCCTAAC	200	[CTG]13	HEX	Lara Schmittmann
Ar12F	CTGCAGAAATCACTTTGGACA	Ar12R	CCACAAGGTTGACAGCATTC	248	[TGAT]14	FAM	Lara Schmittmann
Ar13F	AAAACAAAACGGTGTCATCTTG	Ar13R	TGACTATTGAACTCTTCAGTCAACG	120	[AAAT]10	HEX	Lara Schmittmann
Ar14F	TGCCCCATTTTATTTGTTGG	Ar14R	GCAGAAGTATGAGCACCCATAAG	152	[TGTT]12	HEX	Lara Schmittmann
Ar15F	TCCCCATTTTTGCTAGTGATTT	Ar15R	GGTATCCTTCAACAAAATGCAA	200	[ATCT]10	HEX	Lara Schmittmann
Ar16F	TCCTTGTCTCCTGTAAAGTGCT	Ar16R	CAAAGAGTTGGAGAGTGCTGT	100	[TTA]16	HEX	Lara Schmittmann
Ar17F	AGCTTAACTGTTTATATCGGCCA	Ar17R	CCTTTCCCACACCCAATTGA	122	[TGTC]13	FAM	Lara Schmittmann

Ar18F	GCCCAACCTCATCTGCATTAG	Ar18R	ATGCTGAGGTGTATGGGAAAA	115	[TTG]16	HEX	Lara Schmittmann
Ar19F	AGCTGGAACGCAGCTTCT	Ar19R	GGAGTCACCCGGATTTTGTT	157	[CAG]29	FAM	Lara Schmittmann
Ar20F	GTTGTTCTTGTCGTCGCTGT	Ar20R	GCGACAACAGCAACATTAACAC	150	[TGT]26	HEX	Lara Schmittmann
Ar21F	AGCTTCTTCTGGTCGTCTTCA	Ar21R	AGCAGGTTGAGGTTGTAGCT	109	[GCT]18	FAM	Lara Schmittmann
Ar22F	TCGCCCTTTACATACTGTTTGG	Ar22R	ACCGTGGCTGCTTACTATCA	122	[ATCA]15	HEX	Lara Schmittmann
Ar23F	GTGGACCAAAGACAACACCAA	Ar23R	GGCTGTTTGGTTCGTTCGAA	145	[AGG]13	FAM	Lara Schmittmann
Ar24F	TGATGATGATGAAGCTAACGTCT	Ar24R	CCGTCGCATCTTCATCATCT	125	[GAC]11	HEX	Lara Schmittmann
Ar25F	TTGATCATTCCGAGACCCCA	Ar25R	TCTTGTCGCCGTTTTCAGAG	90	[AGC]16	FAM	Lara Schmittmann
Ar26F	TCACTCTCATCAGCTTCAAAGAC	Ar26R	CCGTGGATGGTGGAGAAGAA	130	[TCT]13	HEX	Lara Schmittmann
Ar27F	CCAAGAAAGAGGGCCAAGGA	Ar27R	TGGTCTTGTGAAGCAGCTCT	89	[GAG]10	FAM	Lara Schmittmann
Ar28F	ATGTTTCAGGGTATGCTGCG	Ar28R	TTCTTTTGGAGCGCACTTCC	109	[CTG]16	HEX	Lara Schmittmann
Ar29F	TCTAGACGCAAATTCCTGGTT	Ar29R	CAAACCCAGCGTCAGTTCTA	114	[AG]16	HEX	Lara Schmittmann

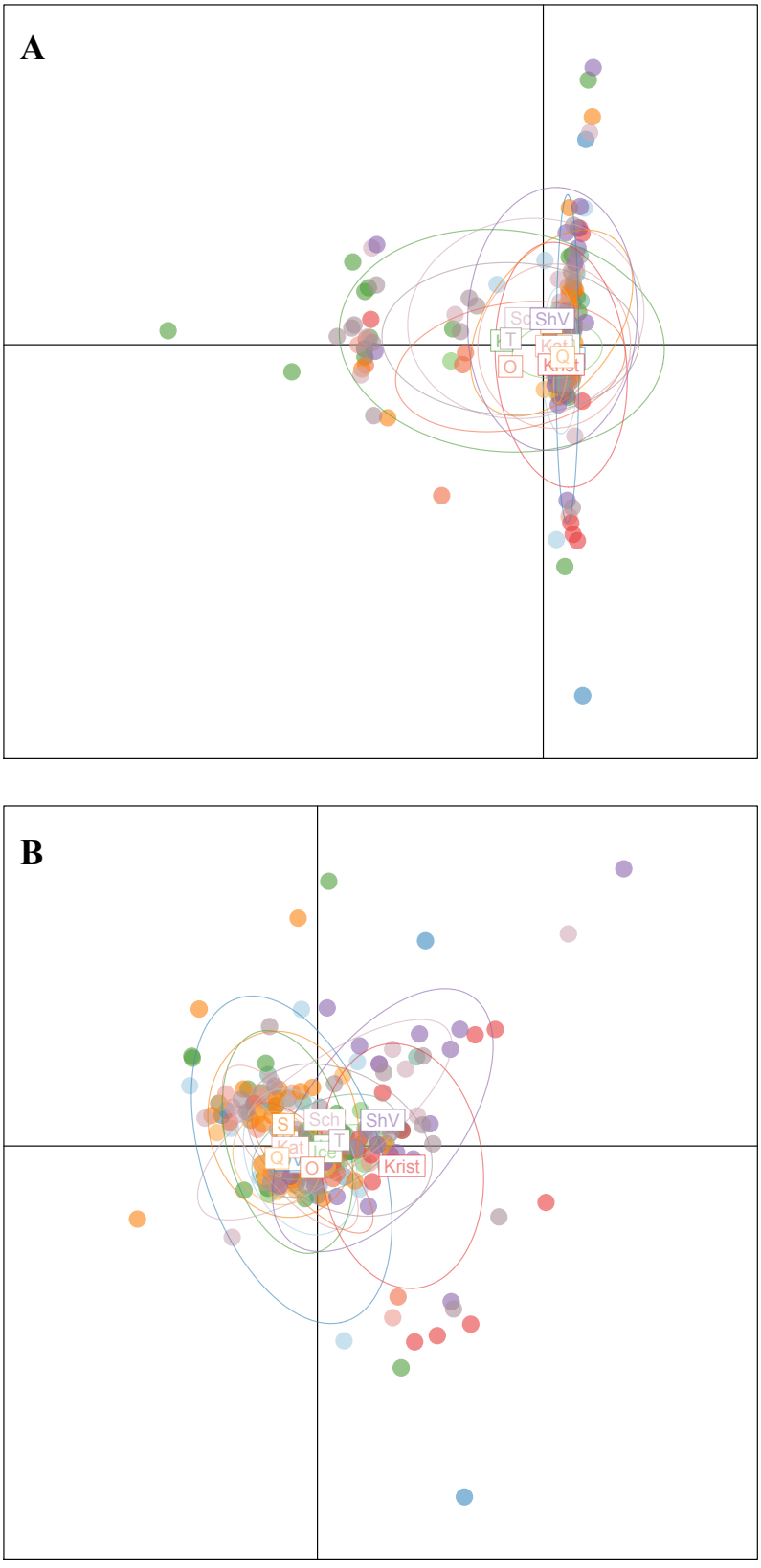

Figure 25: Principle component analysis based on allele frequencies. Eigenvalues of the principle components are displayed in the lower left corner. Loadings of PC1, PC2 and PC3 are shown in **Figure 26**, **Figure 27** and **Figure 28**.

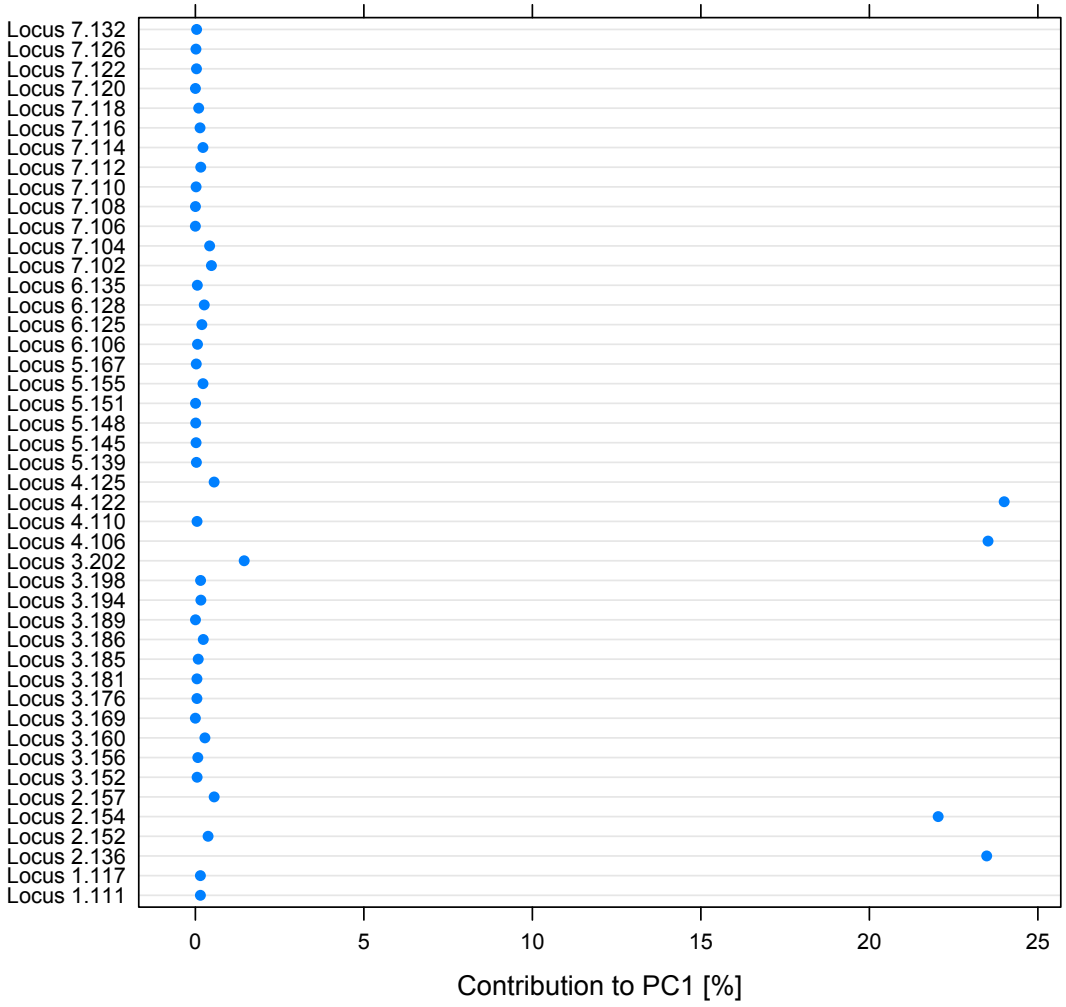

Figure 26: Relative contribution of single allele frequencies to the principal component 1. Allele names are displayed on the y-axis and sorted by the different loci. Locus 1 = Ar1, Locus2 = Ar5, Locus3 = Ar14, Locus4 = Ar17, Locus5 = Ar19, Locus6 = Ar27, Locus7 = Ar29.

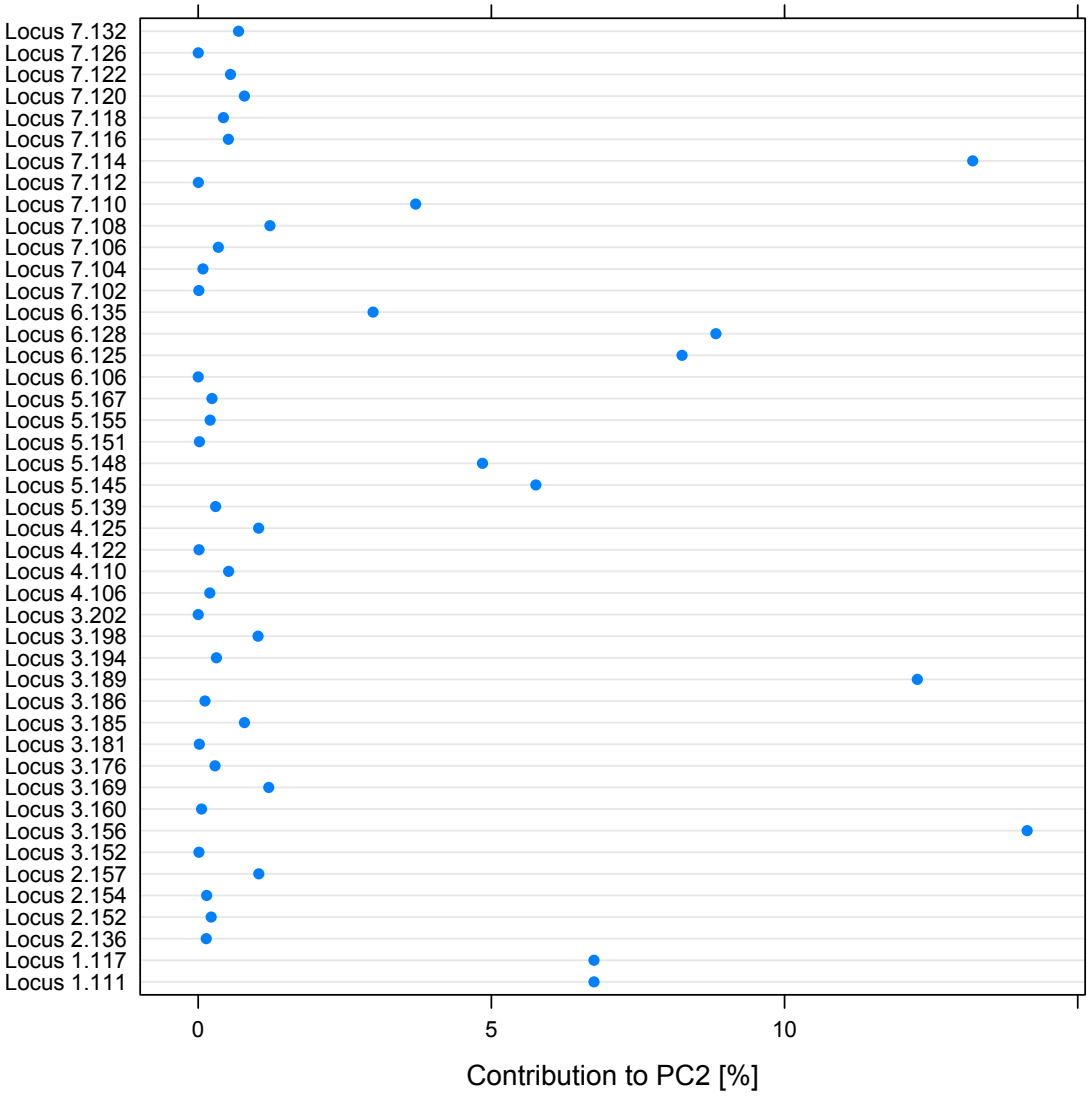

Figure 27: Relative contribution of single allele frequencies to the principal component 2. Allele names are displayed on the y-axis and sorted by the different loci. Locus 1 = Ar1, Locus2 = Ar5, Locus3 = Ar14, Locus4 = Ar17, Locus5 = Ar19, Locus6 = Ar27, Locus7 = Ar29.

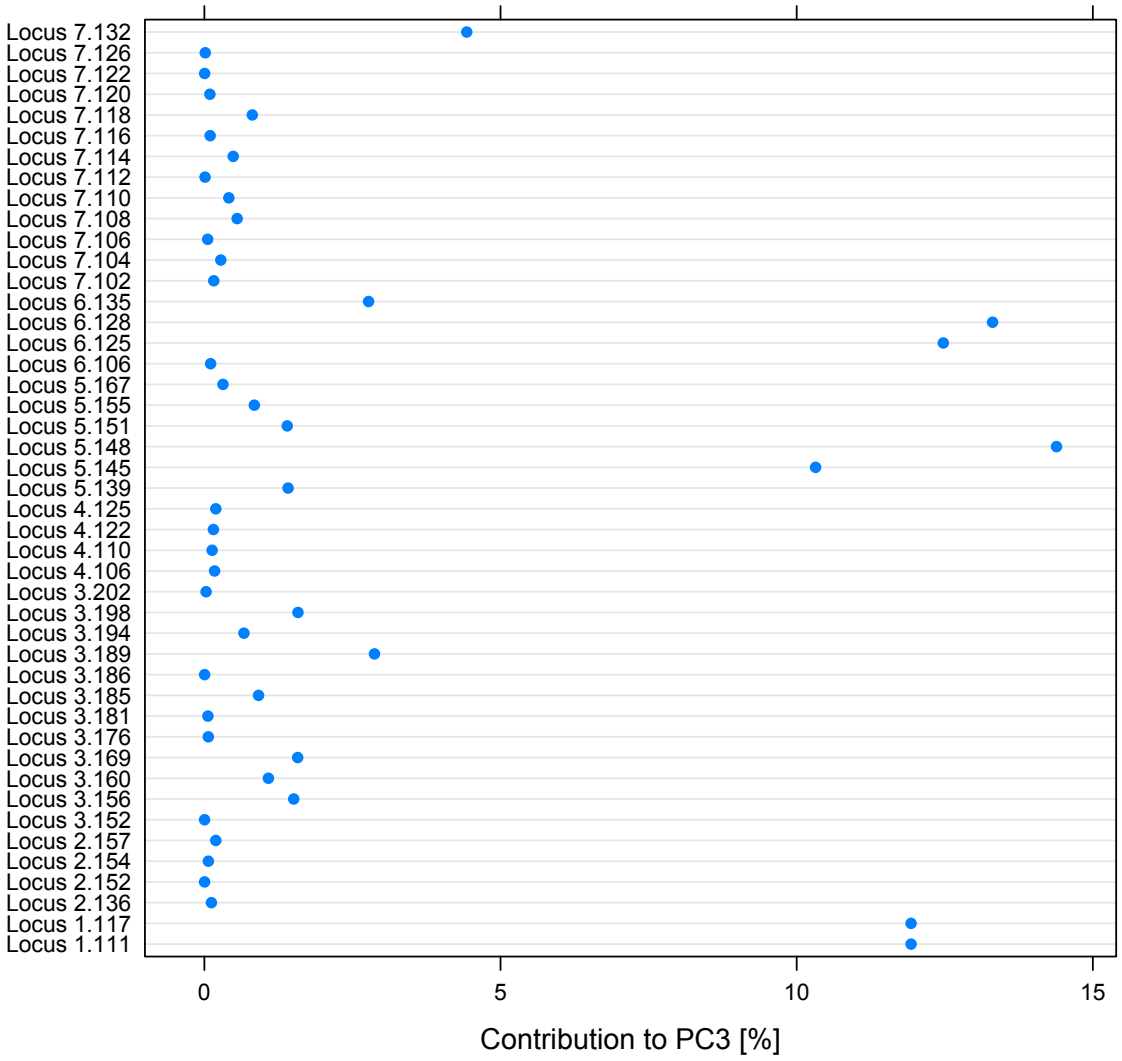

Figure 28: Relative contribution of single allele frequencies to the principal component 3. Allele names are displayed on the y-axis and sorted by the different loci. Locus 1 = Ar1, Locus2 = Ar5, Locus3 = Ar14, Locus4 = Ar17, Locus5 = Ar19, Locus6 = Ar27, Locus7 = Ar29.

Table 12: Null allele frequencies estimated from heterozygosities

Primer	Observed frequency	Median frequency
Ar1	0.010259	0.010700
Ar5	0.013735	0.012525
Ar14	0.066940	0.065809
Ar17	0.000921	0.000370
Ar19	-0.00108	-0.001050
Ar27	0.012768	0.011463
Ar29	0.04467	0.043130

Table 13: Linkage disequilibrium for each locus pair across all populations (Fisher's method).

Locus pair	Chi^2	df	p-value
Primer1 & Primer5	8.872914	14	0.839104
Primer1 & Primer14	11.733161	22	0.962647
Primer5 & Primer14	20.566116	18	0.301865
Primer1 & Primer17	12.110901	16	0.736311
Primer5 & Primer17	Infinity	16	Highly sign.
Primer14 & Primer17	10.682849	16	0.828625
Primer1 & Primer19	2.085636	16	0.999986
Primer5 & Primer19	2.786316	14	0.999395
Primer14 & Primer19	9.144545	16	0.907342
Primer17 & Primer19	0.000000	16	1.000000
Primer1 & Primer26	14.627922	18	0.687337
Primer5 & Primer26	1.090800	12	0.999977
Primer14 & Primer26	6.200696	20	0.998598
Primer17 & Primer26	1.528298	12	0.999856
Primer19 & Primer26	3.298646	12	0.993043
Primer1 & Primer29	17.353026	22	0.743584
Primer5 & Primer29	12.023865	16	0.742335
Primer14 & Primer29	23.437954	24	0.494083
Primer17 & Primer29	15.519303	14	0.343602
Primer19 & Primer29	7.188435	16	0.969456
Primer26 & Primer29	12.748314	20	0.887920

Table 14: Pearson's correlation results of F_{st} with geographical distance (IBD) and with environmental distance, in this case salinity (IBE). geogr. dist. = geographical distance; sal. diff = salinity difference.

Measure	Genetic distance	Geogr. dist. / Sal. diff.	DF	Residual std. error	R^2	Adjusted R^2	F-statistics	p-value
IBD	F_{st}	geogr. dist.	89	0.0556	0.02277	0.01179	2.073	0.1534
	F_{st}	log(geogr. dist.)	89	0.05612	0.00431	-0.0069	0.3854	0.5363
	$log(F_{st})$	geogr. dist.	89	3.067	2.20e-06	-0.0112	0.0002	0.9889
	$log(F_{st})$	log(geogr. dist.)	89	3.066	0.00067	-0.0105	0.0601	0.807
	$(F_{st})/(1-F_{st})$	log(geogr. dist.)	89	0.0712	0.00529	-0.0058	0.4737	0.4931
IBE	F_{st}	sal. diff.	89	0.05621	0.00107	-0.0101	0.0955	0.758
	F_{st}	log(sal. diff.)	89	0.0558	0.0158	-0.0047	1.429	0.2351
	$log(F_{st})$	sal. diff.	89	3.065	0.00098	-0.0102	0.0874	0.7682
	$log(F_{st})$	log(sal. diff.)	89	3.056	0.00706	-0.0041	0.6328	0.4284

Table 15: MANTEL test results of F_{st} with geographical distance (IBD). geogr. dist. = geographical distance.

Genetic distance	Geogr. dist.	R^2	p-value
F_{st}	geogr. dist.	0.0207	0.1690
F_{st}	log(geogr. dist.)	3.476e-03	0.3160
$log(F_{st})$	geogr. dist.	4.795e-04	0.4040
$log(F_{st})$	log(geogr. dist.)	7.189e-05	0.4800